A nanoLC-MS-based platform for peptide analysis

Rieux, Laurent

A nanoLC-MS-based platform for peptide analysis

The work described in this thesis was performed in the research group Pharmaceutical Analysis part of the Groningen Research Institute for Pharmacy (GRIP) at the University of Groningen, the Netherlands.

Cover: Saline (detail) de Valerio Cugia, 2004, huile sur toile (50×75 cm).
Printed by: PPI Partner, the Netherlands.

Rijksuniversiteit Groningen

A nanoLC-MS-based platform for peptide analysis

Proefschrift

ter verkrijging van het doctoraat in de
Wiskunde en Natuurwetenschappen
aan de Rijksuniversiteit Groningen
op gezag van de
Rector Magnificus, dr. F. Zwarts,
in het openbaar te verdedigen op
maandag 20 november 2006
om 16:15 uur

door

Laurent Rieux

geboren op 21 februari 1976
te Chambray lès Tours, Frankrijk

Promotores:	Prof. Dr. R.P.H. Bischoff Prof. Dr. E. Verpoorte
Copromotor:	Dr. H.A.G Niederlander
Beoordelingscommissie:	Prof. Dr. B.H.C. Westerink Prof. Dr. H. W. Frijlink Prof. Dr. T. Hankemeier

ISBN: 90-367-2815-0

Contents

CHAPTER 1

Introduction

1.1 Proteomic analysis: state-of-the-art

The identification and quantification of the complete set of proteins from an organ, a cell or a body fluid at any one time requires powerful analytical techniques. Much like genomics in the 1990's, proteomics is a rapidly expanding field of research which requires sensitive and selective technologies. The following set of techniques, each with its own advantages and disadvantages, has been used to analyse proteomics samples:

- Surface-enhanced laser desorption/ionisation (SELDI) coupled to mass spectrometry (MS)
- Protein arrays
- Two-dimensional polyacrylamide gel electrophoresis (2D-PAGE)
- Capillary electrophoresis (CE) coupled to MS
- Liquid chromatography (LC) coupled to MS

Surface-enhanced laser desorption/ionisation (SELDI) is a modified version of matrix-assisted laser desorption/ionisation (MALDI). SELDI is an ionisation technique often coupled to mass spectrometry (MS) for the analysis of proteins. It

has the potential to fractionate complex protein mixtures without much sample manipulation prior to MS analysis. However, sensitivity is limited by the small amount of sample that can be deposited on a chip [1]. In addition, non-specific binding of proteins [1] and low reproducibility of signal-to-noise ratio (S/N) and normalised intensity [2] remain an issue with this technique.

Protein arrays consist of biomolecules (e.g. oligonucleotides, proteins, small molecules) immobilised on substrates such as microscope glass slides or microwells on/in which samples are applied. Proteins with affinity for the molecules immobilised are retained on the array and other matrix components are removed by washing. The array is then subjected to detection either by MS, surface plasmon resonance (SPR), fluorescence or electroluminescence. For reasons of selectivity, non-specific binding of biomolecules to the surface must be minimised. In this context, the surface chemistry of these microarrays is still a major research subject [3]. Furthermore, the wide range of protein concentrations observed in proteomics samples complicates their use, and ligand choice in relation to selectivity presents additional limitations.

Two-dimensional polyacrylamide gel electrophoresis (2D-PAGE) has long been the method of choice for the analysis of complex protein mixtures, due to its very high resolving power. It enables the separation of thousands of proteins in a single run according to their isoelectric point (pI) in the first dimension and to their molecular weight in the second [4]. 2D-PAGE requires numerous steps (including sample handling and preparation of the gel) to identify protein spots, and the resolution of polypeptides with an extreme size, pI or hydrophobicity is difficult. Reproducibility, sensitivity and dynamic range [5] as well as automation are still problematic.

Capillary electrophoresis (CE) is a technique with high separation efficiency and speed and is suitable to separate a wide range of analytes. CE requires low injection volumes, which can be regarded as both an advantage (low sample consumption) and a drawback (limited sensitivity). An important parameter to be considered in CE is the large influence of the sample matrix on the electrophoretic separation. Peptides and proteins tend to adsorb to the silica surface of the capillary, resulting in band broadening, tailing and memory effects. In addition, adsorption to the capillary wall influences the electro-osmotic flow (EOF) and, consequently, migration times and separation efficiency. As a result, much research has been undertaken to coat silica capillaries [6–8]. Selectivity is enhanced by coupling size-exclusion chromatography (SEC) to CE for the analysis of tryptic peptides [9], and further improved by combining SEC, reversed-phase chromatography (RP) and CE in a multidimensional system [10]. However, coupling of LC

and CE remains difficult, as demonstrated by the off-line RPLC-CE system developed by Issaq et al. [11]. Though CE is a powerful separation technique that has been frequently used in proteome analysis [12], coupling of CE to other separation techniques or to MS, and loading capacity, sensitivity and reproducibility of this technique remain important issues. Therefore, LC-based separation schemes seem more promising alternatives.
With LC, separation is accomplished through a partitioning or adsorption equilibrium between a liquid mobile phase and a stationary phase. The nature of the stationary phase determines the mode of LC. An overview of these different modes is presented later in this Introduction. The composition of the mobile phase influences the state of equilibrium and thereby the selectivity of the separation. Elution can be performed under either isocratic (constant mobile phase composition) or gradient conditions (changing mobile phase composition). Peptide analysis is almost exclusively performed under gradient elution conditions. LC coupled to MS (LC-MS) presents several advantages over the aforementioned techniques. On-line coupling to MS is relatively easily achieved, though the LC-MS interface needs to be thoroughly characterised to enable quantitative analysis. Miniaturised versions of LC-MS allow the sensitive analysis of peptides. Contrary to CE, which is limited by its loadability, nanoLC set-ups making use of a trap column tolerate the injection of large sample volumes. The development of novel LC separation media permits very fast and efficient separation to be performed. LC is a very versatile and highly selective technique. In its multidimensional forms, it offers potential to achieve separation efficiencies approaching those of 2D-PAGE. It is easily automated and coupled to MS, unlike CE. Additionally, sample pretreatment steps can be included in the automated analytical set-up.

1.2 Miniaturisation of LC systems. Theory and practice

1.2.1 Theory

When a sample is injected onto a LC system under isocratic elution conditions, it will be subjected to chromatographic dilution (D), which is expressed by the following equation [13]:

$$D = \frac{C_o}{C_{max}} = \frac{\epsilon \pi r^2 (1+k)\sqrt{2\pi LH}}{V_{inj}} \tag{1.1}$$

where C_o is the initial compound concentration in a sample (before injection into the LC system), C_{max} the final compound concentration at the peak maximum, r the column radius, k the retention factor, L the column length, H the column plate height, ϵ the column porosity and V_{inj} the sample volume injected. D increases proportionally with the square of the column radius and with the square root of the length of the column. Thus, a reduction in column dimensions results in lower chromatographic dilution, whereby C_{max} increases and a lower limit of detection (LOD) can be achieved. Though this reasoning is only strictly valid under isocratic elution conditions, the consequences are commonly extrapolated to gradient elution conditions as well. Under gradient elution conditions, dilution is partly counteracted by increasing the strength of the mobile phase over time. This approach already results in an initial gain in sensitivity. However, a reduction in column dimensions provides an additional gain. Such a reduction in size is also beneficial for analyte detectability when a miniaturised electrospray interface is employed, as is discussed below. The gain in sensitivity due to the use of an LC column of smaller internal diameter (ID) can be approximated by the following relation [13, 14]:

$$f \approx \frac{d_1^2}{d_2^2}, d_1 > d_2 \tag{1.2}$$

where d_1 and d_2 are the diameters of the conventional and nano HPLC columns, respectively. Therefore, downscaling the column used in an analytical method from 4 mm ID to 50 μm ID should result in a 6400-fold gain in sensitivity. However, direct comparison of the sensitivity of two systems is only possible if every separation parameter apart from columns inner diameter is kept constant.
While miniaturisation of an LC system essentially involves the reduction of the column ID of the column, extracolumn peak-broadening effects must be reduced accordingly in order to preserve optimal performance. Excessive extracolumn band-broadening causes considerable loss of separation efficiency and, thereby, sensitivity. Ideally, the contribution of extracolumn peak broadening should be negligible compared to the peak broadening caused by the separation process on the analytical column. Generally, a 5-10% reduction in chromatographic performance is considered as acceptable [13]. Extracolumn band broadening can be divided into two categories, pre-column band broadening and post-column band-broadening. The former, also the most trivial, causes gradient delay. The latter can cause eluting peaks to broaden significantly, and result in loss of resolution and sensitivity. The following equation can be used to approximate the effect of

post-column dead volumes on the volume of a peak [14]:

$$V_{p,obs} = V_p \sqrt{\left(1 + \frac{V_{ex}}{V_p}\right)} \tag{1.3}$$

where $V_{p,obs}$ is the volume of a peak as observed in the detector, V_{ex} corresponds to the post-column dead volumes and V_p is the volume of a peak eluting off a column.

1.2.2 Practical aspects of miniaturisation

Miniaturisation of an LC system implies that all system components should be downscaled, including column, connecting tubing, injector and detector or detection interface. LC columns of 75 μm ID or less require flow rates of 200 nL/min or less. To reach the very high sensitivity often required in proteomics analysis, it is necessary to deliver a stable and reproducible flow at rates at which miniaturised electrospray interfaces perform best. Flow-splitting systems, in which the flow is split between the pump and the injector, are often used because they allow the use of conventional HPLC pumps in combination with an easily constructed flow-splitting device. The simplest system splits both the flow and the sample (i.e. splitting after the injector). However, this type of set-up results in great sample losses [15]. More recently reported systems allow injection of the whole sample onto the LC column by splitting the flow in front of the injection device [16] (cf. Chapter 4). A "split/splitless" scheme with a splitter after the injector is also possible [14] (cf. Chapter 5). The main drawback of flow-splitting systems is related to the fact that the split ratio is defined by the resistance-to-flow of the two paths. As a result, the split ratio varies during gradient elution or when flow resistance in the column increases, for example due to partial clogging of the column. In the worse case, complete clogging of the column is not noticed, because most of the flow is directed through the split line anyway. To overcome these problems, systems integrating flow-feedback have been developed [16, 17].
An alternative to flow splitting is the use of dual syringe pumps that can generate low-flow gradients and accommodate high backpressures. As the flow is not split with this technique, solvent consumption is very low, allowing for continuous automated analysis even if the syringes can only contain a limited volume. Nevertheless, it is necessary to stop the analysis to refill the syringes from time to time. The use of a single pump, either a syringe pump [18] or pneumatic pump [19], in combination with a relatively large mixing chamber has been shown to generate exponential gradient profiles [18, 19]. Exponential and sigmoidal gradients were

generated using two syringe pumps, a relatively large mixing chamber and two 4-port valves [20]. Recently, gradients were generated using two reservoirs under equal gas pressure, which are interconnected with PEEK tubing (Fig. 1.1). The difference in solvent height between the reservoirs ensures dilution of the solvent in reservoir A by that contained in reservoir B, which is pushed out by the gas pressure applied. The inner diameter and length of the PEEK tubing are parameters that can be adjusted to modify the gradient profile [21]. Alternatively, various gradient generators have been reported in which eluents of different compositions were supplied through the loops of switching valves [22–26]. Ericson [27] described an approach based on the thermal expansion of the LC solvent inside a tubular spiral when heated in a water bath. This pump was shown to achieve very low volumetric flow (0.01-10 μL/min) and high pressures (>20000 bars). It is, however, difficult to manipulate the gradient because of solvent diffusion inside the loop. Hence, most of the systems described above are not as versatile for gradient profile control or as practical as binary/quaternary piston pumps. Therefore, flow-splitting set-ups are most commonly used.

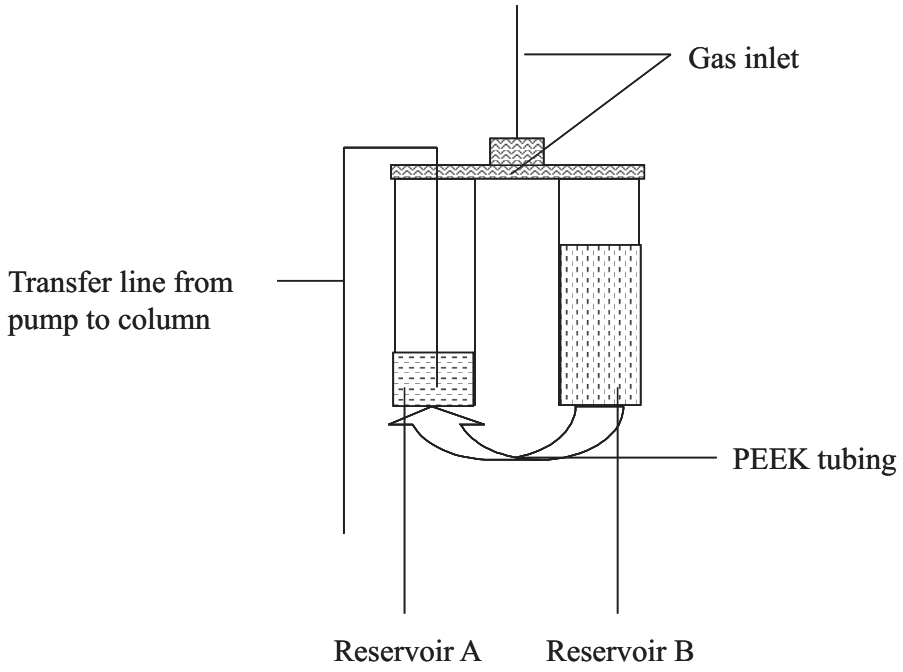

Figure 1.1: Schematic diagram of a nanoLC pump based on the difference in solvent height in two reservoirs under equal pressure.

Miniaturised LC systems can only accommodate nL injection volumes [17,28]. However, sensitivity is proportional to the absolute amount of sample loaded on the column. Therefore, a lower injection volume results in diminished sensitivity and thus a higher LOD (see Equation 1.1). The first miniaturised LC separations were performed using conventional LC pumps with flow splitting between the injection loop and the column, thus leading to great sample losses [15]. To overcome this problem, different methodologies were investigated, such as off-line preconcentration, large-volume injection directly onto the analytical column, and on-line preconcentration (using a relatively short and wide LC column). Off-line preconcentration is usually performed either using a vacuum centrifuge, ultrafiltration or an LC column of different selectivity. Any of these techniques can be used to greatly reduce the sample volume and allow the injection of the whole sample onto a nanoLC column. However, sample loss due to peptide adsorption on the wall of sample vials (cf. Chapter 6) or other parts of an analytical system [29] may still reduce the sensitivity and reproducibility of the system. As an alternative, it has been shown that large sample volumes (1.8 μL) can be loaded directly onto miniaturised LC columns (25 μm ID) in 5 min at high flow rate, while elution is performed at low flow rates [30]. This methodology, however, requires the sample to be dissolved in a solvent significantly weaker (20-30% less organic solvent) than the solvent necessary to elute the analytes off the LC column [13]. As a result, large direct on-column injections are only possible when the analyte is strongly retained, such as in the case of a neuropeptide on a reversed phase (RP) stationary phase material [31]. Apart from the sample volume and solvent, the nature of the analyte plays an important role. The maximum amount to be injected is determined by the analyte in a mixture that is least retained [31]. For example, it was not possible to inject more than 100 nL of a nucleotide solution on a 75-μm-ID RP column without a loss in separation efficiency [28]. Even much smaller sample volumes were shown to be deleterious to the quality of the separation [15]. Therefore, the need arose to develop a column-switching technique that allowed the injection of large volumes (>1 μL) on a trap column (also known as preconcentration column) without overloading the analytical column. Trap columns enable fast sample loading through use of high fllowrates compared ot the separation. While loading 1.8 μL directly onto a 25-μm-ID column took 5 min, systems incorporating a trap column could load 10-100 μL in 5 min or less [32] (cf. Chapter 5). A trap column also provides efficient protection of the analytical column against clogging. Two different column-switching procedures are possible; namely the back-flush [16, 33] (cf. Chapter 4) and forward-flush elution [14] (cf. Chapter 5 & 6).

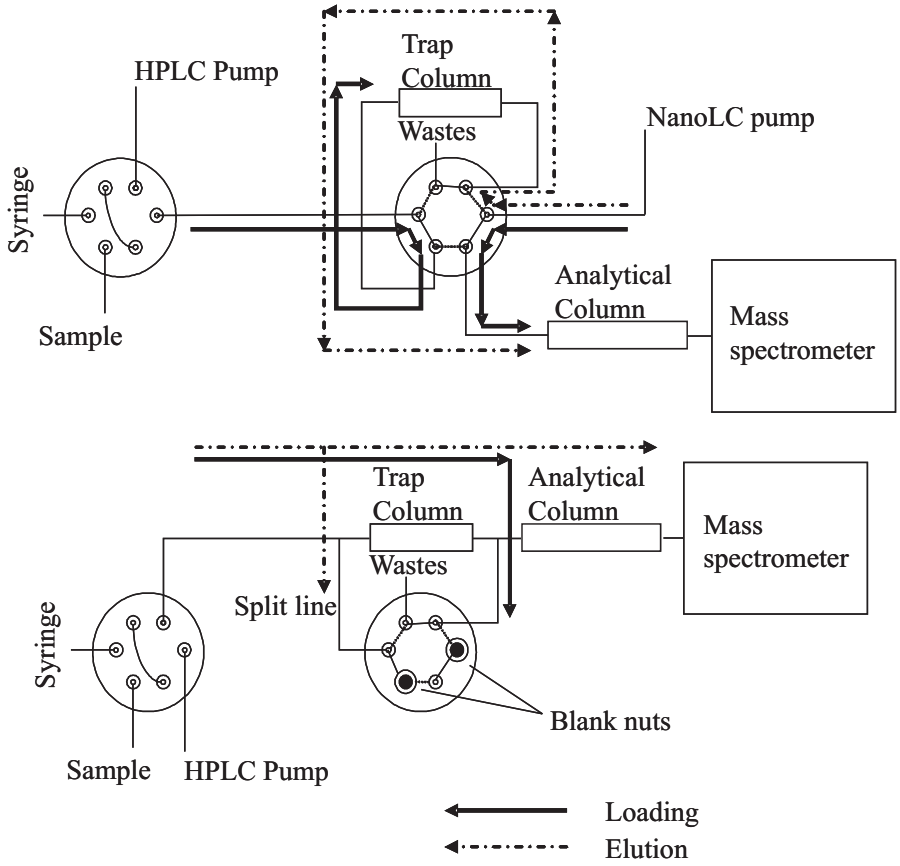

Figure 1.2: Schematic diagram of back-flush (top) and forward-flush (bottom) nanoLC-MS set-ups. More details can be found in Chapter 4 about a back-flush set-up used for the characterisation of a 50-μm reversed-phase monolith. Chapter 5 describes a novel forward-flush set-up we developed. Depending on the connection scheme, a back-flush set-up can be turned into a forward-flush set-up using the exact same components.

A back-flush procedure requires a set-up (Fig. 1.2) incorporating two pumps , with a trap column mounted on an additional switching valve. The sample plug is injected and concentrated on the trap column using the loading pump and the flow is further directed to waste during sample loading. The nanoflow pump is also connected to this switching valve, in order to elute the analytes off the trap column onto the analytical column. Though back-flush set-ups require two pumps, they also present clear advantages. Back-flush elution prevents exces-

sive migration of trapped peptides through the trap column and enables focusing of the sample components as narrow bands on top of the nanoLC column [33]. Whereas the back-flush design is often preferred because it minimises band broadening, forward-flush has been used to protect the analytical column from possible impurities at the head of the analytical column. Meiring et al. [14] designed a forward-flush set-up making use of only a single pump (Fig. 1.2).

The most striking feature of this set-up is the switching valve, which is placed outside the sample stream to manage both sample loading onto the trap and elution from the trap to the analytical column. In addition, this valve controls switching on and off of the split line. Inter-column dead volumes are minimised by the use of a nanoT piece to connect the trap and analytical columns. Moreover, delay in gradient delivery during analytical separation is of little importance because flow splitting is performed just in front of the trap column. The effect of precolumn dead volumes is compensated for by simultaneously switching the valve to start splitting the flow and increasing the pump flow rate. Band broadening was very limited and chromatographic peaks of 4-5 s were obtained [14]. A set-up incorporating a RAM column in front of the nanoLC system was developed based on the configuration described in [14], and yielded similar narrow peaks (cf. Chapter 5). Precolumns with a 300-μm ID have a sufficiently large capacity not to be easily overloaded and can be used in line with nanoLC columns without influencing the delivery of the gradient [34]. Larger trap columns cannot be considered for use with nanoLC columns because these trap columns introduce large void volumes into forward-flush systems resulting in large delays in solvent delivery.

1.3 Nanospray. Coupling nanoLC to MS using electrospray ionisation

Since the introduction of electrospray ionisation (ESI) [35] and MALDI [36] for the analysis of large biomolecules, these techniques have become the most powerful tools for protein identification and characterisation. ESI is a soft ionisation technique allowing the transfer of liquid-phase ions to the gas-phase through a gentle process that facilitates the sensitive analysis of non-volatile and thermolabile compounds [35]. ESI is currently the most popular interface for coupling LC to MS in proteomic analysis.

1.3.1 Theory

When a high voltage difference is applied between an electrode and a counter electrode, a strong electric field is created. In the case of ESI, the high voltage is applied to the end of a capillary (also referred to as tip or emitter) delivering the analyte solution. This capillary is often connected to an LC column for analyte separation. The solvent extends from the tip of the emitter in the shape of a cone, known as Taylor cone [37]. When the coulombic (electrostatic) repulsion between charged molecules at the surface of the Taylor cone is stronger than the surface tension of the solution (or Rayleigh limit), charged droplets are expelled from the cone. Droplet disintegration, assisted by solvent evaporation, results in ever smaller offspring droplets. As the solvent evaporates, the droplets shrink further and the coulombic repulsion increases. Finally, ions are expelled from the remaining solvent and travel toward the counter electrode along the lines of the electric field [38]. The mechanism by which the Taylor cone is established is to date not fully understood.
Most conventional ESI interfaces operate with maximum sensitivity at flow rates in the low-to-mid μL/min range, whereas nanoESI interfaces perform best at flow rates in the low nL/min range. Solvent flow rate [37,39], emitter ID, solvent composition and electrolyte concentration can all influence the quality of the spray [40]. The size of the droplets sprayed from the Taylor cone is highly dependent on flow rate and emitter ID and thus critical to efficient ionisation of the analytes. Lowering the flow rate from the μL/min range to the nL/min range results in the formation of smaller droplets (100-1000 times) [39]. Since smaller droplets contain less solvent, ionisation is more efficient; because lesser fission events are required to produce gas-phase ions [37–39]. With fewer, smaller droplets, more analyte enters the mass spectrometer and thus higher sensitivity is achieved [37]. Thus, coupling of nanoLC with MS has greatly benefited from the design of novel low-volume ESI interfaces - referred to as nanoelectrospray ionisation (nanoESI).

1.3.2 Fabrication

The term nanoelectrospray ionisation (nanoESI) initially referred to off-line spraying [39]. The importance of nanoLC in proteomic analysis and the technological progress in this area resulted in nanoESI now being used for both on-line and off-line techniques applying nL/min flows.
When coupling nanoLC to MS, the spray voltage can be either applied on the outside of the emitter or directly to the liquid to be sprayed. The former requires a conductive layer on the outside of the emitter [39, 41] while the latter, referred

to as a "liquid junction", makes use of uncoated silica emitters [41]. The emitters used in liquid-junction interfacing are, therefore, easier and cheaper to prepare. However, they require a higher voltage to obtain a stable spray as a result of the significant voltage drop through the solvent. In some cases, LC columns were prepared inside nanoESI tips, thereby dramatically minimising post-column dead volumes [42]. Similarly, several groups sprayed directly from the LC column, especially when columns were of the monolithic type [43, 44]. NanoESI can also be performed with capillaries packed without need of a frit. In this case, silica beads arrange themselves in a manner like stones in an arch [45]. However, these set-ups still require electric contact to be made with the LC eluent and are not commonly used.

The fabrication of nanoESI emitters is often a two-step process, making and coating the tip. The first nanoESI emitter was made from a borosilicate capillary heated using a laser and pulled at the same time to a fine tip with a capillary puller. It was then coated with gold by vapour deposition [37]. However, the difficulties associated with making nanoESI emitters this way, including their fragility and their low reproducibility, led to the development of other procedures. Stainless steel (SS) emitters were employed with varying success. While untapered emitters did not give a satisafactory spray [41], tapered tips did, with very stable sprays ultimately [46]. Emitters with a tapered end of smaller ID and with thinner walls gave the best results in terms of sensitivity and stability at low flow rates [46]. No adsorption of peptides to the stainless steel walls was detected. However, this might become problematic at very low flow rates, as observed with glass and fused-silica capillaries [46]. Moreover, peptides are likely to form adducts with alkali-metal ions when peptides are allowed to make contact with metal during spraying [47]. Microfabrication has been used to produce nanospray emitters from different materials including: glass [48], silicon [49] and polymers, such as polydimethylsiloxane (PDMS) [50, 51], polyimide [52, 53], cycloolefin [54], polycarbonate [55, 56] and poly(methylmethacrylate) [55, 57].

Initially, gold was the material of choice for coating nanoESI emitters, whether it was vapour-deposited [39] or sputtered [58]. However, gold coatings are very sensitive to electrical discharge. Part of the coating peels off with every discharge and the emitter performs less effectively with increasing loss of coating [59]. Thus, more stable coatings were necessary. Silver and gold with or without an intermediate chromium layer to improve adhesion have been investigated, but have not yielded a stable coating. Silver was probably unsuccessful due to oxidation, changing it into an insulator. More robust tips were obtained by vapour-depositing a thin film of gold on the outer surface of the capillary following treatment with

an organosilane [60]. Graphite has been used as an intermediate coating to make gold adhere more strongly to silica capillaries. Coatings made of graphite [61], a mixture of polyimide and graphite [62], or polypropylene and graphite [63] were successfully applied to nanoESI using silica-based emitters. Graphite-based coatings show much greater mechanical stability than gold coatings, and stable spraying may be performed for a week or more [62]. Moreover, graphite-coated tips are electrochemically more stable than metal-coated tips [61]. Polyaniline-coated nanotips showed high sensitivity and durability and were resistant to electrical discharge (probably because of the thick polyaniline coating) [64]. Whereas novel methodologies have addressed, sensitivity and ruggedness issues, reproducibility is still problematic with most approaches.

1.3.3 Practical considerations

An additional advantage of the reduced number of disintegration events is the higher tolerance of nanoESI toward salts, resulting in less spectral background noise [40]. At very low flow rates (low nL/min), signal suppression can be greatly reduced as compared to that at higher flow rates (>50 nL/min) [65]. LC separations are often performed in the reversed-phase mode, where the mobile phase is generally a mixture of acidified water and an organic modifier. The lower surface tension and boiling points of the organic solvent facilitate the formation of gas-phase ion [40,66]. Since solvent evaporation plays an important role in the mechanism of electrospray ionisation, it is not surprising that a low flow rate, together with a high percentage of organic modifier, improves the efficiency of droplet size reduction and, thus, the release of ions from droplets. It was found that, at certain solvent compositions, the signal intensity decreased dramatically [41]. Such a drop in intensity is likely to happen at different mobile phase compositions in nanoLC-ESI-MS. Eluent flow rate and composition, emitter ID and geometry, as well as analyte concentration, are all likely to influence the stability of the spray [40] and its morphology [67]. Moreover, a shift in the charge state of peptides has been observed as a result of changing experimental parameters in nanoESI [68]. Therefore, it can be difficult to obtain a stable and reproducible spray and an optimal signal when the mobile phase composition changes. Consequently, coupling nanoLC to MS by means of a nanoESI interface requires a careful investigation of the influence of all the aforementioned parameters on the spray stability and peptide spectra.

1.4 Column technology

Since 2D-PAGE has difficulties resolving either very small or very large proteins as well as polypeptides with extreme pI, size and/or hydrophobicity [4], chromatographic alternatives have emerged. In chromatography, the analytical column is the heart of the technique. Its performance will be of paramount importance to achieve efficient and rapid separation. Consequently, much research has focused on the synthesis of more suitable chromatographic stationary phases (SP). The characteristics of the solid support that bears the stationary phase play an immense role in the separation efficiency of proteins and peptides and thus, much attention must be paid to parameters such as particle and/or pore size as well as to the porosity of the stationary phase. Moreover, the material from which the stationary phase is made will determine the boundary conditions under which separations can be carried out.
The Van Deemter equation (cf. Chapter 3) summarises the different terms contributing to band broadening on a chromatographic column. These are the "Eddy diffusion term" (A-term), the "axial diffusion term" (B-term) and the "resistance-to-mass-transfer term" (C-term). These terms are influenced by the aforementioned structural parameters (particle and pore size). The understanding of the relation between the structural parameters of a column and its chromatographic performance drove the development of more efficient stationary phases. Additionally, stationary phases must be chemically and physically stable. They need to be stable at extreme pH values and at the high pressures at which they are operated (up to 5000 bars in extreme cases [69]). Furthermore, they should not swell when in contact with organic solvents. In order to achieve the analysis of low-level peptides and proteins, a large loading capacity is also required. Using stationary phase supports with different physico-chemical properties might be a way to vary the selectivity of a chromatographic separation (i.e. by using different pHs). Materials used for the preparation of chromatographic SP support materials include silica, organic and inorganic polymers, as well as materials with enhanced thermal, chemical and physical stability such as zirconia and titanium. Naturally-occuring organic polymers exhibit a porosity adequate for protein analysis, and are stable over a large pH range ($3<\text{pH}<13$) [70]. Unfortunately, they are mechanically weak and swell easily [70]. Moreover, such particles are usually rather large (10-60 μm dp) and often exhibit large size distribution, thereby contributing to larger A and C terms in the Van Deemter equation. Silica is the most commonly used stationary phase support material in HPLC, due to its resistance to high pressures and its well-known chemistry. Commonly, porous silica beads

in the 3-10 μm size range are used to separate biomacromolecules. Peptides are usually analysed on supports with a mean pore diameter of 300 Å, while bigger proteins are analysed on supports with pores up to 1000 Å [70]. Though efficient separations are possible with such materials, intra-particle mass transfer is still an issue. 1-μm particles resulted in more efficient separations at the expense of much greater backpressures [71]. Jorgenson introduced injectors, pumps and chromatographic stationary phase support materials able to cope with the pressures (up to 5000 bars) required to perform chromatography with such small particles [69, 72], accordingly termed ultra-high pressure liquid chromatography (UHPLC). Only recently, an LC system working at up to 1000 bars with 1.7-μm particles was commercialised [73]. In open-tubular columns, the walls of silica capillaries have been derivatised with e.g. carbon chains to obtain a reversed-phase retention mechanism [74–76]. Very high efficiencies were achieved, but loading capacity was too low to achieve satisfactory sensitivity. Non-porous particles were developed to avoid band broadening due to stagnant mobile phase transfer [77], but these also exhibited limited loading capacity. To avoid the problems related to the need for very high pressures associated with 1-μm ID particles and the low capacity of open-tubular columns and non-porous media, perfusion chromatography was introduced at the beginning of the 90's [78]. However, at low pressures, the mobile phase and analytes tended to go around the particles without penetrating them [79]. Shortly after, the first monolithic columns were synthesised. These stationary phase support materials, based on polymer or silica, are characterised by high porosity and low flow resistance (only low pressures are required) leading to efficient and fast separations. The synthesis, characterisation and application of silica-based monoliths are described in more detail in Chapter 3 and 4. Though silica-based stationary phases are stable when used with organic liquid phases, silica hydrolyses rapidly at extreme pHs [80]. This greatly stimulated research on chromatographic supports based on other inorganic materials that are chemically and physically more stable than silica- and organic-based SP support materials. Monoliths synthesised from metal oxides such as zirconium [81, 82] and hafnium [81] were successfully applied to chromatographic separations. The surface of these monoliths was either derivatised with C_{18} chains or left unaltered. The latter offers different selectivities as compared to conventional silica materials. A monolithic column was prepared from a graphitised phenolic resin [83]. Unfortunately, it has not yet been used for the separation of proteins and peptides.

1.5 Multidimensional chromatography

The proteome of an organism is generally too complex to be analysed by applying only a single separation step without considerable loss of information. Therefore, multiple-step analyses are required. A multidimensional separation system like 2D-PAGE subjects analytes to two or more orthogonal (based on different partitioning mechanisms) separations, which results in greater selectivity and peak capacity. This is explained by the fact that during separation, multiple compounds may show similar properties and thus interfere with the analysis. When different separation mechanisms are used, chances of co-elution diminish.

1.5.1 Interaction of proteins with chromatographic stationary phase

Protein retention in chromatography is determined by the physico-chemical properties of the proteins (charge, hydrophobicity and conformation) and the system parameters, namely retention mode and nature of the chromatographic support and mobile phase [70]. In the RP retention mode, the distribution of hydrophobic groups on a protein surface has been shown to influence protein retention. Following studies of digestion of proteins in solution and adsorbed onto RP stationary phases, it was suggested that adsorption of a protein might occur through several amino acids [84]. Assuming that digested regions of proteins were in contact with the solvent and non-digested regions contacted the RP stationary phase, the regions that were inaccessible to tryptic digestion were found to correspond to hydrophobic domains on the protein surface [85]. Protein retention in RPLC has been modelled by Regnier and Geng [82]. In their model, retention is a function of the number of moles (Z) of solvent required to displace the protein from the stationary phase and of the displacing agent concentration. Z was found to be directly proportional to the molecular weight of a series of proteins when 60% formic acid was used as additive. Retention also depends on other characteristics of mobile phase additives (e.g. buffer type and concentration). Study of the retention mechanism in ion-exchange chromatography (IEC) showed that the 3-D structure of a protein was strongly related to its retention. Areas with especially high charge density, rather than the total protein charge, seem to dictate the behaviour of a given protein [86, 87]. Though only protein separation mechanisms in RPLC and IEC have been thoroughly investigated, it seems that peptides and proteins almost always interact with the stationary phase through superficial adsorption sites.

Ideally, a stationary phase should not display non-specific adsorption of proteins and peptides. Non-specific interactions of peptides and proteins with the stationary phase cause peaks to tail, leading to deterioration of chromatographic resolution. Residual silanol groups on silica support materials are especially notorious for their influence on chromatographic efficiency. By decreasing the surface concentration of accessible silanol groups through derivatisation, chromatographic resolution can be improved. This process is referred to as end-capping. System performance (efficiency and selectivity) is greatly related to the nature of the derivatising agent as well as its structure. With small molecule derivatising agents, a high degree of coverage of residual silanol groups on a solid support and/or capillary wall can be achieved. An alternative to end-capping is the encapsulation of the stationary phase (e.g. silica particles) with polymers. The resulting particles had mechanical properties similar to those of common inorganic supports and chemical behaviour similar to polymeric beads [88]. The selectivity and physicochemical properties (i.e. resistance to pH) of stationary phases can be drastically changed following coating. While silica hydrolyses rapidly at extreme pHs [80], inorganic materials such as titania or zirconia are chemically and physically more stable than silica- and organic-based stationary phases. Silica supports have been coated with titanium for the analysis of nucleotides [89] and phosphopeptides [90], or with zirconium [91] for the analysis of a range of small molecules.

1.5.2 Separation mechanisms

1.5.2.1 Reversed-phase

Reversed-phase (RP) LC is the most commonly used mechanism for the separation of peptides and proteins. Separation is achieved on the basis of differences in hydrophobicity between analytes. In RP mode, elution is achieved with mobile phases based on aqueous buffers to which organic modifiers such as acetonitrile (ACN) and methanol (MeOH) are added. In multidimensional systems, RP is the favourite mode of separation for the last LC dimension. This is because coupling of RPLC to MS is facilitated by the volatility of the organic modifiers traditionally used to perform RPLC separations. On a few occasions, 2D-LC setups applying the RP separation mechanism for both dimensions, have even been used. Variation of the selectivity between the first and second dimensions was achieved by using different organic solvents [92] or pHs [93]. Since each organic modifier or buffer has a different influence on solute-solvent interactions, 2D-RP-RP-LC using different mobile phases exhibits orthogonal selectivity [94].

1.5.2.2 Ion-exchange

Ion exchange (IEX) is the favourite mode of separation for the purification of intact proteins and the prefractionation of peptides. In IEX, the charges and their distribution over the surface of a protein determine the interactions between the protein and the charged surface groups on the packing material, thus dictating protein retention [86,87]. Which amino acid residues are charged is mainly dependent on pH. In IEX, controlling the pH of the mobile phase is therefore of utmost importance for successful peptide separation. At a pH $\leq$ 3, the carboxyl groups of peptides are neutral, while basic amino acids (arginine, lysine and histidine) as well as the peptide N-terminus contribute to a net positive charge of the peptide.

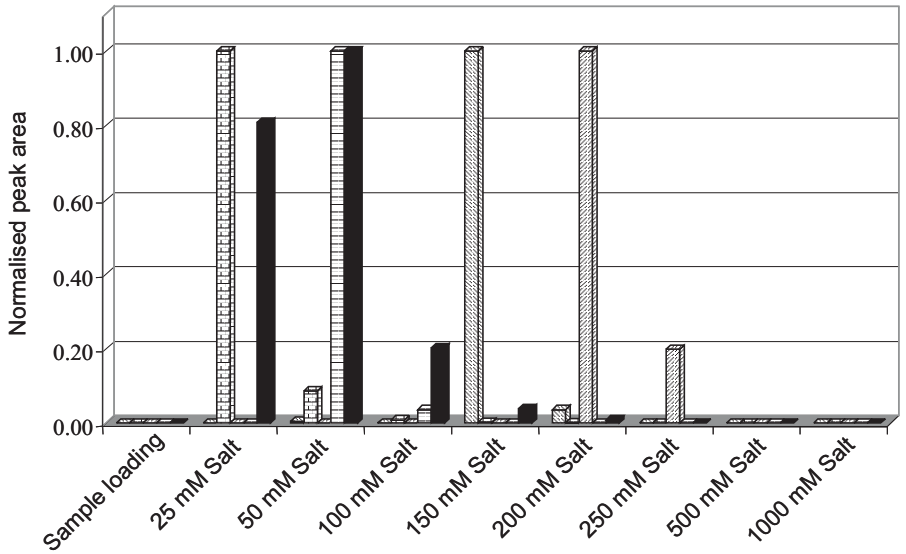

Figure 1.3: Elution profile of some of cytochrome c tryptic peptides using a strong cation-exchanger coupled on-line with RP nanoLC-MS. Columns with different patterns represent different peptides of cytochrome c having mid-range hydrophobicity. The SCX column was a BioSCX II (Agilent, Waldbronn, Germany), and elution was performed in steps of increasing concentration of ammonium formate. The nanoLC-MS set-up was as described in Chapter 6. Every peptide elutes over 2-4 salt fractions.

The fully protonated peptides can be fractionated by cation-exchange chromatography at the same pH as for a possible second-dimension RP separation. In anion-exchange chromatography, a high pH is required. However, completely deprotonated basic residues may require a pH >12, which will lead to hydrolysis

of the silica support material. Novel stationary phases (i.e. based on zirconium and titanium) are therefore required for the analysis of highly basic proteins and peptides. IEX is a general term that encompasses four types of ion-exchangers, namely weak anion-exchanger (WAX), weak cation-exchanger (WCX), strong anion-exchanger (SAX) and strong cation-exchanger (SCX). While weak ion exchangers exhibit their ion-exchanging capabilities over a relatively narrow pH range, strong ion-exchangers are charged at most pH values. Elution is performed by varying the mobile phase pH or the concentration of a salt added to the mobile phase to displace peptides from the stationary phase. In most cases, elution is performed by increasing the salt concentration in steps. As the strength of the eluting solvent does not increase continuously when performing step gradient elution, desorption of a peptide often takes place over several steps or fractions (Fig. 1.3).

Applying a continuous salt gradient will solve this problem, but is practically more difficult to implement [95]. With respect to the nature of the salt displacer, ammonium acetate [96] or formate are often preferred to alkali salts. This is because, in contrast to Na^+ and K^+ (Fig. 1.4), ammonium ions do not show adduct formation with the proteins to be separated.

Although the major property governing peptide retention during IEX involves ionic interactions, it has been noted that IEX sorbents suffer from non-specific interaction due to the hydrophobicity of the IEX stationary phase, which often results in incomplete recovery, poor peak shape or elution of peptides over several fractions [97]. Adding an organic solvent to the IEX mobile phase alleviates these problems but may interfere with the separation in a second-dimension separation step if RPLC is chosen for that dimension [93]. The lack of stability of silica support materials, and the need to exchange buffers before entering a possible second-dimension RP separation when working a high pH, explains why SCX is the preferred fractionation mode for multidimensional analysis of peptides. An efficient SCX-RP system using direct injections of fractions from the SCX column onto the RP column allowed the identification of 480 proteins from a cell lysate in 20 h [98]. Yates et al. combined SCX with RP LC-MS/MS using a single, biphasic column [96, 99]. About 25% of the complete proteome of S. cerevisiae was identified in a single run using this approach [96]. Further improvements made this set-up more reproducible, with variation on retention times about 0.5% between analyse [99].

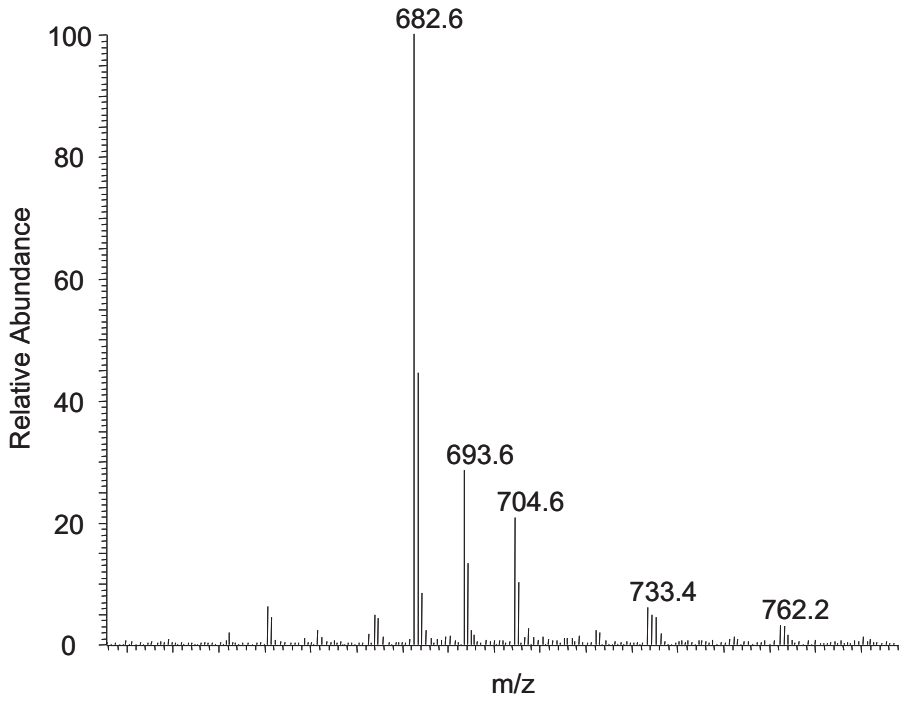

Figure 1.4: MS spectrum (between m/z 620 and 790) of Na^+ and K^+ adducts of the oxidised form of substance P, a very hydrophobic, 11-amino acid peptide. The doubly-protonated ion of SP is the most intense at 682.6. The following Na adducts were found: SP-Na and SP-Na2 at m/z of respectively 693.6 and 704.6. Other peaks were observed at 733.4 and 762.2 and might be attributable to the K-adducts: SP-Na-K2 and SP-K4, respectively. Adducts complicate the understanding of MS spectra and result in a decrease in intensity, which can prove extremely deleterious to quantitation.

1.5.2.3 Affinity chromatography and high-abundance protein depletion

The presence of particular structural features such as phosphorylation, glycosylation, nitration or histidine residues can be exploited for the selective enrichment of proteins and peptides using affinity chromatography (AC). AC is based on the selective interaction between two molecules, one of them being, in our case, a protein or peptide to be retained. For the second molecule immobilised on a solid support material, the following options have been applied:

- an antibody (immunoaffinity chromatography (IAC))
- a metal ion (immobilised metal affinity chromatography (IMAC))
- a ligand; e.g. lectin, dye or a small molecule

In IAC, antibodies are generally immobilised on stationary phases with limited pressure stability (e.g. agarose-based materials), and more rarely on silica and vinyl polymers [100]. IAC owes its selectivity to the specificity of antibodies, which define the performance of the method. Selectivity can be explained by the precise 3D arrangement of amino acids within an antibody's binding site, which can undergo various non-covalent interactions (H bonding, ionic, dipole-dipole and nonpolar interactions) [101]. The probability of an antibody cross-reacting with more than just a single protein determines the specificity of the interaction. In other words, specificity is determined by the uniqueness of the steric (tridimensional) match of antigen and antibody, as well as by the number of molecular interactions taking place between both molecules. In a specific case, where 11 antibodies were tested against 5000 proteins of the yeast proteome, every antibody exhibited a certain degree of cross-reactivity, in addition to binding its respective antigen. Comparing the amino acid sequence of antibody and antigens showed similarities that could partially explain cross-reactivity, but was not able to predict it a priori [102]. In order to preserve the tridimensional structure of the immobilised antibodies, buffers with a composition and pH close to physiological conditions are used during equilibration, loading and washing of the column. In contrast, elution is generally performed using acidic buffers [103–105] that disrupt the 3D structure of antibodies significantly to release the antigen. IAC has been used for the extraction of structurally-related amino acids and proteins. Antibodies specific for nitrotyrosine have been used for immunoprecipitation [106]. Such antibodies have also been immobilised on chromatographic media [105], extending the seminal work by Helman and Givol [104]. Protein A and Protein G form complexes with immunoglobulins. This feature is exploited in the depletion of proteomic samples of very abundant proteins, and is detailed in a later paragraph.

IMAC is a technique making use of the formation of complexes between metal ions and specific amino acids or functional groups. In principle, the side-chains of lysine, methionine, asparagine, arginine, tyrosine and histidine, as well as the N- and C-termini of peptides and proteins, complex with metal ions. However, it has been demonstrated that interactions mainly take place through surface histidine groups [107]. Cu^{2+}-IMAC is often used in proteomics analysis for the selective retention of histidine-containing proteins and peptides [107]. Other metal ions can

be applied as well, however. Recombinant ovine growth hormone was purified using both Ni^{2+} and Cu^{2+}-IMAC [108]. The Ni^{2+} column was found to retain more protein and result in a purer fraction. Phospho-proteins and amino acids bind to immobilised Fe^{3+} ions [109–111]. Ga^{3+} [112], Lu^{3+}, Sc^{3+} and Th^{4+} ions [110] were found to have similar properties to Fe^{3+} ions. Metal oxides based on aluminium [113], zirconium [114] and titanium [114, 115] were used to selectively retain phosphopeptides from complex mixtures. Column preparation is more straightforward with these metal oxides than with other IMAC materials, since the ion chelation and washing steps required for preparation of IMAC columns can be avoided. Elution of IMAC columns usually takes place by increasing pH or by introducing imidazole [108] or phosphate ions [110]. The main problem of IMAC lies in its rather low selectivity when the sample contains peptides with multiple aspartate and glutamate residues. Moreover, current methods are often limited to the identification of phosphoserine and phosphothreonine residues. This retention mode provides the advantages of low cost and high stability of the support media.

Among the many types of post-translational modifications, glycosylation is the most common and the most complex [116]. Lectins are proteins that target oligosaccharide structures recognising specific glycosylation motifs, though overlap in specificity has been observed [117, 118]. It has been shown that concanavalin A (Con A) mainly recognizes α-mannose [118] whereas wheat germ agglutinin (WGA) exhibits affinity for N-acetylglucosamine (GlcNAc) [118] and sialic acid [117]. Jacalin specifically recognises galactose-N-acetylgalactosamine (Gal-GalNAc) and more generally O-type glycopeptides [119]. Lotus tetragonolobus agglutinin (LTA) has been used for its high affinity for fucose-containing glycoconjugates [120, 121]. Sambucus nigra agglutinin (SNA) has been employed to select and compare the concentration of sialic acid-containing glycopeptides [122]. The buffers used during loading and elution of lectin columns contain a Tris buffer and NaCl; Ca^{2+} and Mn^{2+} may also be added. Elution buffers generally contain a higher NaCl concentration and 0.2 to 0.8 M sugar. The eluting glyco-peptides or proteins are enzymatically deglycosylated prior to second dimension RPLC-MS analysis, as the presence of oligosaccharide moieties complicates MS determination of molecular mass and sequence [120].

Highly abundant proteins often mask proteins and peptides of lower abundance and thus prevent or hinder their detection and identification. Albumin for example constitutes ≈60% of the total human serum protein content [123]. As in serum [124], the high albumin concentration in urine interferes with protein separation [125]. Several approaches are available to lower the level of highly

abundant proteins based on either specific antibodies, dye ligands or protein A and G. Albumin depletion is performed using either a dye such as Cibacron-Blue [126] or Affi-Gel Blue [125], or serum albumin antibodies. Removal of some IgG is performed using immobilised protein A [127] and even better using protein G [127, 128] columns. Effective depletion of human serum with respect to albumin and/or γ-globulins was achieved using both dyes and antibodies. A column designed to bind both albumin and γ-globulins yielded the highest protein concentration in the flow-through, maybe due to its proven lower effiency in albumin removal [103]. Most depletion columns (if not all) also exhibit non-specific binding of proteins and peptides of lower abundance. As a result, combining several columns might lead to considerable loss of information, which may well be the main limitation in applying depletion columns to proteomics studies.

1.5.2.4 Miscellaneous retention modes

Other retention mechanisms have been used for the analysis of proteins and peptides, though their use is much less common than the other aforementioned mechanisms. Size-exclusion chromatography (SEC) makes use of a matrix with different pore sizes that the protein and peptide analytes can enter or not, depending on their size. The large proteins can enter a lower number of pores than the small peptides and therefore elute first. Restricted-access media (RAM) are porous silica materials used in chromatography for the separation of low-molecular-weight analytes from matrix components like albumin, by a combination of size exclusion and conventional adsorption chromatography. The outside of the silica particles is often coated with a hydrophilic layer while the inside of the pores is derivatised with RP or IEX chains. RAMs are often used in pharmaceutical analysis to simplify and automate sample preparation. Though the applicability of RAM materials for the analysis of peptides has been demonstrated [129], RAM chromatography is seldom used in proteomics. Normal-Phase chromatography (NP), hydrophilic interaction liquid chromatography (HILIC) and hydrophobic interaction chromatography (HIC) are other alternatives that have been seldom (or not) used in proteomics applications. NP was used as a clean-up step in conjunction with ethylacetate extraction of a peptide before further analysis by LC-MS [130]. To our knowledge, this is the only application of NP LC to proteomic studies. Hydrophilic interaction liquid chromatography (HILIC) exploits the same separation mechanism as NP-LC. However, the stationary phases are different. Whereas bare-silica particles are normally used in NP LC, silica particles are coated with hydrophilic moeities in HILIC. Applications of NP LC and HILIC to proteomics

are limited due to the poor peptide solubility in mobile phases containing large amounts of ACN or MeOH. Hydrophobic interaction chromatography (HIC) is often used for the separation of proteins because of its mild non-denaturing properties. Even if HIC is based on the same retention principle as RPLC, the mobile phases are very different. In HIC, elution is done with aqueous buffers of decreasing ionic strength. Though HIC is commonly applied to the separation of proteins [131], to our knowledge, it has not been used for the multidimensional analysis of peptides by LC.

1.6 Sample pretreatment

1.6.1 Digestion

The enzymatic digestion of the sample (a set of proteins) is a key step in proteomic studies. The resulting mixture of peptides can be analysed using MS-based technologies to generate amino-acid-dependent data. Algorithms were developed to match the observed tandem mass spectrum of a peptide to theoretical mass spectra from protein databases, allowing the identification of proteins present in mixtures. Without prior digestion into sufficiently small fragments, further fragmentation using MS/MS is not possible.
The most commonly used proteolytic enzyme is trypsin, a serine endoprotease with well-defined substrate specificity. Digestion is generally performed in solution, which presents a number of limitations in increasing the efficiency and throughput of the process. Digestion times are long (typically >12 h) due to the necessity to work with low trypsin-to-substrate ratios to prevent autodigestion of trypsin and limit the number of interfering autolytic peptides. Moreover, at low substrate concentrations, obtaining a sufficient number of peptides to allow protein identification is problematic, since the digestion rate is limited by substrate concentration [132]. The secondary and tertiary structure of proteins (i.e. disulphide bridges, hydrophobic cores) can further reduce the digestion rate. Disulphide bridges are usually reduced and alkylated [132, 133] in order to prevent adduct formation during digestion and to improve accessibility to the cleavage sites. To increase the speed and robustness of digestion steps, proteolytic enzymes have been immobilised on solid supports. Immobilisation strongly reduces digestion times because the effective protease concentration on the solid support is very high. Digestion times have been reduced from several hours down to between 1 [134] to 5 min [135] and even 5s [136] for certain proteins using immobilised-enzyme reactors. Moreover, immobilisation stabilises proteases

against denaturation due to organic solvents and chaotropic agents. Last but not least, immobilisation facilitates the incorporation of the digestion step in on-line multidimensional LC systems. Immobilised-enzyme reactors have been prepared in cartridges based on beads [85, 136–138] and monoliths [139, 140]. They have also been made in pipette tips using monoliths [141]. Increased protease activity resulted from the acetylation of lysine residues of trypsin immobilised on a solid support (Fig. 1.5), which also helped in reducing autolytic products [142].

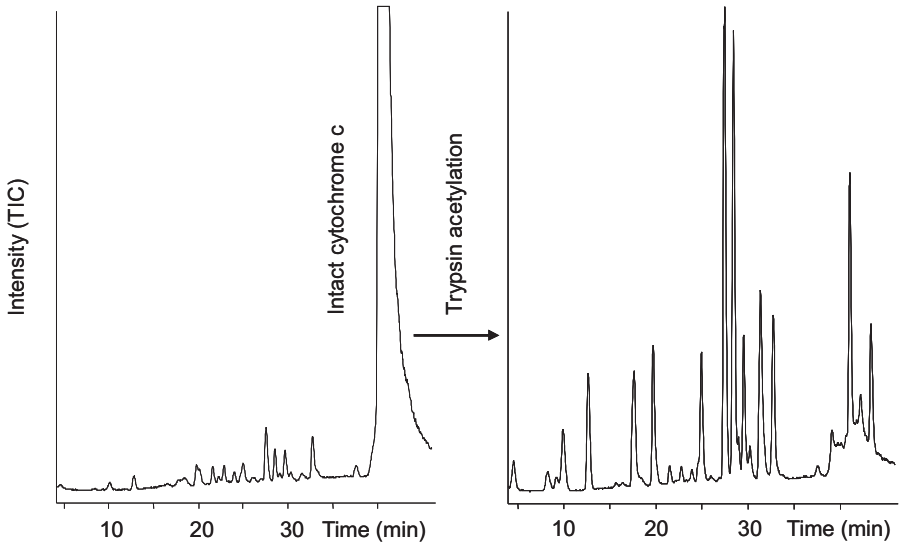

Figure 1.5: Effect of acetylation on the trypsin digestion rate of 4 μM cytochrome c, analyzed by LC-MS. Digestion was performed in 1-mm cartridges at a flow rate of 40 μL/min (residence time 4 s). Without acetylation, most of cytochrome c is still intact after 4s whereas acetylated trypsin does not show any residual cytochrome c [142].

1.6.2 Protein precipitation

Protein precipitation is a sample-preparation technique that has only seldom been used in automated/on-line systems. It is more likely to be incorporated in off-line or at-line schemes. Precipitation is performed under harsh conditions and is the consequence of denaturation. After precipitation, samples are usually centrifuged, and the supernatant is further evaporated and reconstituted before LC-MS analysis. The whole procedure normally takes between 5 min [143] and 1h [144]. Precipitation of serum or plasma is performed by mixing it with a large volume of an organic solvent such as ACN [143], ethanol [145], MeOH [144] or acetone [146].

A combination of organic solvent and acid has also been used, in which case the addition of as little as 1% trifluoroacetic acid (TFA) to ACN was necessary for proteins to precipitate [143]. Solvents can be cooled to less than 4°C [144] to limit protein solubility, or heated to 82°C [146] to denature proteins. Precipitation is also performed using salts [147]; the use of ammonium sulphate is still widely reported [148]. The lack of selectivity of most precipitation methodologies can lead to great losses as a result of coprecipitation.
More selective methods require the use of antibodies (immunoprecipitation) [149, 150], in which case the compounds precipitated are the compounds of interest. Alternative methods use metal ions [146] to form a complex with the analyte following the same mechanism as that used in IMAC. Affinity precipitation makes use of an affinity macroligand (AML), generally a polymer to which one or more types of affinity ligand are bound. Proteins or peptides bind to their corresponding affinity ligands and thus are indirectly bound to the polymer backbone. Precipitation using AMLs is reversible and triggered by a change in pH or temperature [151]. It results in rather high recovery ($\geq 75\%$) of the target molecule. High specificity is also ensured by the use of affinity ligands.
The advantages of precipitation include their ease of use and the low cost of chemicals and reagents (with the exception of immunoprecipitation). Automation is possible using a pipetting robot. However, the centrifugation step remains difficult to automate.

1.6.3 Solubility and adsorption of peptides

Proteins and peptides interact with the solvent and walls of the container in which they are held. The physico-chemical properties of a peptide will determine its solubility in a given solvent in a given container. If a peptide does not show sufficient "affinity" for the solvent in which it is dissolved, it will tend to adsorb to the walls of the container [152], leading to a lower peptide concentration than in the original matrix. However, this fact is overlooked in most proteomic analytical methods, even those designed to allow quantification. Adsorption has been shown to present an important limitation in the quantitative analysis of various peptides [153–155]. In the previous sections, the chemical nature of peptides was demonstrated to be of great importance to their solubility. The material of which containers are made also has a great impact on the solubility of peptides [156]. The influence of pH, container material, surfactants and organic modifiers on adsorptive behaviour has been studied [152, 155, 156]. Calcitonin adsorbed to the wall of a glass vial according to a Langmuir isotherm at pH ≈ 4 suggesting that

calcitonin formed a monolayer at the glass/solution interface. On the other hand, it adsorbed according to a Freundlich equation at neutral to basic pHs, suggesting the formation of aggregates and/or multilayers on the glass wall [152]. The addition of 1% TFA to the solvent significantly improved the solubility of a relatively large peptide [143], but no such effect was observed in the case of the analysis of microcystins [155]. The addition of salt (NaCl) also did not improve peptide recovery [155]. Surfactants were successfully used in the analysis of membrane proteins [143], in which they proved to minimise adsorption effects and improve quantitation. However, surfactants would interfere with MS detection. The addition of 1% n-nonyl-β-D-glucopyranoside to the solvent decreased the adsorption of a 36-amino-acid peptide during extraction from animal and human plasma [143] but, like surfactants, sugars are also likely to suppress the ionisation of analytes. Adding ACN [143] and MeOH [154, 155] greatly improved the solubility of hydrophobic peptides. Depending on the peptide to be quantified, the optimal percentage of organic solvent varies. Unfortunately, the presence of an organic solvent can also interfere with RPLC separation. Therefore, selection of the organic solvents used is important. Dimethylsulfoxide (DMSO) proved to be a better solvent than ACN or MeOH for improving the solubility of hydrophobic peptides due to its weaker eluting power in RPLC (cf. Chapter 6).

1.7 Plan of the thesis

In order to study the biochemical processes underlying pharmacological and medical events, a sensitive and selective analytical method is necessary. The miniaturisation of LC-MS allows detection of amol and even zmol LOD levels and seems to be the most promising technique to tackle these challenges. To achieve the high throughput and ease necessary in routine comparative proteomic studies, several limitations of nanoLC-MS need to be overcome. Systems must become even more sensitive, more selective, more reproducible, more robust, faster and easier to use. This thesis presents several studies in which various aspects and components of a nanoLC-MS system have been optimised, with the aim to overcome the limitations listed. In Chapter 2, the characterisation of the nanoESI interface we built is presented. Working toward quantitative analysis of low-level peptides using nanoLC-MS, it is necessary to know how a nanospray interface responds to changes in the mobile phase composition, spray voltage and morphology and position of the nanoESI emitter. The morphology of the nanospray tip - ID and geometry of the tip opening, the presence (or absence) of a conductive coating - was shown to influence the optimal working conditions and the resulting

spectra. Parameters such as tip diameter, flow rate, analyte concentration and solvent composition can all affect the observed ions and the charge states.
In Chapter 3, the state of the art in silica-based monolith synthesis, characterisation and application is presented, while in Chapter 4, the detailed evaluation of the performance of a new 50-μm-ID monolithic column and its application to peptide analysis is demonstrated. Traditionally, chromatographic stationary phases are prepared from naturally-occurring organic polymers (e.g. agarose) or silica. Silica beads are the most commonly used solid support materials in the LC-MS analysis of peptides. The smaller the silica beads, the higher the back-pressure. The larger the beads, the lower the separation efficiency and flow resistance. Moreover, highly porous beads have a higher capacity. Thus, the structure of the stationary phase will be of paramount importance to achieve efficient, rapid and sensitive separation. Much research has been focused on the synthesis of higher-performance chromatographic stationary phases. The latest advance in column technology was the synthesis of monolithic phases, first organic phases followed later by silica phases. A number of groups are working to prepare better monolithic columns and understand the underlying principles of their working.
In Chapter 5, a novel set-up allowing on-line albumin depletion and sample fractionation is presented. By increasing the efficiency, selectivity and loading capacity of an analytical system, multidimensional approaches increase the number of peptides that can be analysed in a complex sample. One of the many advantages offered by multidimensional chromatography is the possibility to deplete samples of high-abundance proteins (e.g. albumin).
In Chapter 6, a study of the repeatability issues in LC-MS is presented. Poor repeatability of peak areas is a problem frequently encountered in peptide analysis with nanoLC-MS. As a result, quantitative analysis is seriously hampered, unless the observed variability can be corrected for. Currently, labeling techniques or addition of internal standards are often applied to this end. However, these procedures are often elaborate and error prone, and do not always improve repeatability. The addition of salt (NaCl) did not improve peptide recovery [155] and is likely to result in the formation of adducts and/or ionisation suppression of the peptides. Surfactants were proven to minimise adsorption effects [143] and improve quantitation. However, surfactants interfere with MS detection and are not the most favourable solution to improve solubility in proteomics studies. Adding organic solvents [143, 154, 155] can greatly improved the solubility of hydrophobic peptides. Unfortunately, the presence of an organic solvent can interfere with RPLC separation. Therefore, selection of the organic solvents is important. We used dimethylsulfoxide (DMSO) to increase peptide solubility and thereby pep-

tide recovery (cf. Chapter 6). Depending on the peptide to be quantified, the optimal percentage of organic solvent varies.
Finally, in Chapter 7, an outlook for the further development of this nano-LC-MS platform will be provided.

References

[1] N. Tang, P. Tornatore, S. R. Weinberger; *Mass Spectrometry Reviews* **23**, 34 (2004)

[2] D. A. Colantonio, D. W. Chan; *Clinica Chimica Acta* **357**, 151 (2005)

[3] M. Cretich, F. Damin, G. Pirri, M. Chiari; *Biomolecular Engineering* **23**, 77 (2006)

[4] P. H. O' Farrell; *Journal of Biological Chemistry* **250**, 4007 (1975)

[5] S. P. Gygi, G. L. Corthals, Y. Zhang, Y. Rochon, R. Aebersold; *PNAS* **97**, 9390 (2000)

[6] B. Verzola, C. Gelfi, P. G. Righetti; *Journal of Chromatography A* **874**, 293 (2000)

[7] L. Castelletti, B. Verzola, C. Gelfi, A. Stoyanov, P. G. Righetti; *Journal of Chromatography A* **894**, 281 (2000)

[8] E. Olivieri, R. Sebastiano, A. Citterio, C. Gelfi, P. G. Righetti; *Journal of Chromatography A* **894**, 273 (2000)

[9] J. P. Larmann, A. V. Lemmo, A. W. Moore, J. W. Jorgenson; *Electrophoresis* **14**, 439 (1993)

[10] A. W. Moore, J. W. Jorgenson; *Analytical Chemistry* **67**, 3456 (1995)

[11] H. J. Issaq, K. C. Chan, G. M. Janini, G. M. Muschik; *Electrophoresis* **20**, 1533 (1999)

[12] P. G. Righetti, A. Castagna, B. Herbert, F. Reymond, J. S. Rossier; *Proteomics* **3**, 1397 (2003)

[13] J. P. C. Vissers; *Journal of Chromatography A* **856**, 117 (1999)

[14] H. D. Meiring, E. van der Heeft, G. J. ten Hove, A. P. J. M. de Jong; *Journal of Separation Sciences* **25**, 557 (2002)

[15] F. J. Yang; *Journal of Chromatography A* **236**, 265 (1982)

[16] E. Nagele, M. Vollmer, P. Horth; *Journal of Chromatography A* **1009**, 197 (2003)

[17] J. P. Chervet, M. Ursem, J. P. Salzmann; *Analytical Chemistry* **68**, 1507 (1996)

[18] T. Takeuchi, D. Ishii; *Journal of Chromatography A* **253**, 41 (1982)

[19] J. E. MacNair, G. J. Opiteck, J. W. Jorgenson, M. A. Moseley; *Rapid Communications in Mass Spectrometry* **11**, 1279 (1997)

[20] A. Ducret, N. Bartone, P. A. Haynes, A. Blanchard, R. Aebersold; *Analytical Biochemistry* **265**, 129 (1998)

[21] T. Le Bihan, D. Pinto, D. Figeys; *Analytical Chemistry* **73**, 1307 (2001)

[22] T. Takeuchi, T. Niwa, D. Ishii; *Journal of Chromatography A* **405**, 117 (1987)

[23] K. Deguchi, S. Ito, S. Yoshioka, I. Ogata, A. Takeda; *Analytical Chemistry* **76**, 1524 (2004)

[24] T. Natsume, Y. Yamauchi, H. Nakayama, T. Shinkawa, M. Yanagida, N. Takahashi, T. Isobe; *Analytical Chemistry* **74**, 4725 (2002)

[25] A. Cappiello, G. Famiglini, C. Fiorucci, F. Mangani, P. Palma, A. Siviero; *Analytical Chemistry* **75**, 1173 (2003)

[26] M. T. Davis, D. C. Stahl, T. D. Lee; *Journal of the American Society for Mass Spectrometry* **6**, 571 (1995)

[27] C. Ericson; *Electrochromatography and liquid chromatography: microtechniques, instrumentation and application*; Phd thesis; Uppsala University, (1999)

[28] K. Vanhoutte, W. Van Dongen, I. Hoes, F. Lemiere, E. L. Esmans, H. Van Onckelen, E. Van den Eeckhout, R. E. J. van Soest, A. J. Hudson; *Analytical Chemistry* **69**, 3161 (1997)

[29] A. T. Timperman, R. Aebersold; *Analytical Chemistry* **72**, 4115 (2000)

[30] K. J. Skogerboe, D. S. Hage, D. J. Anderson; *Analytical Chemistry* **65**, 416R (1993)

[31] Y. Shen, N. Tolic, C. Masselon, L. Pasa Tolic, D. G. Camp, K. K. Hixson, R. Zhao, G. A. Anderson, R. D. Smith; *Analytical Chemistry* **76**, 144 (2004)

[32] G. Mitulovic, M. Smoluch, J. P. Chervet, I. Steimacher, A. Kungl, K. Mechtler; *Analytical and Bioanalytical Chemistry* **376**, 946 (2003)

[33] L. Rieux, D. Lubda, H. A. G. Niederlander, E. Verpoorte, R. Bischoff; *Journal of Chromatography A* **1120**, 165 (2006)

[34] J. B. Fenn, M. Mann, C. K. Meng, S. F. Wong, C. M. Whitehouse; *Science* **246**, 64 (1989)

[35] M. Karas, F. Hillenkamp; *Analytical Chemistry* **60**, 2299 (1988)

[36] M. S. Wilm, M. Mann; *International Journal of Mass Spectrometry and Ion Processes* **136**, 167 (1994)

[37] A. P. Bruins; *Journal of Chromatography A* **794**, 345 (2002)

[38] M. S. Wilm, M. Mann; *Analytical Chemistry* **68**, 1 (1996)

[39] M. Karas, U. Bahr, T. Dulcks; *Fresenius Journal of Analytical Chemistry* **366**, 669 (2000)

[40] K. Vanhoutte, W. Van Dongen, E. L. Esmans; *Rapid Communications in Mass Spectrometry* **12**, 15 (1998)

[41] M. R. Emmett, R. M. Caprioli; *Journal of the American Society for Mass Spectrometry* **5**, 605 (1994)

[42] F. C. Leinweber, D. G. Schmid, D. Lubda, B. Sontheimer, G. Jung, U. Tallarek; *Journal of Mass Spectrometry* **39**, 223 (2004)

[43] T. Koerner, K. Turck, L. Brown, R. D. Oleschuk; *Analytical Chemistry* **76**, 6456 (2004)

[44] Y. Ishihama, J. Rappsilber, J. S. Andersen, M. Mann; *Journal of Chromatography A* **979**, 233 (2002)

[45] Y. Ishihama, H. Katayama, N. Asakawa, Y. Oda; *Rapid Communications in Mass Spectrometry* **16**, 913 (2002)

[46] K. W. Y. Fong, T. W. D. Chan; *Journal of the American Society for Mass Spectrometry* **10**, 72 (1999)

[47] G. A. Schultz, T. N. Corso, S. J. Prosser, S. Zhang; *Analytical Chemistry* **72**, 4058 (2000)

[48] C. H. Chiou, G. B. Lee, H. T. Hsu, P. W. Chen, P. C. Liao; *Sensors and Actuators B: Chemical* **86**, 280 (2002)

[49] J. S. Kim, D. R. Knapp; *Journal of the American Society for Mass Spectrometry* **12**, 463 (2001)

[50] N. Lion, J. O. Gellon, H. H. Girault; *Rapid Communications in Mass Spectrometry* **18**, 1614 (2004)

[51] H. Yin, K. Killeen, R. Brennen, D. Sobek, M. Werlich, T. van de Goor; *Analytical Chemistry* **77**, 527 (2005)

[52] Y. Yang, J. Kameoka, T. Wachs, J. D. Henion, H. G. Craighead; *Analytical Chemistry* **76**, 2568 (2004)

[53] M. Svedberg, A. Pettersson, S. Nilsson, J. Bergquist, L. Nyholm, F. Nikolajeff, K. E. Markides; *Analytical Chemistry* **75**, 3934 (2003)

[54] K. Tang, Y. Liu, D. W. Matson, T. Kim, R. D. Smith; *Analytical Chemistry* **73**, 1658 (2001)

[55] A. Muck, A. Svatos; *Rapid Communications in Mass Spectrometry* **18**, 1459 (2004)

[56] J. F. Kelly, L. Ramaley, P. Thibault; *Analytical Chemistry* **69**, 51 (1997)

[57] M. Mazereeuw, A. J. P. Hofte, U. R. Tjaden, J. van der Greef; *Rapid Communications in Mass Spectrometry* **11**, 981 (1997)

[58] M. S. Kriger, K. D. Cook, R. S. Ramsey; *Analytical Chemistry* **67**, 385 (1995)

[59] M. Wetterhall, O. Klett, K. E. Markides, L. Nyholm, J. Bergquist; *The Analyst* **128**, 728 (2003)

[60] S. Nilsson, M. Wetterhall, J. Bergquist, L. Nyholm, K. E. Markides; *Rapid Communications in Mass Spectrometry* **15**, 1997 (2001)

[61] M. Wetterhall, S. Nilsson, K. E. Markides, J. Bergquist; *Analytical Chemistry* **74**, 239 (2002)

[62] E. P. MaziarzIii, S. A. Lorenz, T. P. White, T. D. Wood; *Journal of the American Society for Mass Spectrometry* **11**, 659 (2000)

[63] A. Schmidt, M. Karas, T. Dulcks; *Journal of the American Society for Mass Spectrometry* **14**, 492 (2003)

[64] R. Juraschek, T. Dulcks, M. Karas; *Journal of the American Society for Mass Spectrometry* **10**, 300 (1999)

[65] R. Juraschek, F. W. Rollgen; *International Journal of Mass Spectrometry* **177**, 1 (1998)

[66] Y. Li, R. B. Cole; *Analytical Chemistry* **75**, 5739 (2003)

[67] J. E. MacNair, K. D. Patel, J. W. Jorgenson; *Analytical Chemistry* **71**, 700 (1999)

[68] M. Leonard; *Journal of Chromatography B: Biomedical Sciences and Applications* **699**, 3 (1997)

[69] I. Halasz, R. Endele, J. Asshauer; *Journal of Chromatography A* **112**, 37 (1975)

[70] J. E. MacNair, K. C. Lewis, J. W. Jorgenson; *Analytical Chemistry* **69**, 983 (1997)

[71] I. D. Wilson, J. K. Nicholson, J. Castro-Perez, J. H. Granger, K. A. Johnson, B. W. Smith, R. S. Plumb; *Journal of Proteome Research* (2005)

[72] J. W. Jorgenson, E. J. Guthrie; *Journal of Chromatography A* **255**, 335 (1983)

[73] T. Tsuda, K. Tsuboi, G. Nakagawa; *Journal of Chromatography A* **214**, 283 (1981)

[74] T. Tsuda, K. Hibi, T. Nakanishi, T. Takeuchi, D. Ishii; *Journal of Chromatography* **158**, 227 (1978)

[75] K. K. Unger, O. Jilge, J. N. Kinkel, M. T. W. Hearn; *Journal of Chromatography A* **359**, 61 (1986)

[76] N. B. Afeyan, N. F. Gordon, I. Mazsaroff, L. Varady, S. P. Fulton, S. B. Yang, F. E. Regnier; *Journal of Chromatography A* **519**, 1 (1990)

[77] A. I. Liapis, Y. Xu, O. K. Crosser, A. Tongta; *Journal of Chromatography A* **702**, 45 (1995)

[78] T. N. M. Bernards; *Silicate sol-gel chemistry as studied by hydrolysis-gelation time curves*; Phd thesis; Utrecht University, (1997)

[79] D. C. Hoth, J. G. Rivera, L. A. Colon; *Journal of Chromatography A* **1079**, 392 (2005)

[80] J. Randon, S. Huguet, A. Piram, G. Puy, C. Demesmay, J. L. Rocca; *Journal of Chromatography A* **1109**, 19 (2006)

[81] C. Liang, S. Dai, G. Guiochon; *Analytical Chemistry* **75**, 4904 (2003)

[82] X. Geng, F. E. Regnier; *Journal of Chromatography* **296**, 15 (1984)

[83] M. I. Aguilar, D. J. Clayton, P. Holt, V. Kronina, R. I. Boysen, A. W. Purcell, M. T. W. Hearn; *Analytical Chemistry* **70**, 5010 (1998)

[84] J. G. Dorsey, J. P. Foley, W. T. Cooper, R. A. Barford, H. G. Barth; *Analytical Chemistry* **62**, 324R (1990)

[85] W. R. Melander, Z. El Rassi, C. Horvath; *Journal of Chromatography A* **469**, 3 (1989)

[86] Y. Shen, X. Shao, K. Neill, J. S. Bradshaw, M. L. Lee; *Journal of Chromatography A* **866**, 1 (2000)

[87] S. Miyazaki, M. Y. Miah, K. Morisato, Y. Shintani, T. Kuroba, K. Nakanishi; *Journal of Separation Science* **28**, 39 (2005)

[88] S. Miyazaki, K. Morisato, N. Ishizuka, H. Minakuchi, Y. Shintani, M. Furuno, K. Nakanishi; *Journal of Chromatography A* **1043**, 19 (2004)

[89] Z. G. Shi, Y. Q. Feng, L. Xu, M. Zhang, S. L. Da; *Talanta* **63**, 593 (2004)

[90] T. Ikegami, T. Hara, H. Kimura, H. Kobayashi, K. Hosoya, K. Cabrera, N. Tanaka; *Journal of Chromatography A* **1106**, 112 (2006)

[91] M. Gilar, P. Olivova, A. E. Daly, J. C. Gebler; *Analytical Chemistry* **77**, 6426 (2005)

[92] N. Tanaka, H. Goodell, B. L. Karger; *Journal of Chromatography* **158**, 233 (1978)

[93] Y. Wagner, A. Sickmann, H. E. Meyer, G. Daum; *Journal of the American Society for Mass Spectrometry* **14**, 1003 (2003)

[94] M. P. Washburn, D. A. Wolters, J. R. Yates III; *Nature Biotechnology* **19**, 242 (2001)

[95] A. J. Alpert, P. C. Andrews; *Journal of Chromatography A* **443**, 85 (1988)

[96] S. Gu, Y. Du, J. Chen, Z. Liu, E. M. Bradbury, C. A. A. Hu, X. Chen; *Journal of Proteome Research* **3**, 1191 (2004)

[97] D. A. Wolters, M. P. Washburn, J. R. Yates III; *Analytical Chemistry* **73**, 5683 (2001)

[98] J. R. Freije, R. Bischoff; *Drug Discovery Today: Technologies* **3**, 5 (2006)

[99] D. S. Hage, M. A. Nelson; *Analytical Chemistry* **73**, 199A (2001)

[100] G. A. Michaud, M. Salcius, F. Zhou, R. Bangham, J. Bonin, H. Guo, M. Snyder, P. F. Predki, B. I. Schweitzer; *Nature Biotechnology* **21**, 1509 (2003)

[101] N. I. Govorukhina, A. Keizer-Gunnink, A. G. J. van der Zee, S. de Jong, H. W. A. de Bruijn, R. Bischoff; *Journal of Chromatography A* **1009**, 171 (2003)

[102] M. Helman, D. Givol; *Biochemical Journal* **125**, 971 (1971)

[103] X. Zhan, D. M. Desiderio; *International Journal of Mass Spectrometry* **In Press, Corrected Proof**

[104] L. A. MacMillan-Crow, J. A. Thompson; *Methods in Enzymology* **301**, 135 (1999)

[105] V. Gaberc-Porekar, V. Menart; *Journal of Biochemical and Biophysical Methods* **49**, 335 (2001)

[106] V. Gupta, A. N. S. Eshwari, A. K. Panda, G. P. Agarwal; *Journal of Chromatography A* **998**, 93 (2003)

[107] S. B. Ficarro, M. L. McCleland, P. T. Stukenberg, D. J. Burke, M. M. Ross, J. Shabanowitz, D. F. Hunt, F. M. White; *Nature Biotechnology* **20**, 301 (2002)

[108] L. Andersson, J. Porath; *Analytical Biochemistry* **154**, 250 (1986)

[109] H. Michel, D. F. Hunt, J. Shabanowitz, J. Bennett; *Journal of Biological Chemistry* **263**, 1123 (1988)

[110] L. Riggs, E. H. Seeley, F. E. Regnier; *Journal of Chromatography B* **817**, 89 (2005)

[111] F. Wolschin, S. Wienkoop, W. Weckwerth; *Proteomics* **5**, 4389 (2005)

[112] H. K. Kweon, K. Hakansson; *Analytical Chemistry* **78**, 1743 (2006)

[113] M. W. H. Pinkse, P. M. Uitto, M. J. Hilhorst, B. Ooms, A. J. R. Heck; *Analytical Chemistry* **76**, 3935 (2004)

[114] Z. Yang, W. S. Hancock; *Journal of Chromatography A* **1053**, 79 (2004)

[115] V. P. Bhavanandan, A. W. Katlic; *Journal of Biological Chemistry* **254**, 4000 (1979)

[116] J. T. Gallagher, A. Morris, T. M. Dexter; *The Biochemical Journal* **231**, 115 (1985)

[117] F. T. Saulsbury; *The Journal Of Rheumatology* **24**, 2246 (1997)

[118] L. Xiong, F. E. Regnier; *Journal of Chromatography B* **782**, 405 (2002)

[119] L. Xiong, D. Andrews, F. E. Regnier; *Journal of Proteome Research* **2**, 618 (2003)

[120] R. Qiu, F. E. Regnier; *Analytical Chemistry* **77**, 2802 (2005)

[121] N. L. Anderson, N. G. Anderson; *Molecular and Cellular Proteomics* **1**, 845 (2002)

[122] N. Ahmed, G. E. Rice; *Journal of Chromatography B* **815**, 39 (2005)

[123] J. Oh, J. H. Pyo, E. H. Jo, S. I. Hwang, S. C. Kang, J. H. Jung, E. K. Park, S. Y. Kim, J. Y. Choi, J. Lim; *Proteomics* **4**, 3485 (2004)

[124] E. Gianazza, P. Arnaud; *Biochemical Journal* **201**, 129 (1982)

[125] B. Akerstrom, T. Brodin, K. Reis, L. Bjorck; *Journal of Immunology* **135**, 2589 (1985)

[126] B. Akerstrom, L. Bjorck; *Journal of Biological Chemistry* **261**, 10240 (1986)

[127] T. C. Pinkerton, K. A. Koeplinger; *Journal of Chromatography A* **458**, 129 (1988)

[128] C. A. J. Hajee, H. A. van Rhijn, J. J. P. Lasaroms, H. J. Keukens, J. de Jong; *Analyst* **126**, 1332 (2001)

[129] M. Careri, A. Mangia; *Journal of Chromatography A* **1000**, 609 (2003)

[130] M. Quadroni, P. James; *electrophoresis* **20**, 664 (1999)

[131] N. Lundell, T. Schreitmuller; *analytical biochemistry* **266**, 31 (1999)

[132] S. Ekstrom, P. Onnerfjord, L. Nilsson, M. Bengtsson, T. Laurell, G. Marko-Varga; *Analytical Chemistry* **72**, 286 (2000)

[133] G. Marie, L. Serani, O. Laprevote; *Analytical Chemistry* **72**, 5423 (2000)

[134] C. Wang, R. Oleschuk, F. Ouchen, J. Li, P. Thibault, D. J. Harrison; *Rapid Communications in Mass Spectrometry* **14**, 1377 (2000)

[135] A. Doucette, D. Craft, L. Li; *Journal of the American Society for Mass Spectrometry* **14**, 203 (2003)

[136] R. K. Blackburn, R. J. Anderegg; *Journal of the American Society for Mass Spectrometry* **8**, 483 (1997)

[137] D. S. Peterson, T. Rohr, F. Svec, J. M. J. Frechet; *Journal of Proteome Research* **1**, 563 (2002)

[138] A. K. Palm, M. V. Novotny; *Rapid Communications in Mass Spectrometry* **18**, 1374 (2004)

[139] D. Craft, A. Doucette, L. Li; *Journal of Proteome Research* **1**, 537 (2002)

[140] J. R. Freije, P. P. Mulder, W. Werkman, L. Rieux, H. A. Niederlander, E. Verpoorte, R. Bischoff; *Journal of Proteome Research* **4**, 1805 (2005)

[141] M. K. Lawless, S. Hopkins, M. K. Anwer; *Journal of Chromatography B: Biomedical Sciences and Applications* **707**, 213 (1998)

[142] C. S. Yang, S. T. Chou, L. Liu, P. J. Tsai, J. S. Kuo; *Journal of Chromatography B: Biomedical Sciences and Applications* **674**, 23 (1995)

[143] J. Carstens, K. T. Jensen, P. Ivarsen, L. M. Rasmussen, E. B. Pedersen; *Clinical Chemistry* **43**, 638 (1997)

[144] K. Nostelbacher, M. Kirchgessner, G. I. Stangl; *Journal of Chromatography B: Biomedical Sciences and Applications* **744**, 273 (2000)

[145] W. Melander, C. Horvath; *Archives of Biochemistry and Biophysics* **183**, 200 (1977)

[146] L. Jiang, L. He, M. Fountoulakis; *Journal of Chromatography A* **1023**, 317 (2004)

[147] R. Wolf, T. Hoffmann, F. Rosche, H. U. Demuth; *Journal of Chromatography B* **803**, 91 (2004)

[148] R. Wolf, F. Rosche, T. Hoffmann, H. U. Demuth; *Journal of Chromatography A* **926**, 21 (2001)

[149] F. Hilbrig, R. Freitag; *Journal of Chromatography B* **790**, 79 (2003)

[150] S. Law, C. Shih; *Drug Development and Industrial Pharmacy* **25**, 253 (1999)

[151] K. H. Song, H. M. An, H. J. Kim, S. H. Ahn, S. J. Chung, C. K. Shim; *Journal of Chromatography B* **775**, 247 (2002)

[152] P. Hyenstrand, J. S. Metcalf, K. A. Beattie, G. A. Codd; *Toxicon* **39**, 589 (2001)

[153] P. Hyenstrand, J. S. Metcalf, K. A. Beattie, G. A. Codd; *Water Research* **35**, 3508 (2001)

[154] M. R. Duncan, J. M. Lee, M. P. Warchol; *International Journal of Pharmaceutics* **120**, 179 (1995)

[155] H. Grohganz, M. Rischer, M. Brandl; *European Journal of Pharmaceutical Sciences* **21**, 191 (2004)

[156] H. Grohganz, O. Schlafli, M. Rischer, M. Brandl; *Journal of Pharmaceutical and Biomedical Analysis* **34**, 963 (2004)

CHAPTER 2

Characterisation of a nanoelectrospray interface

2.1 Introduction

Nanoelectrospray (nanoESI) was developed by Wilm and Mann [1,2]. Though nanoESI first referred to an off-line application, the need for very sensitive analysis in proteomics led to the coupling of nanoliquid chromatography (nanoLC) to MS using nanoESI. In nanoESI, the spray voltage can be applied on a conductive layer on the outside of the emitter [2,3] or directly to the liquid to be sprayed [4–6]. Both set-ups present advantages and drawbacks. The metal coatings used as conductive layer deteriorate following corona discharge [7]. Moreover, they adhere poorly to silica and often show limited lifetime [8]. When applying the voltage directly to the liquid to be sprayed in a so-called "liquid-junction" set-up, non-coated silica emitters are used [4–6]. The emitters used in liquid-junction interfacing are easier and cheaper to prepare. However, they require a higher voltage to produce a stable spray than coated needles, due to the significant voltage drop through the solvent, due to solvent resistance. The different means to apply voltage to the sample solvent are likely to influence the quality of the spray and the resulting spectra. Additionally, eluent flow rate and composition, as well as the internal diameter of the nanoESI tip, influence the stability of the spray [9] and its morphology [10]. It was found that, at certain solvent compositions, signal intensity drops dramatically. Such a decrease is likely to happen at various mobile phase

compositions in nanoLC-ESI-MS as well. The use of tapered gold-coated tips ensures efficient ionisation over a much wider range of mobile phase composition [3]. At very low flow rates (<50 nL/min), ionisation suppression is greatly reduced compared to that at higher flow rates [11]. Emitters with a tapered end of smaller ID and thinner walls gave the best results in terms of sensitivity and stability at such low flow rates. A reduction in flow rate was found to be concomitant with a decrease in the optimal spray voltage [12]. With respect to the resulting spectra, parameters such as tip diameter, flow rate, analyte concentration and solvent composition can all affect the ions observed and their relative intensity [13]. In addition, positioning of the nanoESI tips, the type of emitters and their dimension are also of importance. Consequently, in order to characterise a nanoESI interface for proteomic analysis, it is necessary to investigate the impact of varying the aforementioned parameters on the spray and the spectra. In this study, our home-built nanoESI interface was characterised in order to allow selection of optimal experimental conditions for further developments of the nanoLC-MS-based platform.

2.2 Materials and methods

2.2.1 Materials

Formic acid (98-100% pure) was purchased from Merck KGaA (Darmstadt, Germany) and acetonitrile (HPLC Supra-Gradient grade) from Biosolve B.V. (Valkenswaard, The Netherlands). Bovine insulin ($\geq$ 27 USP units per mg) was obtained from Sigma Aldrich (Zwijndrecht, The Netherlands), SSI stainless steel (SS) union (1/16" tubing OD, 0.015" bore), 1/16" SS nuts and 1/16" SS ferrules and 1/16" PEEK tubing (0.02" ID) from Supelco (Zwijndrecht, The Netherlands). PEEK microCross (38 nL dead volume) and microtight PEEK tubing sleeves (395 μm ID) were purchased from Upchurch. Fused-silica capillaries (100 μm ID, 360 μm OD) were from Composite Metal Service (Ilkley, UK), and tapered fused-silica nanospray needles (360 μm OD, 75, 50 or 20 μm ID and tapered to 15, 8 or 5 μm ID, respectively) from New Objectives (Woburn, MA, USA). Nanospray (nanoESI) needles (also referred to as tip, spray tip, or emitter) were either platinum-coated at the tapered or distal end, or uncoated. To differentiate between the three kinds of nanoESI needles, we will refer to them as fully-coated for the tapered-end platinum-coated needle, distal-coated for the distal-end platinum-coated emitter, and bare-silica for the non-coated spray tip. When referring to a nanoESI tip by its ID, the ID will be the one at the tapered end of the emitter (i.e. 15, 8 or 5 μm

ID. Nanotips may require "opening" by gently tapping the tapered end of the tip against the end plate of the MS [2]. Their ID at the tapered end was thus larger than specified by the company.

2.2.2 Sample preparation

Solutions of 600 nM bovine insulin (BI) were prepared by sequential dilution in solvent containing water, acetonitrile (ACN) and formic acid (FA). The amount of water, ACN and FA in the solvent were varied in accordance with the parameter that was investigated (i.e. %ACN, pH). The solvent composition is explicitly given in the relevant parts of the "Results and Discussion" section.

2.2.3 Set-up

Different means of connecting a transfer capillary or a liquid chromatography column to a nanoESI emitter were investigated (Fig. 2.1). The different nanoESI interfaces were mounted on a home-built micrometric table placed in front of an LCQ ion trap MS (Thermo Electron, Breda, The Netherlands). The micrometric table allowed the accurate positioning of the nanoESI tip with respect to the inlet of the MS, which is in the center of the MS heated capillary. Electrical contact was made by applying the high voltage on the outside of a platinum-coated nanoESI tip (cf. scheme D Fig. 2.1) or directly to the liquid to be sprayed (cf. schemes A,B & C, Fig. 2.1), in which case the interface is referred to as a "liquid junction". Most experiments described here were performed using the set-up shown in schemes A and B with a bare-silica needle, unless otherwise stated.
Different parameters are likely to influence the quality of the spray and the spectra. These include spray voltage, distance between nanospray tip and MS inlet, mobile phase composition (% organic modifier and acid), dimensions of nanospray tips and possible coating.
The coordinates of the nanospray tip were varied so as to investigate the impact of the distance between the nanoESI tip and the MS on the MS signal. For every set of coordinates, a stable spray was obtained by adjusting the spray voltage, and spectra were recorded for 1 min. The spectra were averaged over the whole sampling period (1 min). The intensity and signal-to-noise ratio (S/N) of the resulting spectra were used to compare the influence of the parameters investigated in this study. In the following paragraphs, S/N refers to the intensity of the MS signal with respect to the spectral noise. S/N in the spectral domain is important for the discovery of biomarkers by nanoESI-MS. The S/N in the time domain will

be of greater importance than the S/N in the spectral domain for monitoring of peptides, though the former is influenced by the latter.

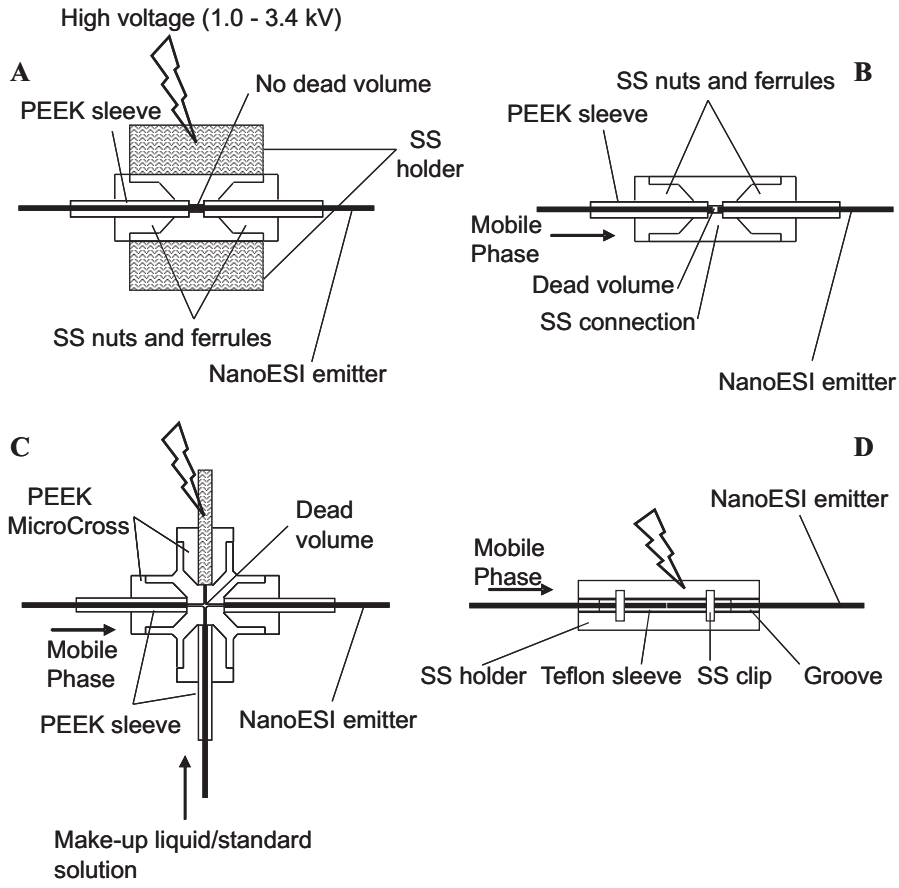

Figure 2.1: Different means of connecting a transfer capillary or a nanoLC column to nanoESI tips. A and B are views of a "liquid junction"-type connection making use of an SSI stainless steel union (1/16" tubing O.D., 0.015" bore). High voltages were directly applied to the stainless steel connection. In C, electrical contact is also made through a "liquid junction" within the PEEK microcross (38 nL dead volume). The microcross allowed the addition of a make-up liquid or of a standard solution. In D, ionisation is achieved by applying the high voltage on the outside of a fully-coated nanoESI tip. The capillary or nanoLC column is butt-connected to the nanoESI tip using a Teflon sleeve ensuring minimal dead volumes.

The procedure was the same for every parameter that was studied (angle of the nanospray tip with the MS heated capillary, mobile phase composition,

dimensions of nanospray tips and type of coating if present). Since the aim of this study was to gain a better understanding of the nanoLC-MS interface and the optimal conditions under which it should be used and not to acquire analytical data per se, experiments were not replicated.

2.2.4 MS settings

Optimisation of the MS transmission parameters (capillary voltage, tube lens offset, voltage on the octapoles and the interoctapole lens) was performed using the pneumatically-assisted electrospray interface and software provided with the LCQ ion trap MS (Thermo Electron, Breda, The Netherlands). A solution of 6 μM BI in 0.1% FA in water:ACN (1:1) was infused through the ESI interface at 5 μL/min. The ion-transmission parameters are independent of the flow rate used during tuning of the MS, but are characteristic of an analyte. Later tuning/control of the MS settings was performed using a 600 nM solution of BI in 0.1% FA in water:ACN (1:1) infused through the home-built nanoESI interface at 200 nL/min. Tuning of the different transmission parameters was done by varying the parameters manually and subsequent visual inspection of the resulting MS spectra. The optimum parameters are summarised in Table 2.1. Clear protein spectra with little spectral noise could be obtained using the MS settings shown in this table. The high value found for the optimal capillary voltage for analysis of BI is likely to result in in-source fragmentation in the case of peptide analysis, and could prove detrimental to sensitivity and reproducibility [14, 15]. For the mass spectrometric analysis of substance P, a neuropeptide of importance in many brain pathologies, even the lowest capillary voltages resulted in in-source fragmentation (data not shown). Regular tuning is necessary in order to preserve good sensitivity. Moreover, the optimal MS settings should be investigated whenever analysing a new compound [16].

Heated capillary voltage	>0 V
Tube lens offset	15 to 50 V
2nd octapole	-4.5 to -9.0 V
1st octapole	-3.0 to -4.5 V
Interoctapole lens	-15 to -40 V

Table 2.1: Summary of the optimum transmission parameters for bovine insulin. Clear protein spectra with little spectral noise could be obtained using these MS settings.

2.3 Results & Discussion

2.3.1 Angle of the nanotip with respect to the position of the heated capillary

Positioning the nanoESI tip at an angle with respect to the longitudinal axis of the heated capillary is a generally accepted approach to improve the S/N ratio by decreasing the number of neutral species entering the MS. Alternatively, nanoESI interfaces can be positioned on-axis and very close to the MS inlet to transfer as much as possible of the sample into the MS in order to reach a lower limit of detection (LOD).
To this end, a 600 nM solution of BI in H2O:ACN:FA (70:30:0.1) was infused through an 8-μm-ID uncoated nanospray tip at a flow rate of 200 nL/min using a 250-μL Hamilton syringe and the syringe pump of the LCQ MS. The tip was either in line or at a 20˚angle with respect to the heated capillary.
The coordinates of the nanospray tip were varied so as to investigate the impact of the distance between the nanoESI tip and the MS on the MS signal. Over the whole set of coordinates, the spray voltage was set between 1.0 and 3.4 kV. The further the tip was positioned from the heated capillary, the larger the voltage required to obtain a stable spray. The electric field followed the same trend though it quickly levelled off with distance (Fig. 2.2). The optimal spray voltages appear to be larger when the nanospray tip was at a 20˚angle with the heated capillary than when it was positioned on-axis. It was necessary to "open" nanotips by gently tapping the tapered end of the tip against the end plate of the MS [2]. A simple explanation might therefore be that this operation has led to different geometrical characteristics of the tips and resulted in the observed differences in spray voltage. However, this would need to be confirmed with further experiments.
Though positioning the interface on-axis gave higher intensities for both BI^{5+} and BI^{4+}, operating the interface at an angle seems to result in larger S/N values. When the tip was positioned on-axis and very close to the MS inlet, the sample was sprayed directly into the MS inlet, which would explain the larger intensities. However, when the nanospray tip was positioned further away from the heated capillary, the diameter of the spray was too large for all the ions to enter the MS. Therefore, the increase in signal intensity when the tip was positioned further away from the MS inlet probably resulted from more efficient ion evaporation. Chemical noise results from collisions of charged analytes with neutral species in the MS. When the tip was positioned at an angle, fewer neutral species could enter the MS, which resulted in lower chemical noise and thus larger S/N.

Concluding, positioning the nanospray tip at a 20˚angle with respect to the heated capillary is favourable in obtaining spectra with a low background level, i.e. when screening samples for novel biomarkers. However, when monitoring known species, the interface should be positioned axially to achieve maximal intensity for a single m/z and thereby sensitivity.

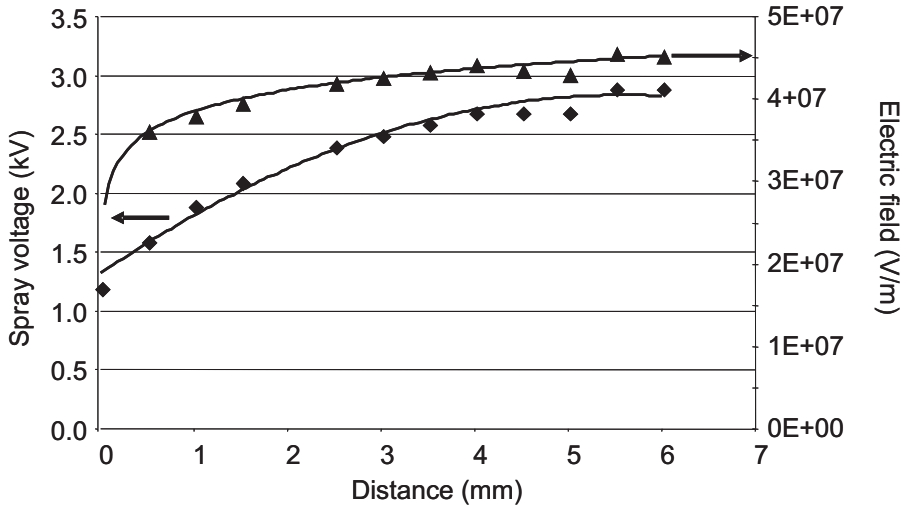

Figure 2.2: Variation of the optimal spray voltage (diamonds) and electric field (triangles) with the distance at which the nanoESI tip was positioned. A 600 nM solution of BI in H2O:ACN:FA (70:30:0.1) was infused through an 8-μm ID uncoated nanospray tip at a flow rate of 200 nL/min using a 250-μL Hamilton syringe and the syringe pump of the LCQ MS. The tip was positioned at a 20˚angle with respect to the MS heated capillary. The lines indicate the general trend for the variation of the spray voltage and the electric field.

2.3.2 Impact of the percentage acetonitrile (ACN)

To study the impact of an organic modifier on signal intensity, two solutions of 600 nM BI were prepared in H2O:ACN:FA with two different ratios. The percentage FA was fixed at 0.1%, but the percentage ACN was set at either 30 or 60 % (H_2O at either 70 or 40%). Both solutions were infused through an uncoated 8-μm-ID nanoESI emitter at 200 nL/min using a syringe pump. Optimal spray voltages were much lower for the 60% ACN solution (0.9-1.2 kV) than for the 30% ACN solution (1.2-3.4 kV).

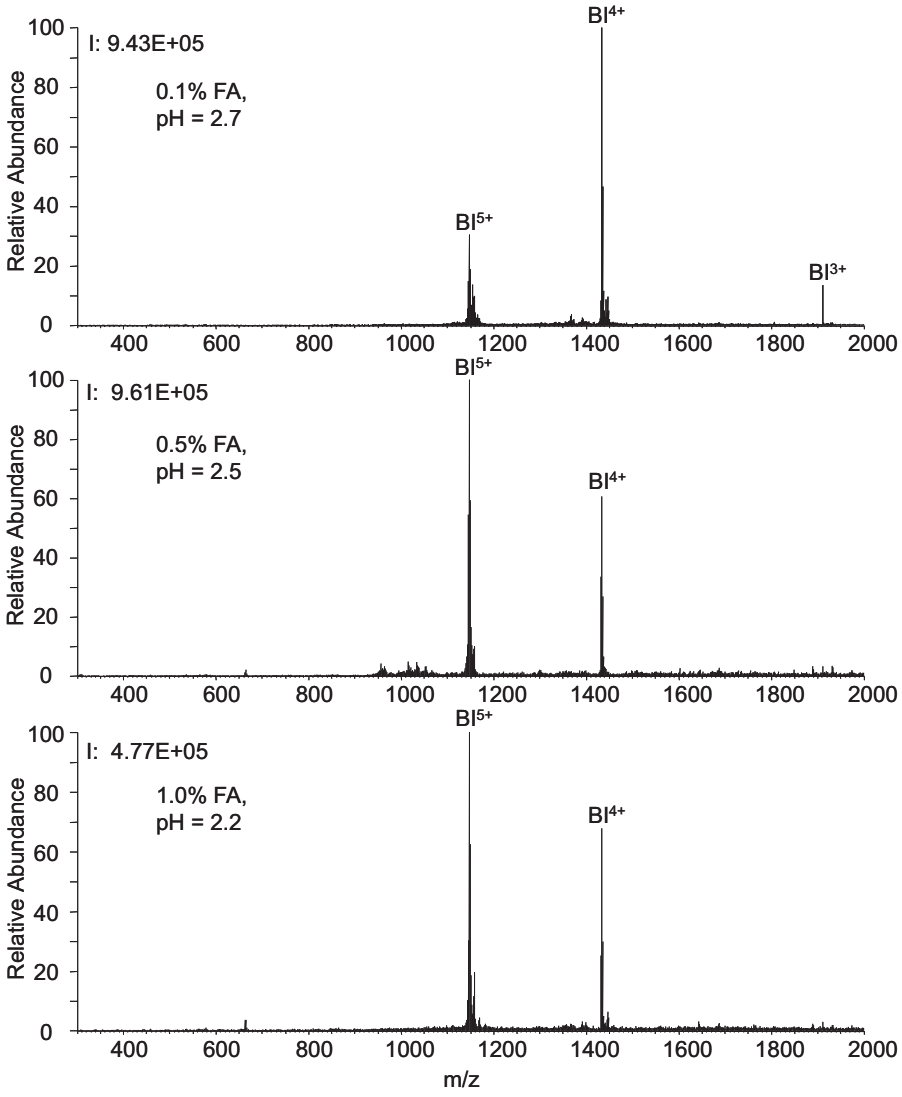

Figure 2.3: Influence of the concentration in FA in the sample solvent on the spectra. Top: 0.1% FA. Middle: 0.5% FA. Bottom: 1.0% FA. All three solutions contained 600 nM BI and were prepared using solvents containing 40% water and 60% ACN. The sample solutions were infused through a non-coated 8-μm-ID nanoESI tip (at a 20˚angle with respect to the MS heated capillary) at 200 nL/min using a 250-μL Hamilton syringe and the syringe pump of the LCQ MS.

The lower surface tension and easier evaporation of the solvent containing

60% ACN are responsible for the much lower spray voltages necessary to obtain a stable spray as compared to the solvent containing 30% ACN. When infusing solutions with little ACN, the spray voltage must be carefully adjusted in order to obtain a stable signal. Spray voltages which are too low result in the solvent sputtering from the nanospray emitter [10]. Spray voltages which are too high, on the other hand, cause the spray geometry to change [10] or induce arcing [7].

In contrast to a solvent containing little ACN, solvents containing a large percentage of organic modifier allow the spray voltage to be set at a much broader range of values while retaining a stable spray and a good S/N. It has been reported that the addition of glycerol and m-nitrobenzyl alcohol to the analyte solutions to be sprayed dramatically increased both the maximum charge state and the signal intensity of the proteins observed [17]. In our study, the amount of ACN did not have any bearing on the charge state, as no significant difference was observed between the intensity ratio for BI^{4+} and BI^{5+} obtained with either 30 or 60% ACN. However, when the sample solution was prepared in 10% ACN (cf. Fig. 2.4 in paragraph 2.3.4), the BI^{6+} ion was also observed, whereas it was not visible at an ACN percentage of 30 and 60%. Probably one of the six nitrogen atoms of BI that are likely to be protonated must have been shielded from the protons of the surrounding solvent, either because of the forced folding of BI or aggregation at higher % ACN.

2.3.3 Influence of the formic acid concentration

Varying the pH (through a change in the FA concentration) is a common approach to improve chromatographic efficiency or to vary the selectivity of a chromatographic column. In addition, a change in pH will affect ionisation and therefore the charge state distribution. Sensitivity might also be affected by changes in pH. It is therefore necessary to find the optimum FA concentration. To study the effect of pH on the MS signal, three solutions containing 600 nM BI were prepared using solvents containing 40% water, 60% ACN and concentrations of FA of 0.1, 0.5 and 1.0 %. The resulting pHs are 2.7, 2.5 and 2.2 respectively. The sample solutions were infused through an uncoated 8-μm-ID nanoESI tip at 200 nL/min. At 0.1 % FA, three distinct charge states of BI are observed, namely triply, quadruply and quintuply charged. At 0.5 and 1.0 % FA, only BI^{4+} and BI^{5+} are observed (Fig. 2.3). However, signal intensity decreased strongly with 1.0 % FA in the mobile phase while, at 0.5 % FA, it was comparable to that obtained at 0.1 % FA. BI^{4+} was most intense at low % FA when the tip was positioned close to the MS. At high % FA, the position at which BI^{4+} was most

intense was further away from the MS inlet.

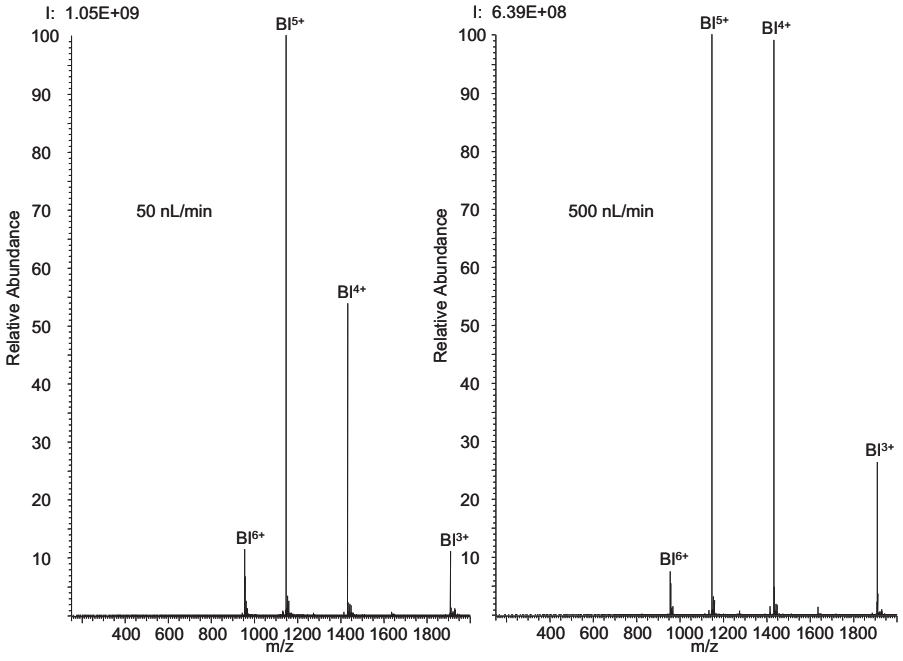

Figure 2.4: Effect of varying the flow rate on the resulting spectrum. Left: 50 nL/min. Right: 500 nL/min. A 6-μM solution of BI in H2O:ACN:FA (90:10:0.1) was infused through a 15-μm-ID uncoated nanospray tip positioned axially with the MS heated capillary. The flow was generated using a 250-μL Hamilton syringe and the syringe pump of the LCQ MS.

The shift of the charge envelop towards lower m/z likely resulted from the higher proton concentration in the solution. As already observed, the use of more acidic conditions led to an increase in the average charge for a range of peptides and proteins [13]. Interestingly though, no BI^{6+} was observed, even when the sample solution was prepared in 1% FA, whereas it was visible when applying a lower organic modifier concentration (10% ACN) at only 0.1% FA (Fig. 2.4). The charge distribution over a smaller number of ions and the large signal intensity at 0.5% FA might be an advantage for sensitive monitoring of the elution of BI. The decrease in signal intensity observed at 1%FA is likely to be due to ion-pairing effects between BI and FA or to an increase in the surface tension of the mobile phase as has been suggested for trifluoroacetic acid [18].

However, the opposite has been reported as well [19]. From a practical point of view, cases where an increase in FA concentration would be necessary are limited as a result of problems in obtaining a stable spray. Whereas the nanospray tip can be positioned rather freely at low FA concentrations, a stable spray at a high FA concentration could only be obtained at a few coordinates. Therefore, positioning the spray tip and obtaining a stable spray at high FA concentrations requires much care and attention, and is not recommended.

2.3.4 Impact of the flow rate

Eluent flow rate was shown to influence the stability of the spray [9] and its morphology [10]. Moreover, the average charge state of the analytes also varies as a result of changing the flow rate: the lower the flow rate, the higher the charge state [13]. Therefore, the influence of varying the flow rate on spectral intensity, as well as on the shape of the charge envelop for BI, was assessed using an 8- and a 15-μm-ID uncoated nanoESI tip. Tips were installed on the nanointerface at a 20˚angle with respect to the heated capillary while infusing a solution of 6M BI in H2O:ACN:FA (90:10:0.1). Flow rates were varied between 50 and 300 nL/min for the 8-μm-ID nanoESI emitter and between 50 and 500 nL/min for the 15-μm-ID tip.
Larger flow rates required larger spray voltages (1.7-2.4 kV for the 15-μm-ID tip) to obtain a stable spray, as has previously been reported [12]. The 15-μm-ID tip was most sensitive at 100 nL/min. Signal intensity was a little lower though very stable at higher flow rates. The smaller-ID tip exhibited maximum performances at 50 nL/min and performed similarly to the 15-μm-ID tip at higher flow rates. The flow rates studied were not sufficiently high to see a clear advantage in using larger-ID nanoESI tips. As has already been reported [13], the charge envelop shifted toward lower m/z at lower flow rates. The ratio of intensities between BI^{6+} and BI^{3+} on one hand and between BI^{5+} and BI^{4+} varied respectively from 0.5 to 1 and from 1 to 2 when the flow was lowered from 500 down to 50 nL/min (Fig2.4). Using tips with a smaller ID (i.e. 5 μm) resulted in a greater shift in the envelop toward high charges and more intense MS signal as a consequence of the greater electric field strength and the resulting more efficient protonation of the analytes. Therefore, 5-μm nanoESI tips were used in the experiments dealing with coupling a 50-μm-ID packed column with MS (cf. Chapter 5).

2.3.5 Bare-silica, distal-coated & fully-coated nanotips

Nanospray emitters are generally uncoated or gold-coated. The simple metal-liquid junction used in conjunction with uncoated nanoESI tips is expected to conduct current efficiently from the point where the potential is applied up to the opening of the nanotip. Unfortunately though, there is a voltage drop along the tip, due to eluent resistance. This voltage drop justified the development of coated needles. However, gold does not adhere well to fused-silica capillaries and tends to peel off quickly. An alternative was developed by New Objective, based on a proprietary multi-layer platinum coating. The coating was either applied at the distal end of the nanotip or on the complete emitter. Bare-silica emitters were compared to coated nanoESI tips. The influence of every type of coating on the spray voltage required to obtain a stable spray and on the spectra was assessed using an 8-μm-ID nanoESI tip at 200 nL/min. Tips were installed on the nanointerface at a 20˚angle with respect to the heated capillary while infusing a solution of 600 nM BI in H2O:ACN:FA (70:30:0.1) at a flow rate of 200 nL/min. A much lower spray voltage was required to obtain a stable spray with fully-coated tips than with bare-silica tips. Optimal spray voltages for distal-coated tips are about half those required with the bare-silica tips (0.9-1.4 kV and 0.9-2.8kV respectively, depending on the distance at which the nanoESI tip is positioned). Only very low voltages are required to obtain a stable Taylor cone when the nanospray tip is positioned at or very close to the MS inlet for both distal-coated and bare-silica tips. The fully-coated tips, however, are very susceptible to arcing because the electric potential is applied at the very end of the nanospray emitter. Therefore, no measurements were performed with these tips at less than 1 mm from the heated capillary.

Signal intensities are much larger (>10-times) for coated tips than for bare-silica tips (Fig. 2.5). Uncoated needles gave slightly more intense signals when the tip was positioned at about 3 mm from the heated capillary. In contrast, coated tips perform better when positioned close to the heated capillary (optimum at 1mm). The larger intensities found for coated tips are not accompanied by larger S/Ns. S/Ns are in fact larger for bare-silica than for coated nanospray tips. No hypothesis can be made as to why this is. However, it is to be noted in this context that coated needles require a longer time than bare-silica needles for Taylor cone stabilisation. This period is even longer in the case of fully-coated than distal-coated needles.

Even though fully-coated tips are fragile and require a relatively long equilibration time, they were applied for all further experiments. The more intense protein

signal provided by fully-coated tips should translate into an improvement in sensitivity in the time domain. The tip was always positioned on-axis and at 1 mm from the heated capillary.

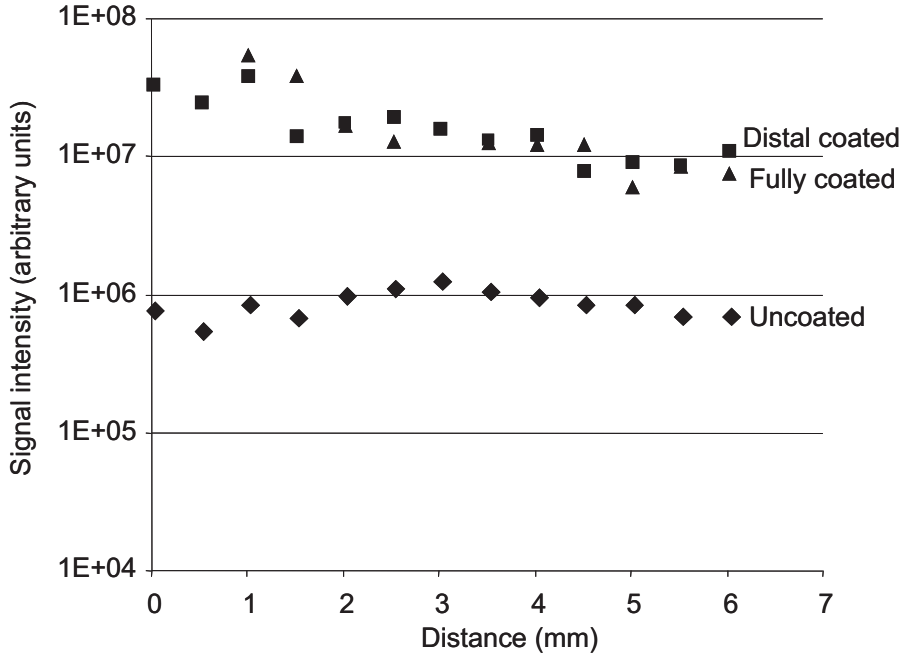

Figure 2.5: Influence of the type of nanospray tip on the intensity of the BI^{4+} ion signal; bare silica (diamond), distal-coated (square) and fully-coated (triangle). A 600 nM solution of BI in H2O:ACN:FA (70:30:0.1) was infused through the 8-μm-ID nanospray tip at a flow rate of 200 nL/min using a 250-μL Hamilton syringe and the syringe pump of the LCQ MS. The tip was positioned under a 20°angle with the MS heated capillary.

2.3.6 Coupling nanoLC to MS

Different means of connecting a transfer capillary or a liquid chromatography column to a nanoESI emitter were investigated (Figure 2.1). Electrical contact was made by applying the high voltage on the outside of a fully-coated nanoESI tip (cf. scheme D, Figure 2.1) or directly to the liquid to be sprayed (cf. schemes A,B & C, Figure 2.1). The main difference between the set-ups lies in their ease of use and, most important, in their respective dead volumes. Most experiments described until now have been performed using the set-up shown in schemes A and B (Figure 2.1). Positioning the nanoESI tip inside the stainless steel connec-

tion without additional void volumes proved to be a difficult task. However, dead volumes remained significant. Moreover, schemes A and B require the use of relatively long nanoESI tips (≈ 4.0-5.0 cm), which contributed to post-column dead volumes. This resulted in very broad chromatographic peaks when the interface (scheme A in Figure 2.1) was used in conjunction with a 50-μm-ID column. Set-up C (Figure 2.1) was investigated because the internal geometry of the PEEK microcross is well-characterised and allows the easy and reproducible positioning of emitters while limiting post-column dead volumes. The bore of the microcross was smaller than the external diameter of both the column and the emitter. Their respective ends could thus be positioned against the inner walls of the microcross. The dead volume of set-up C depended on the PEEK connection. A PEEK microcross introduced 38 nL dead volumes. The nano-ESI tips required for set-up C were still relatively long (≈ 2.5-3.0 cm) and chromatographic peaks remained broad when coupled with a 50μm-ID packed column. However, such a set-up can probably be successfully used with packed columns with larger IDs or monolithic columns that accommodate larger flow rates, in which case dead volumes of the magnitude observed here are of less importance. This set-up presents the advantage of ease of use and modularity. Using the microcross, a make-up liquid can be added when a nanoLC separation requires non-volatile buffers to be used. Additionally, the microcross allowed infusion of a standard solution for tuning of the MS parameters.

Only set-up D (Fig. 2.1) allows the reduction of post-column dead volumes sufficiently to retain the separation efficiency achieved with 50-μm-ID columns. This set-up is built according to the set-up developed by Meiring et al. [20], in which the nanoLC column and the nanoESI tip are butt-connected. The Teflon sleeve used in this set-up allows visual inspection of possible dead volumes introduced in the system. However, this set-up requires fully-coated needles that are more fragile and sensitive to arcing [2, 7]. Nevertheless, set-up D proved to be useful for connecting packed and monolithic columns to the MS with satisfactory performance under most flow regimes. At high flow rates (≥1.0 μL/min), the spray became rather unstable [21](cf. Chapter 4). To accommodate for these higher flow rates, a commercially available interface, built for μL/min flow rates and allowing for a nebuliser gas, was modified according to the butt connection principle of scheme D [22] (cf. Chapter 6).

2.4 Conclusion

Complete characterisation of a nanoESI interface is necessary in order to perform accurate, precise, rapid and reproducible quantitative analysis. A nanoESI interface was built in-house and the different parameters likely to influence the quality of the spray and the spectra were investigated. Positioning the nanospray tip at a 20°angle with respect to the heated capillary led to better S/Ns, probably as a result of the reduced introduction of neutral species into the MS. However, signal intensity was maximum when the interface was positioned axially and close to the heated capillary. Larger % ACN in the mobile phase required lower spray voltages to obtain a stable spray, due to the lower surface tension and the facilitated evaporation of the mobile phase. At low % ACN (i.e. 10%), the spray voltage must be carefully adjusted in order to obtain a stable signal, whereas a much wider spray voltage range will give a stable spray at high %ACN. High %ACN resulted in a narrower distribution of the charge envelop. To date we have no explanation for this observation. Varying the FA concentration had a clear impact on both the intensity and the charge envelop. Larger %FA made the charge envelop shift toward lower m/z. Too high a %FA, though, led to a strong reduction in signal intensity. This may have been due to an ion-pairing effect between the peptide and formate ions, or to the increased surface tension of the mobile phase. Larger intensities were found for coated needles. Unexpectedly, S/Ns were higher for bare-silica than for coated-nanospray emitters. Lower flow rates required lower spray voltage and resulted in higher charge states of the analyte. Using tips with smaller ID resulted in an even greater shift of the charge envelop toward high charges. In addition a more intense MS signal is obtained as a consequence of the greater electric field strength, leading to more efficient protonation of the analytes.

References

[1] M. S. Wilm, M. Mann; *international journal of mass spectrometry and ion processes* **136**, 167 (1994)

[2] M. S. Wilm, M. Mann; *analytical chemistry* **68**, 1 (1996)

[3] K. Vanhoutte, W. Van Dongen, E. L. Esmans; *Rapid Communications in Mass Spectrometry* **12**, 15 (1998)

[4] M. T. Davis, J. Beierle, E. T. Bures, M. D. McGinley, J. Mort, J. H. Robinson, C. S. Spahr, W. Yu, R. Luethy, S. D. Patterson; *Journal of Chromatography B: Biomedical Applications* **752**, 281 (2001)

[5] M. R. Emmett, F. M. White, C. L. Hendrickson, S. D. H. Shi, A. G. Marshall; *Journal of the American Society for Mass Spectrometry* **9**, 333 (1998)

[6] J. C. Hannis, D. C. Muddiman; *Rapid Communications in Mass Spectrometry* **12**, 443 (1998)

[7] M. Mazereeuw, A. J. P. Hofte, U. R. Tjaden, v. d. G. J.; *Rapid Communications in Mass Spectrometry* **11**, 981 (1997)

[8] G. A. Valaskovic, F. W. McLafferty; *american society for mass spectrometry* **7**, 1270 (1996)

[9] M. Karas, U. Bahr, T. Dulcks; *Fresenius' Journal of Analytical Chemistry* **366**, 669 (2000)

[10] R. Juraschek, F. W. Rollgen; *International Journal of Mass Spectrometry* **177**, 1 (1998)

[11] A. Schmidt, M. Karas, T. Dulcks; *Journal of the American Society for Mass Spectrometry* **14**, 492 (2003)

[12] Y. Ishihama, H. Katayama, N. Asakawa, Y. Oda; *Rapid Communications in Mass Spectrometry* **16**, 913 (2002)

[13] y. li, r. b. cole; *analytical chemistry* **75**, 5739 (2003)

[14] r. d. smith, J. A. Loo, C. J. Barinaga, C. G. Edmonds, H. R. Udseth; *Journal of the American Society for Mass Spectrometry* **1**, 53 (1990)

[15] D. Robert, T. P. Voyksner; *Rapid Communications in Mass Spectrometry* **5**, 263 (1991)

[16] S. Vaidyanathan, D. B. Kell, R. Goodacre; *Anal.Chem.* **76**, 5024 (2004)

[17] A. T. Iavarone, J. C. Jurchen, E. R. Williams; *Anal.Chem.* **73**, 1455 (2001)

[18] A. Apffel, S. Fischer, G. Goldberg, P. C. Goodley, F. E. Kuhlmann; *Journal of Chromatography A* **712**, 177 (1995)

[19] H. Toll, H. Oberacher, R. Swart, C. G. Huber; *Journal of Chromatography A* **1079**, 274 (2005)

[20] H. D. Meiring, E. van der Heeft, G. J. ten Hove, A. P. J. M. de Jong; *Journal of Separation Sciences* **25**, 557 (2002)

[21] L. Rieux, D. Lubda, h. a. g. niederlander, E. Verpoorte, r. bischoff; *Journal of Chromatography A* **1120**, 165 (2006)

[22] P. van Midwoud, L. Rieux, r. bischoff, E. Verpoorte, h. a. g. niederlander; *Journal of proteome research* **In preparation** (2006)

CHAPTER 3

Silica Monolithic Columns: Synthesis, Characterisation and Applications to Proteomics

3.1 Introduction

Proteomics deals with the analysis of large sets of proteins. Like genomics, proteomics research has fostered the development of novel technologies in the areas of separation science, mass spectrometry and bioinformatics. Analysis for proteomics has relied on two-dimensional polyacrylamide gel electrophoresis (2D-PAGE), which provides unprecedented separation power for proteins. 2D-PAGE has long been the method of choice for the analysis of complex protein mixtures, as it enables the separation of thousands of proteins in a single run according to their isoelectric point (pI) in the first dimension and to their molecular weight in the second [1]. More recently, two- and multi-dimensional chromatographic approaches have proven complementary to 2D-PAGE. The chromatographic stationary phases employed need to exhibit very high resolving power and provide fast turnaround times per analysis.

Since 2D-PAGE has difficulties resolving either very small or very large proteins as well as polypeptides with an extreme pI and/or hydrophobicity [2], chromatographic alternatives have emerged. Making use of the high resolving power of high-pressure liquid chromatography (HPLC) for peptides, the so-called "shot-

gun" proteomics approach has been developed, where all proteins are digested with trypsin prior to separation [3]. While rendering the sample more amenable to HPLC separation, tryptic digestion increases the number of sample components by a factor of approximately 25 to 50. This overwhelming separation problem has initiated interest in coupled-column liquid chromatography (2D-LC) in order to increase peak capacity to a level that allows the mass spectrometer to detect, quantify and identify individual peptides. However, comprehensive 2D-LC of complex samples often implies spending 12 to 24 hours on the analysis of a single sample [4],due mainly to the rather long LC run times. As a result, great efforts have been made to optimise the separation efficiency of columns and reduce analysis times. Several approaches to achieve this goal are being explored, such as Ultra-High Pressure Liquid Chromatography (UHPLC), electrically driven separations, and columns with low flow resistance. While particle-based stationary phases continue to play a dominant role, it is the recent development of monolithic materials that promises to advance the possibilities of HPLC in proteomics. Silica-based monoliths have already gained an important place in separation science, but mainly for low molecular weight analytes.
In order to better understand the advantages of monolithic columns, the limitations of conventional chromatographic stationary phases should be considered. The following equations for plate height [5,6] shed light on these limitations.

$$H = Au^{1/3} + B/u + Cu \tag{3.1}$$

$$H = \frac{1}{[(1/C_e d_p) + (D_m/C_m d_p^2 u)]} + C_d D_m/u + C_{sm} d_p^2 u/D_m \tag{3.2}$$

Equation 3.1 summarises the different terms contributing to band broadening, the "Eddy diffusion term" (A), the "axial diffusion term" (B) and the "resistance to mass transfer term" (C). The individual terms are given in more detail by Equation 3.2. Apart from some column specific constants (C_e, C_m, C_d and C_{sm}) and the linear flow velocity (u), particle diameter (d_p) and solute diffusion in the mobile phase (characteriSed by the diffusion coefficient, Dm) determine separation efficiency to a large extent. The last term in Equation 3.2 describes diffusion-limited transport (i.e. relating to D_m) in the mobile phase over a distance related to the particle diameter (i.e. $\approx d_p^2$), required to reach the interface with the stationary phase over which the partitioning equilibrium takes place. Especially at high mobile-phase flow velocities (fast separations), this term determines separation efficiency to a large extent. In contrast, the A-term is responsible for most of the band broadening at low linear flow velocities [7].
Until recently, chromatographers have achieved more efficient, faster separations

by using smaller particles and thereby reducing the contribution of both the A- and the C-terms to band broadening. This was first demonstrated using 1 μm particles by Halasz et al. in 1975 [8]. However, improved efficiency also implied, in this case, much greater backpressure. Instrumentation to produce such high pressures was at that time not commercially available, which prevented the more widespread use of small particles. With the advent of novel, high-pressure-stable silica particles and special equipment, UHPLC was introduced by Jorgenson [9, 10]. This approach allows the use of 30-cm-long capillaries packed with 1 μm particles to yield efficiencies as high as 670 000 plates/m. Alternatively, electrically driven separations like capillary electrochromatography (CEC) can be used to obtain very high plate numbers, but it remains difficult to couple CEC with MS [11], which is the detector of choice in proteomic studies. Non-porous particles were used by Unger [12] to avoid peak broadening due to stagnant mobile phase transfer. However, such particles also show very limited binding capacity. To avoid the problems related to the need for very high pressures and the low capacity of non-porous media, a new technique named perfusion chromatography was introduced in 1990 by Afeyan et al. [13]. This technique makes use of particles with very large pores (6000 to 8000 Å) that proteins can enter through a combination of convective and diffusional transport, resulting in relatively low pressures. However, up to a given pressure, the mobile phase and analytes tend to go around the particles without penetrating them. Shortly thereafter Tennikova, Svec and co-workers introduced a new support for chromatography in which separation takes place on very short, wide macroporous polymeric monoliths [14]. High porosity and low pressure are features characteristic of such monolithic materials. Instead of particle diameter (Equation 3.2), separation efficiency for these materials is related to structural parameters as discussed later. Monoliths can be prepared by one of two routes.

- polymerisation of organic monomers
- polymerisation of alkoxysilane monomers

The first type of monolith has been the subject of intense research over the past years [15, 16]. The synthesis of organic monoliths involves mixing monomers, initiators, crosslinkers and porogenic solvents in a mould and subjecting them to UV light or heat to initiate polymerisation. In this approach, the porogenic solvent acts as an emulsifier and creates the porous structure. However, organic polymers are often subject to swelling or shrinking in organic solvents and show pores [17], whose size (<2 nm) hinders the motion of analytes in and out of the pore.

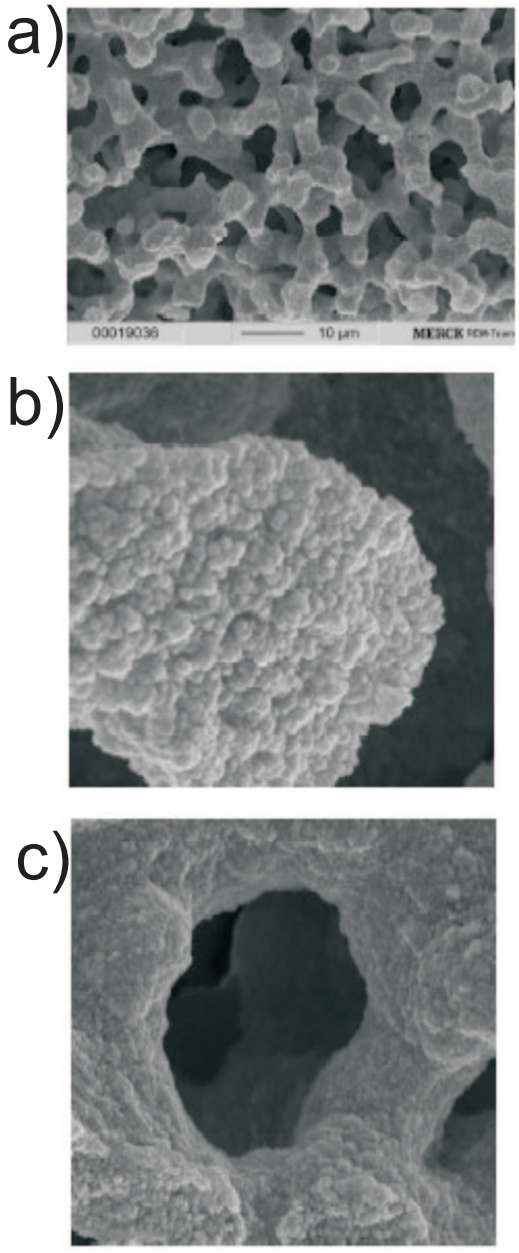

Figure 3.1: Scanning Electron Microscopy (SEM) of (a) the skeleton-throughpore network of a silica-based monolithic column, (b) the mesoporous structure on the surface of the skeleton and (c) a throughpore. (reprinted with permission from Cabrera, K., Journal of Separation Science 2004, 27, 843; copyright 2004 Wiley-VCH).

It was not until 1996 that a silica-based monolith was synthesised for use in HPLC [18], where the skeleton defines the throughpores and contains the mesopores (Figure 3.1). Whereas the latter provide the specific surface area and thus binding capacity, the flow-through pores are responsible for the hydraulic permeability of the monolith. Silica-based monoliths differ from their organic counterparts in that they only exhibit μm-size flow-through pores constituting a macroporous network and nm-size mesopores in the skeleton, but no pores smaller than 2 nm. Moreover, silica monolithic columns do not show the tendency to swell or shrink when they are used with organic liquid phases [17]. Desmet and coworkers [19] devised a model to investigate the effect of interstitial porosity (which can be assimilated to the porosity associated with throughpores) on column performance. It showed that increasing interstitial porosity from 0.4 to 0.9 yielded an up to a 2-fold improvement in separation efficiency. Therefore, the skeleton size, which refers to the average thickness of the silica network (Figure 3.1), is an important parameter when designing new and efficient separation media based on monoliths. Another structural parameter often referred to in publications related to HPLC on silica-based monoliths is the domain size, which is equal to the sum of the skeleton and the throughpore size.
This review will focus on silica monoliths first outlining the principle chemical reactions and their effect on the chemical and structural properties, which influence the chromatographic performance of the resulting columns. Subsequently, applications of silica monoliths to proteomics research will be outlined.

3.2 Synthesis

More than thirty years ago, Hansen and Sievers [20] prepared liquid chromatography columns from polyurethane. The very low backpressure allowed a very high speed of analysis. Similarly, Hjerten [21] successfully separated proteins using a compressed polyacrylamide gel. However, both stationary phases lacked mechanical strength and it was not until the beginning of the 90's that monolithic stationary phases with satisfactory mechanical properties could be synthesised. The successful combination of sol-gel reaction and phase separation for the preparation of silica-based monoliths was first demonstrated by Kaji et al. [22]. Following acid and/or base catalysis, reactive alkoxysilanes polymerise to form a gel. Inorganic polymerising systems undergo a phase separation (or spinodal decomposition) driven by the increase in free energy for solvation due to the reaction of the different species present in the starting sol.

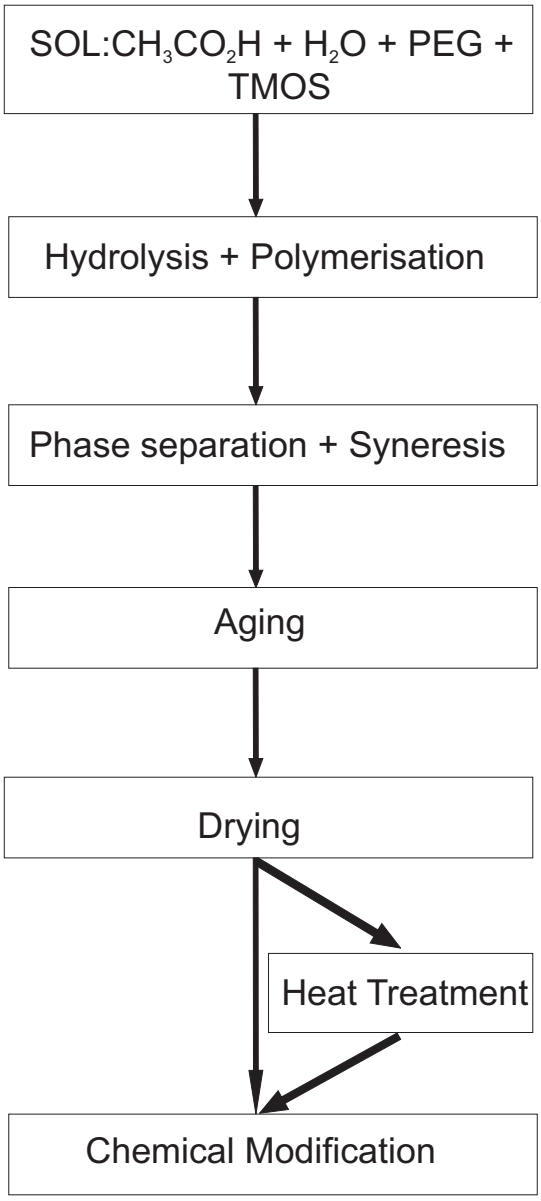

Figure 3.2: Schematic representation of the synthetic steps for the preparation of silica-based HPLC monoliths. (Heat treatment is optional).

Synthetic variables				Resulting structural parameters					
Silanes	Porogens	Additives	Aging reagent	Skeleton size (μm)	Throughpore size (μm)	Mesopore size (nm)	Domain size (μm)	Throughpore/ Skeleton Ratio	Reference
TMOS	*PEG*		*NH_4OH*	*1.1-2.4*	*1.3-3.5*	*13.0-25.0*	*2.3-5.9*	1.3-1.4	[27]
TMOS	PEG		*NH_4OH*	1	1,7	*14.0 or 25.0*	2,7	1,7	[18]
TMOS	*PEG*		*NH_4OH*	*1.0-2.3*	*1.3-3.4*	*5.0-25.0*	*2.3-5.7*	*1.0-1.7*	[24]
TMOS	PEG		NH_4OH	2,2	8,0	14,0	10,2	3,6	[28]
TMOS	*PEG*		NH_4OH	*1.0-2.3*	*1.2-3.5*	NA	*2.2-5.8*	*1.2-1.5*	[35]
TMOS or TMOS + MTMS	*PEG*		*urea*	1.0-2.0	2.0-8.0	NA	3.0-10.0	1.33-4.0	[36]
TMOS	*PEG*	CTAB	*NH_4OH*	*1.0-2.0*	*1.2-3.5*	*10-15*	*2.2-5.5*	*1.2-1.75*	[29]
TMOS	PEG		*urea*	NA	≈ 1.0	*8.0-413.0*	NA	NA	[37]

Table 3.1: Effects of the variation of different synthetic parameters on the structure of silica-based monolithic columns using acetic acid as catalyst of the sol-gel process. The parameters that were varied in the corresponding article are shown in italics. (NA) stands for not available.

63

The resulting gel separates into solid- and liquid-rich domains that further react with each other to give the gel its final structure. This process, called syneresis [23], results in shrinkage of the network and in an expulsion of liquid from the pores. The inorganic sol-gel transition to form an alkoxysilane network freezes the domains as permanent morphology [24]. After aging and drying of the gel, a highly porous monolith is obtained. A typical route for the preparation of silica-based HPLC monoliths is summarised in Figure 3.2. The pore structure and the mechanical strength of the monolith depend on the competition between the kinetics and thermodynamics of the sol-gel transition and of phase separation [23, 24]. Therefore, the nature and concentrations of the starting materials will be of great importance to control both the time and the speed at which both gelation and phase separation take place.
Brinker et al. investigated the dependence of hydrolysis and condensation reactions on pH [25]. The rate of hydrolysis at low pH is relatively high and decreases linearly with increasing pH up to 7. At higher pH, hydrolysis becomes faster again. At the same time, condensation is minimal around pH 3 and greatly increases over the pH range 7-9. At higher pH, condensation rate falls due to increased depolymerisation. Therefore, a low pH, resulting in long gelation and phase separation times, is favoured to obtain small throughpores [26]. Tanaka et al. [18, 24, 27, 28] advocated the use of tetramethoxysilane (TMOS) as silica monomer in the sol. This is now the most commonly used alkoxysilane to prepare HPLC grade monoliths. The mechanical strength of the monolith increases with increasing TMOS concentration whereas too low a concentration in alkoxysilane results in poor interconnectivity of the skeleton and, consequently, in poor mechanical strength [29].

While condensation of the alkoxysilanes proceeds, the resulting network becomes less soluble and hastens phase separation. Consequently, the use of other alkoxysilanes will lead to morphological and chromatographic differences. In addition, alkoxysilanes can be used to introduce functionalities for later derivatisation of the stationary phase or for direct tailoring of chromatographic properties. The following alkoxysilanes have been used separately or in combinations: tetraethoxysilane (TEOS) [30], methyltrimethoxysilane (MTMS) [31], ethoxytrimethoxysilane (ETMS) [32], 2-cyanoethyltriethoxysilane (CEOS) [33], (3-aminopropyl)triethoxysilane (APTES) [34] and diglycerylsilane (DGS) [30,34]. Table 3.1 summarises the effects different synthetic parameters have on the monolith structure and Table 3.2 gives an overview over other reagents that have been used in the preparation of monoliths in order to vary their bimodal structure and/or their selectivity.

Silanes	Catalysts	Porogens	Additives	Aging reagent	Throughpore size (m)	Mesopore size (nm)	Ref.
Potassium silicate		Formamide			NA	NA	[38]
TMOS	HCl		BPA antibodies in PBS		NA	NA	[39]
TMOS	HCl		buffer				
TMOS	HCl & NaOH		*Enzyme immobilised on beads*		NA	NA	[40]
TMOS	HAc	PEG	Tetraisopropyltitanate	Urea	NA	9.0-12.0	[41]
TMOS	HAc	PEG	Zirconium oxychloride	NH_4OH	NA	NA	[42]
TMOS	HAc	F127			NA	9.0-10.0	[43]
TMOS	TFA in water (also contains di- or tri-) peptides)	CTAB or Triton X-114	CHCA in MeOH		NA	NA	[44]
TMOS	HCl	*PEG*			*1.0-2.0*	*3.0-5.0*	[45]
TMOS	HAc	PEG		*NH_4OH*	NA	$\approx$ 10.0	[46]
TMOS:MTMS (1:4)	HCl		Enzyme in PBS buffer and dextrin		NA	NA	[47]
TEOS or DGS	*(HCl and Tris pH 8.25) or Tris*		*Enzyme in Tris buffer + NaCl + $CaCl_2$*		NA	*$\approx$ 5.0*	[30]
BTME	HNO_3	*Pluronic P123*	*TMB*		*Great variations*	*Great variations*	[32]
TMOS	HCl PBS buffer pH 7.0			Water	NA	NA	[48]
DGS	HCl	*PEO + APTES + protease in HEPES buffer pH 7.5*	*PAM or DM-DMS*		*0.5-3.0*	*$\approx$ 2.0*	[44]
TEOS, CEOS, TMAOH	*NH_3, NaOH, HCl*	*CTAB, F127*			NA	NA	[33]
TEOS + $CH_3(CH_2)_nSi(OR)_3$	n-hexadecylamine	n-hexadecylamine			NA	NA	[49]

Table 3.2: Effects of the variation of different synthetic parameters on the structure of silica-based monolithic columns using also other catalysts for the sol-gel process. Different alkoxysilanes and porogens, a different pH as well as additives allowed to tailor the bimodal. The parameters that were varied in the corresponding article are shown in italics. (NA) stands for not available.

65

As alkoxysilanes are poorly water soluble, a chemical additive is often required to increase solubility. Additives also have two other functions. They can act as templates for the monolith's pores (in which case they are also referred to as porogens or templates) and retard the phase separation process. For the preparation of HPLC monoliths, the most common porogen is poly(ethylene)glycol (PEG) [18, 24, 27]. An increase in PEG concentration leads to a decrease in both throughpore- and domain-size due to a retarded phase separation relative to the sol-gel transition [24, 27, 29, 31]. The abundant cross-linking sites in monolithic structures having a small domain size give mechanically stronger monoliths [29]. The molecular weight of the porogen also has an impact on the morphology of the monolith; the larger the porogen, the larger the throughpores and mesopores [45]. Aging is the first step involved in tailoring the surface for use in chromatography after a monolith has been synthesised. Aging deals with the enlargement of the mesopores using a process called Ostwald Ripening that leads to round surfaces and a reduced contact area between liquid and solid due to local solubilisation. The most common method to tailor mesopores employs ammonium hydroxide [18,24,27,28], where an increase in concentration results in larger mesopores up to 400 nm [37]. Temperature can be used additionally to tailor mesopore size [37] as an increase in temperature results in a greater syneresis and thus in smaller pores [50]. Urea has been used as a precursor of ammonia in monolith preparation [31]. It hydrolyses to ammonia at high temperature and partially dissolves the silica backbone [41]. The most difficult step in preparing monoliths is the removal of liquid, as gels contract while the liquid evaporates from the pores [23, 51]. The huge stress generated in the mesopores tends to exceed the strength of the network and can cause formation of cracks. This can be avoided by supercritical drying of the gel [52, 53]. Shrinkage can also be eliminated by carefully choosing the solvent present in the monolith during the drying step. To this end, isobutanol, 2-pentanol and iso-octane led to large, crack-free monoliths [54]. Both drying temperature and pressure can be lowered below the critical value for these solvents while still obtaining crack-free monoliths if the pores are large enough [55]. Ionic solvents (e.g. 1-ethyl-3-methylimidazolium bis[(trifluoromethyl)sulfonyl]-amide) have virtually no vapour pressure, thereby greatly simplifying the drying step. They were used as solvents for all steps of the synthesis of the monolith. Their use alleviated the need for solvent exchange [56]. The last step in preparing a silica-based monolithic HPLC column is derivatisation. It is generally performed using octadecyldimethyl-(N,N-diethylamino)silane [18, 24, 27] to obtain a stationary phase for reversed phase separations. Biomolecules have also been chemically attached to monoliths in the preparation

of affinity-based LC columns [57–59]. Affinity ligands can be attached to silica particles [40] before being added to the sol or directly put in the sol [39] prior to the sol-gel process. Alternatively, bio-macromolecules can be immobilised at the surface of monoliths by adsorption [33, 60]. Adsorption was also used to prepare Ti- [41, 61] and Zr-coated [42] monoliths. Tables 3.1 and 3.2 provide an overview of the materials used by various researchers and the parameters that have been varied in the synthesis of silica monoliths by sol-gel reactions.

3.3 Characterisation

3.3.1 Physical characterisation of monoliths

Silica monoliths have to be physically characterised to relate these characteristics to their chromatographic behaviour. The link between morphology and chromatographic performance is of utmost importance in order to design better separation media. Several techniques are used for the physico-chemical characterisation of HPLC monoliths.

Optical methods such as Scanning Electron Microscopy (SEM) [18, 24, 27] and to a lesser extent Transmission Electron Microscopy (TEM) [62, 63] are commonly used for the assessment of the structural parameters of monolithic columns. SEM is used to study the morphology of monoliths after the drying step. It gives an estimate of the size of the throughpores and of the skeleton [18, 24, 27] that will in turn determine the hydrodynamic properties and mechanical strength of the column. Whereas the methods outlined below are better suited to determine the exact size and the size distribution of the throughpores, SEM is the only method that allows gaining data about the skeleton size. However, SEM is mainly used to study transversal slices of a monolith, which does not allow to draw conclusions about the homogeneity of the pore size distribution and homogeneity over the entire column. A longitudinal cut of the monolith gives a better idea of pore size and especially of the homogeneity of its distribution [31].

Techniques such as mercury porosimetry, Size Exclusion Chromatography (SEC) and N_2 adsorption give additional data about the morphology of the investigated monolith. The specific surface area of a chromatographic column relates to the column selectivity and the amount of a given analyte that can be adsorbed. It is measured by N_2 adsorption via the Brunauer-Emmett-Teller (BET) method. This method involves measuring the volume of N_2 adsorbed on the surface of the column. In the case of liquid chromatography columns, monolayer adsorption is assumed. The specific surface area of a column can therefore be easily calculated

from the adsorbed volume of gas and the size of a N_2 molecule [64].
Mercury porosimetry allows determining both the volume of meso- and throughpores in two experiments [65]. By wrapping the sample in a mercury-tight membrane, the volume of throughpores is determined by linearly increasing the mercury pressure. Under the action of pressure, the monolith will be crushed. The volume of the throughpores is calculated as the reduction in volume of the monolith. To assess the mesopore volume, the mercury pressure is linearly increased without using a membrane so that the mercury can now invade the mesopores [65]. The shape of the adsorption curve gives an indication of the size and shape of the pores, a bimodal pore distribution can be evidenced using this technique [66].
SEC makes use of a set of linear polystyrene standards with a molecular weight between 600 and 3.7×10^6 Da (having molecular radii of 2.7 to 453 nm respectively). The molecules that are too large to enter the porous structure elute in the flow-through. By comparing the results obtained for a given monolith to those obtained with a material of known porous structure allows determining the mesoporosity. The results obtained by SEC and mercury porosimetry are comparable. However, the pore size distribution obtained with SEC may appear somewhat broader [67, 68]. SEC has the advantage of being a nondestructive method.

3.3.2 Chromatographic properties of silica monoliths

The macroporous structure of silica monoliths prepared by the sol-gel process is controlled by the composition of the starting mixture. The size of silica skeletons and throughpores can be varied independently. The size of throughpores is normally much larger than the thickness of the skeleton resulting in throughpore size-to-skeleton size ratios up to 4.0 [31]. This porosity is much greater than in the case of packed columns (0.25-0.4) resulting in considerably lower flow resistance. The size of mesopores can be adjusted by varying pH, temperature and reaction time [37]. The size of mesopores as well as their size distribution are important when tailoring the monolith surface for HPLC separations. The smaller the mesopores, the higher the specific surface area and thus the higher the loadability of the column. However, small mesopores will tend to hinder the movement of large molecules such as peptides or proteins in and out of the pores thereby leading to peak broadening.
The small diffusion pathlength provided by the large throughpores and small skeletons results in efficient separations and low operating pressures. Because of these properties, monoliths are able to efficiently separate analytes at flow rates much higher than can be used with packed columns of similar dimensions. Because

monoliths are not prepared from particles, the impedance (number of theoretical plates per unit pressure drop [69]) is often used to compare monoliths to other HPLC columns as it emphasises the high efficiency obtained at low pressures. The size of throughpores for monoliths reported in the literature ranges from 1 μm [70] to 8 μm [28, 31]. In accordance with theory, the smallest throughpores (1.1-2.0 μm) give the lowest plate height (5-8 μm at 1.0-1.5 mm/s linear flow velocity for benzene derivatives with 80% methanol and $\approx$ 15 μm at 0.5 mm/s for insulin using 30% acetonitrile) [70, 71] but also a higher backpressure. Even though monoliths with large throughpores (8.0 μm) [28, 31] show a lower plate number per unit length, their backpressure is so low that very long monoliths can be used to compensate for this effect. Large throughpores also offer the advantage of being able to raise the flow rate and thus shorten analysis time [72]. Apart from the low operating pressures required by monolithic columns, the most prominent feature monoliths offer is a very shallow Van Deemter curve. The reduced contribution of mass transfer to plate height allows to accelerate the separation without sacrificing resolution and efficiency. To evaluate the efficacy of a commercial monolith (100*4.6mm, Merck, Japan) for high-speed RPLC of peptides [73], a digest of cytochrome C was injected at flow rates varying from 2.0 to 25 mm/s (10 mL/min). Little change in resolution and peak elution volume were observed. The morphology of silica monoliths is also described by the throughpore size-to-skeleton size ratio. When this ratio reaches very large values ($\approx$ 4.0) [31], the pressure required to operate such a column is very low and thus the flow can be greatly increased. Such a large ratio is thus favoured when high-throughput analysis is required. However, if the sample is more complex and demands on separation efficiency increase, smaller ratios are preferable. Separation efficiency was also investigated in relation to domain size (throughpore + skeleton). The columns with the smallest domain size gave the lowest plate height. A column with a domain size of 5.8 μm showed a plate height of 15 μm while a column with a domain size of 2.3 μm gave a plate height of 5.0 μm for amylbenzene using 80% methanol [27].

Varying the size of the mesopores proved to be important in terms of both loading capacity and separation efficiency. Mesopores, if too small, can hinder the movement of analytes in and out of the pore. Insulin was more efficiently separated on a monolith with mesopores of 25 nm than 14 nm, where plate heights between 20 μm and 40 μm were obtained for the monoliths with large and small mesopores respectively [18]. When further increasing the size of mesopores (140 nm), it has been suggested that steric hindrance is no longer important and that a flow can be generated inside the mesopores [74]. This suggests that a perfusion mechanism

may take place in very large mesopores. However, using monoliths with mesopores of 12.5 and 20 nm, diffusion-limited mass transfer was still observed [75], while the possibility that convection takes place in larger mesopores was not ruled out though. The same study allowed to calculate equivalent sphere dimensions to compare monoliths and packed columns. An equivalent dispersion particle diameter (d_{disp}) was calculated in view of the contribution of the C-term to band broadening. An equivalent particle diameter based on permeability (d_{perm}) was also described based on the operating pressures obtained at different flow rates. d_{perm} was equal to $\approx$ 15 μm while d_{disp} was found to be 2.5 μm for angiotensin on both the 12.5- and 20-nm mesopore monoliths [75].
Although different from a morphological point of view, monolithic and packed columns are subjected to the same mechanisms involved in band broadening: molecular diffusion, liquid hold-up in the mesopores and stagnant mobile phase at the liquid-solid interface. Therefore, theoretical investigations performed for packed columns may also be applicable to monoliths. The contribution of Eddy diffusion to plate height is mainly affected by the homogeneity of the chromatographic bed, which is inversely related to particle diameter for spherical, particulate LC columns. It was modelled that an improvement in bed homogeneity could yield a reduction in plate height by as much as 50% [19]. Using computational fluid dynamics software, the theoretical band broadening in an ideal monolith was simulated [76]. Reduced plate heights as small as h_{min}=0.8 (equivalent to appr. 1.8 μm) and separation impedances as small as E_{min}=120 for a retained component were predicted. Especially with respect to the Eddy diffusion term, significant improvements (about a factor of 10) as compared to current state-of-the-art monoliths were predicted. This indicates that, as with packed columns, more homogeneous monoliths would give more efficient separations. A mathematical model specifically designed to describe the dynamic behaviour of an analyte in a chromatographic column [77] could help in designing better monoliths with regard to separation efficiency. The model predicts that monoliths should preferably have relatively large throughpores with high interconnectivity and small-sized skeletons with mesopores large enough not to hinder the passage of molecules in and out of the pore [77]. For particulate columns, the effect of the layer of immobilised ligands (e.g. hydrophobic, ionic) on the intraparticle interstitial velocity is rather small, while the effect of the value of the pore connectivity, nT, on the intraparticle interstitial velocity is very large [78]. It can be assumed that this is also valid for monoliths as they exhibit mesopores in the skeleton comparable to the pores in silica particles.
The ideal stationary phase for liquid-based separations should provide a large

surface contact area between stationary and mobile phases, form a homogeneous channel network for the facile transport of mobile phase through the column and maximise channel interconnectivity to limit peak broadening [77, 79]. Silica monoliths possess these characteristics and show very efficient separations, but like porous particles, they still suffer, though to a much lesser extent, from band broadening originating in diffusion-limited mass transfer. Convective mass transfer is very advantageous as it helps to establish an efficient exchange of molecules between stationary and mobile phases, and thus permits raising the velocity of the mobile phase without significantly decreasing column efficiency to achieve fast analysis. The performance of silica-based monoliths under isocratic conditions are well documented [18, 24, 27]. However, they have not been as thoroughly investigated under gradient conditions using proteins and peptides.

3.4 LC-MS of peptides and proteins using silica-based monoliths

The use of three silica-based monoliths exhibiting different morphologies (100*4.6mm, 2.0 μm and 13 nm; 50*4.6 mm, 2.5 μm and 25 nm; 100*4.6 mm, 2.5 μm and 25 nm) was investigated for peptide mapping of a tryptic digest of cytochrome C homologues (from equine, bovine, canine and avian origin) by gradient elution RPLC-MS [72]. Each monolith showed efficient and reproducible separation allowing small differences in amino acid sequence to result in minute and reproducible differences in chromatographic profiles. The main difference between the 2.0-μm and the 2.5-μm throughpore monolith is the flow rate at which they can be operated. The monolith with wider throughpores could be used with flow rates twice as high as the monolith with the smaller thoughpores, though at the cost of decreased capacity and selectivity due to the loss of surface area. Monolithic columns (100*4.6mm [37]; 150*0.1mm and 500*0.1mm [80], and 560*0.05 mm, Chapter 4) were used to evaluate their efficacy for high-speed gradient elution RPLC of peptides using tryptic digests of cytochrome c from bovine heart [73] and horse heart [80]. Resolution and retention volume were found to vary very little when the linear flow was increased from 2.0 to 25 mm/s (10 mL/min) for use with the 4.6-mm id monolith. Similar results were obtained with both the 50- and the 100-μm monolithic columns (Figure 3.3). The 50-μm capillary column was operated at flow rates up to 2.0 μL/min ($\approx$20 mm/s), which is more than 10 times the flow rate applicable with a packed column of similar dimension (Chapter 4). This confirms the applicability of silica monoliths to very

fast separations.

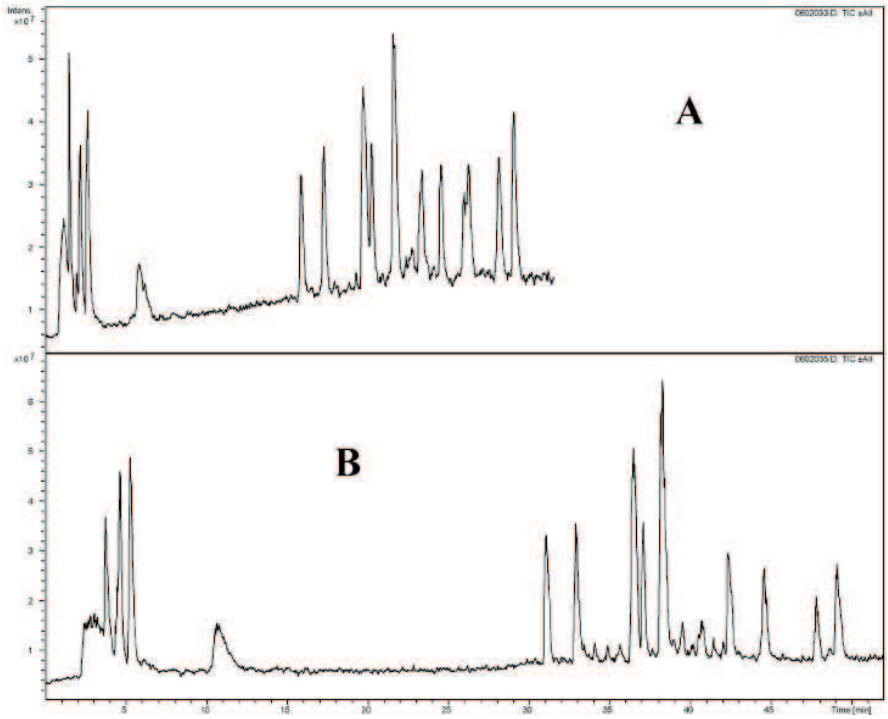

Figure 3.3: Total Ion Current (TIC) chromatograms corresponding to the injection of 2.0 μL of a cytochrome c tryptic digest (0.01 μg/μL) on a Chromolith CapRod RP18e silica-based monolithic capillary column (0.1 mm ID, 15 cm length) run at two different flow rates: A = 4.5 μL/min and B = 2.0 μL/min. Mobile phase A consisted of 0.1% formic acid in water. Mobile phase B consisted 0.1% formic acid in acetonitrile. The gradient slope was kept constant. (reprinted with permission from B. Barroso, D. Lubda, R. Bischoff, Journal of Proteome Research 2003, 2, 633; copyright 2003 American Chemical Society [80])

The very high linear flows (up to 25 mm/s) that can be used with monolithic columns are a great advantage in terms of analysis time. However, they raise several problems when coupling monolithic columns to MS. Large-internal diameter columns are coupled to MS using conventional pneumatically assisted electrospray ionisation sources (ESI). A nebuliser gas and a drying gas are used to help evaporation of the eluent and favour the transfer of the analyte to the gas phase. The low flow rates (<0.5 μL/min) used with narrower packed columns (<100-μm id)

normally enables the coupling of LC columns to MS by means of a nanospray interface, without using a nebuliser gas. Due to their very high porosity, capillary monoliths are often used with higher flow rates. Barroso [80] used flows up to 4.5 μL/min with a 100-μm id reversed-phase silica monolith, coupled to an ion trap mass spectrometer via a commercially available pneumatically-assisted microESI source. In an attempt to eliminate post-column dead volumes altogether, a 100-μm id silica monolith was also directly coupled to the mass spectrometer [81]. The electrospray voltage was connected to the stainless steel union positioned in front of the monolithic column, allowing the effluents to be sprayed directly from the monolith. First demonstrated by Koerner et al. [82] with an organic-based monolith, this set-up was also successful with a silica-based monolith [81]. The good-quality ionisation is claimed to result from the small-sized throughpores that act as a set of tapered-nanospray tips [82]. Such a set-up alleviated the need of a tapered tip, which is easily blocked and whose coating is often fragile and short-lived. A stable spray was obtained at flow rates up to 1.0 μL/min for a wide range of mobile phase compositions. In another application, a 50-μm ID reversed-phase monolithic column (560 mm) was coupled to an ion trap mass spectrometer via an in-house modified nanospray interface or a commercially available microESI source (Agilent, Germany) (Chapter 4). In the nanospray-configuration, the monolithic column was butt connected to a gold coated nanospray emitter using a 360-μm-ID Teflon sleeve and subsequently mounted in front of the nanoESI source entrance. Such a set-up introduced very little post-column dead volumes and allowed to obtain a stable spray at most flow rates and gradient steepnesses. However, spray stability was negatively influenced by higher flow rates and extreme gradient steepnesses (>9% ACN/min). Using the nanospray source, a wide range of flows (up to 1.95 μL/min) and gradient steepnesses (up to 9% ACN/min) could be used. However, efficient ionisation and long-lasting nanospray tips were only possible if the flow rate was kept below 1.0 μL/min. When using a 50-μm ID monolith, a compromise between sensitivity and analysis time has to be reached. Monolithic columns with a smaller internal diameter could be more easily coupled to MS via a nanospray interface while retaining optimum sensitivity and analysis time, however, they are not yet available.

Silica monoliths were mostly used to shorten the analysis time of a single analyte in isocratic elution mode or a relatively simple mixture of peptides in gradient elution. With more complex samples, the excellent separation efficiency also enabled to combine shorter analysis time with good resolution as will be discussed below. Methanolic extracts of microcystins (hepatotoxic cyclic peptides) were prepared from samples of Microcystis PCC7820 and Anabaena sp. [48] and added

to a commercial standard of microcystin-YR and methanolic extracts of Baltic Sea Nodularia. The pooled extracts were diluted with water and concentrated on an SPE cartridge. A reversed-phase monolithic column (100*4.6mm) was used for their separation. The analysis time was reduced from 45-60 to 4.3 min when compared with packed columns of similar dimensions [83] without any loss in resolution or sensitivity.

The analysis of the proteome often requires attaining high sensitivity next to separation efficiency. To analyze combinatorial, synthetic peptide libraries, a 100-μm monolithic column (500 mm long) was coupled to a Fourier Transform mass spectrometer [84]. The first synthetic peptide library was based on the sequence, VSXLY (X = one out of all 20 natural amino acids), whereas the second library had the following characteristics, CWXXXG (X = amino acids E, N, R, F, P, S, W, Y, L, or H). The high resolving power and low operating pressure of the silica monolith added to the high selectivity of the Fourier Transform mass spectrometer allowed to separate all peptides from these libraries in 30 min, while sensitivity remained adequate due to the capillary format of the monolith. A similar monolith (150*0.1mm) was coupled to an ion-trap mass spectrometer for the analysis of different proteomics samples using a commercially available microESI source [80]. Samples of high complexity and of very different nature were used to demonstrate the capacity of reversed-phase silica monoliths for the analysis of these biomedical samples. In one example, elastin, a rather hydrophobic protein, was digested by various proteases and the digests analysed by LC-MS as a basis for discovering biomarkers of pulmonary disease. Peptide identity was ascertained by MS/MS. Broncho-Alveolar Lavage Fluid (BALF) was collected during fiberoptic bronchoscopy. It contains phospholipids, nucleic acids, proteins and peptides in very low concentrations and high amounts of salt. Good peak shape and chromatographic resolution as well as clear MS/MS spectra were obtained. As part of another biomarker discovery study, a sample of serum from a cervical cancer patient was spiked with 1.26 pmol/μL cytochrome c to act as internal standard and depleted of albumin and γ-globulins [85], digested with trypsin and the resulting tryptic peptides fractionated using a strong cation exchange (SCX) column. The sample was analysed by LC-MS on a 50-μm ID reversed-phase monolith. The very short and fast gradient enabled analysis of one sample every 30 min, which is 6 times faster compared to a packed column. This is a great asset in the comparative analysis of biomedical samples.

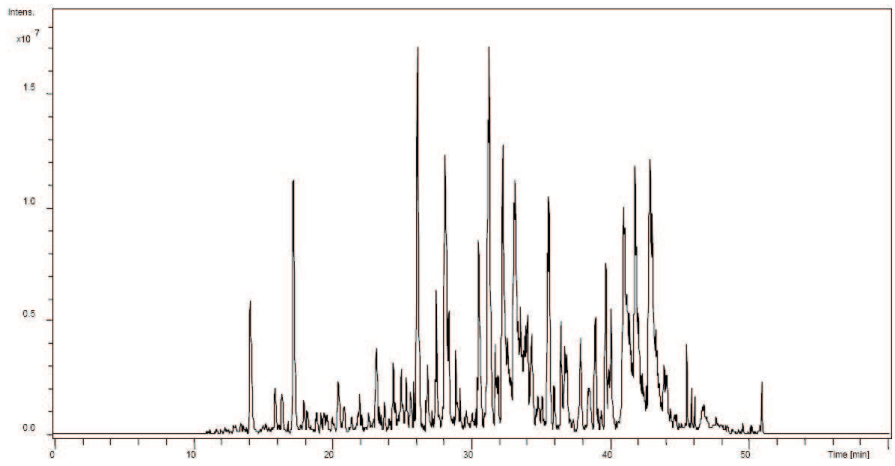

Figure 3.4: Base Peak Chromatogram (BPC) corresponding to the injection of 2.0 μL of an in-gel digest of an excised spot on a nanoLC-MS system making use of a Chromolith CapRod RP18e silica-based monolithic capillary column (0.05 mm id 56 cm length) and a Zorbax 300 SB-C_{18} trap column (0.3 5 mm, 5 μm d_p). After 5 min loading, elution took place at 1.0 μL/min. The gradient steepness was 1% acetonitrile/min. Mobile phase A consisted of 0.1% formic acid in water. Mobile phase B consisted 0.1% formic acid in acetonitrile.

Due to the low backpressure of monolithic columns, column length is not a limiting factor anymore when the efficiency of a separation needs to be improved (Figure 3.4). To this end, a long monolithic column (900*0.2 mm) was used for the analysis of the metabolome of Arabidopsis thaliana [86]. A cold methanol extract of 100 mg fresh weight of ground leaves was diluted with water and injected. A great variety of analytes was detected comprising glucosinates, flavonoids, phenolic compounds, anthocyanines, membrane lipids, porphyrins and chlorophylls. The length of the column proved to be an effective way to limit ionisation suppression by increasing resolution between analytes while analysis time was kept to about 2h.

An alternative to very long columns in order to separate very complex mixtures is the use of 2D-LC. A 2D-LC system was developed for the separation of complex peptide mixtures taking a tryptic digest of bovine serum albumin (BSA) as example [87]. Fractionation took place on a polymer-based cation exchanger (50*2.1 mm, 5μm d_p) followed by analysis of the resulting peptidic fractions on a very short RP monolith (25*4.6 mm) coupled to a time-of-flight mass spectrometer via an ESI interface. Alternatively, a capillary-based monolith (100*0.1mm) was

employed as 2^{nd} dimension with split injection and flow. The monolith in the capillary format resulted in better MS spectra and sensitivity. Runs were 40 min in the 1^{st} and 2 min in the 2^{nd} dimension for the 4.6-mm ID monolith. Due to its greater length, runs making use of the capillary monolith were 4 min long. From the analysis of a BSA digest, a peak capacity of 700 was calculated for the 2D-LC set up (Figure 3.5).

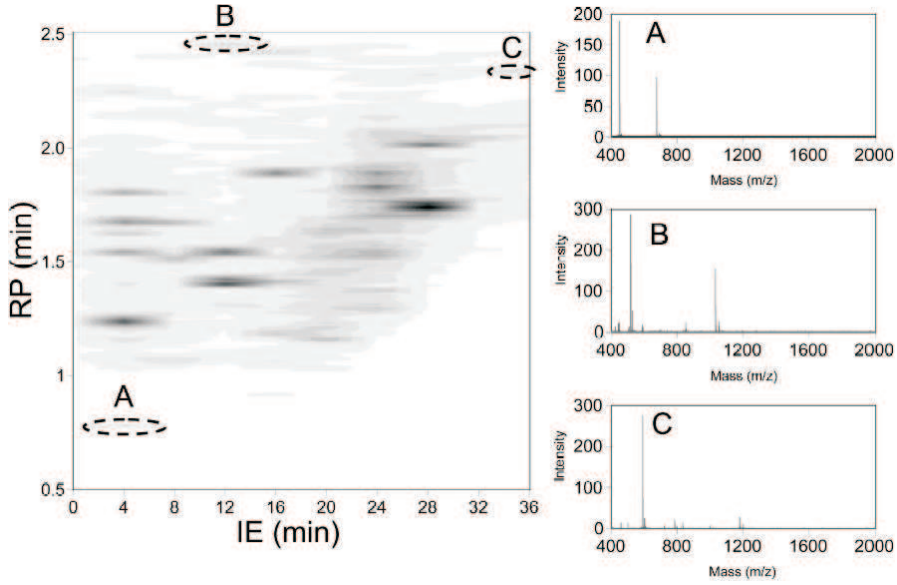

Figure 3.5: Representation of a two-dimensional separation of a bovine serum albumin tryptic digest. A silica-based monolithic capillary column (0.1 mm ID, 10 cm length) was used in the second dimension following prefractionation by strong cation-exchange chromatography. The MS spectra for the spots A, B & C are shown. (reprinted with permission from Kimura H.; Tanigawa T.; Morisaka H.; Ikegami T.; Hosoya K.; Minakuchi H.; Nakanishi K.; Ueda M.; Cabrera K.; Tanaka N.; Journal of Separation Science 2004, 27, 897; copyright 2004 Wiley-VCH).

A shotgun approach (digestion of the whole sample and separation by 2D-LC [3]) was used for the analysis of the proteome of Arabidopsis thaliana after depletion of Rubisco, a high-abundance protein found in plant leafs [88]. The first dimension was based on SCX whereas the second dimension was performed using RPLC. The silica monolith (500*0.1mm) was coupled to the SCX column by means of a 10-port valve and two C_{18} trap columns to desalt the fractionated sample prior to injection on the monolith. Individual RPLC runs were in excess

of 2h. Using this set-up, a total of about 3500 MS/MS spectra were acquired during each run, enabling to identify about 300 unique proteins.
Monoliths appear to be a viable alternative for fast, high-resolution separations of complex samples to the recently introduced UHPLC systems, which require special HPLC pumps and extremely pressure stable stationary phases. We expect that rapid separations by LC-MS using silica-based monoliths will extend the possibilities of LC-MS in proteomics, notably for the comparative analysis of larger sets of samples in biomarker discovery research.

3.5 Other applications of silica-based monoliths in proteomics

In proteomics analysis, the digestion step is of critical importance. In-solution digestion often takes 12h or more. By immobilising proteases on a solid support, digestion kinetics can be greatly enhanced bringing digestion time down to minutes or even seconds [89]. Moreover, immobilisation often results in diminished autolysis [90,91]. Trypsin was adsorbed on monoliths exhibiting different morphological characteristics [33]. Immobilised trypsin was 10-20 times more active than in its free form and was stable for 4-6 weeks when stored at 4 or 25°C. Trypsin activity was monitored by following the catalytic hydrolysis of N-α-benzoyl-DL-arginine-*p*-nitroanilide (BAPNA) [92]. The immobilised trypsin could be reused for up to 6 cycles. At that point, 40% of the original amount of trypsin remained adsorbed. It is important to note that washing and reequilibration of the immobilised-trypsin monolith led to a loss of 10-15% trypsin every time. It was shown that catalytic efficiency (kcat/Km) increased with increasing mesopore diameter indicating that diffusional mass transfer played an important role. When trypsin was adsorbed onto the monolith with the largest pores (average pore size: 18 nm), the catalytic efficiency was almost 30 times higher than for trypsin in solution. Even when trypsin was immobilised on the monolith with the smallest pores (average pore size: 3.3 nm), the catalytic efficiency was twice as high as in solution [33], which shows that accessibility in large pores is crucial for enhanced digestion kinetics. The immobilisation of other enzymes on monoliths was also investigated. For example, the influence of the pre-immobilisation of glucose oxidase on silica beads prior to the sol-gel reaction on their activity was studied [40]. Glucose oxidase was first immobilised on a porous support prior to incorporation in a sol for the sol-gel reaction. Activity was found to decrease by only 10% when the enzyme was pre-immobilised whereas it lost as much as 60% when put directly in the

sol. Moreover, pre-immobilisation eliminated bleeding of the enzyme [40]. When protease P (from Aspergillus melleus) was immobilised, the internal diameter of the monolith was varied and found not to have any influence on the conversion rate of the substrate when the linear flow was kept constant [47]. Three monoliths of the same diameter were butt-connected and the conversion rate increased by as much as 50%. This protease P micro-bioreactor performed better at high flow rate than the control batch experiment whereas it did not match the conversion rates of the batch experiment at lower flow rate. It suggests that convective flow took place in the enzyme reactor at high flow rates and thereby enhanced the digestion rates. Frequently, proteomic samples are separated by 2D-PAGE and individual spots in-gel digested. These samples need to be desalted and enriched prior to off-line nanospray or MALDI analysis. To this end, a platform making use of pre-treatment tips based on monolithic stationary phases with various surface chemistries corresponding to biomolecules of various characteristics (hydrophilic, hydrophobic, phosphorylated) was developed [61]. C_{18} tips were employed for the desalting and concentration of peptide samples. Titania-coated tips were applied to the isolation of phosphopeptides (Figure 3.6), as titanium dioxide recognises phosphorylated substances. These tips exhibited satisfactory sample capacity and dead volumes for protein/peptide analysis and can be integrated in automated sample preparation systems. Further investigations towards the chemical derivatisation of silica monoliths will likely extend possibilities for sample pretreatment. MALDI is widely used for generating gas-phase ions from thermolabile bio-macromolecules notably in proteomics. To enhance its possibilities, a MALDI plate was modified with a silica monolith for the analysis of di- and tri-peptides [44]. The MALDI matrix, α-cyano-4-hydroxycinnamic acid, and the analytes were added to the sol before the sol-gel process took place on the MALDI plate. Different monoliths with varying pore sizes were synthesised but they all gave similar spectra. Though this approach may be beneficial with respect to sample capacity, it still needs to prove its practical relevance for complex proteomics samples.

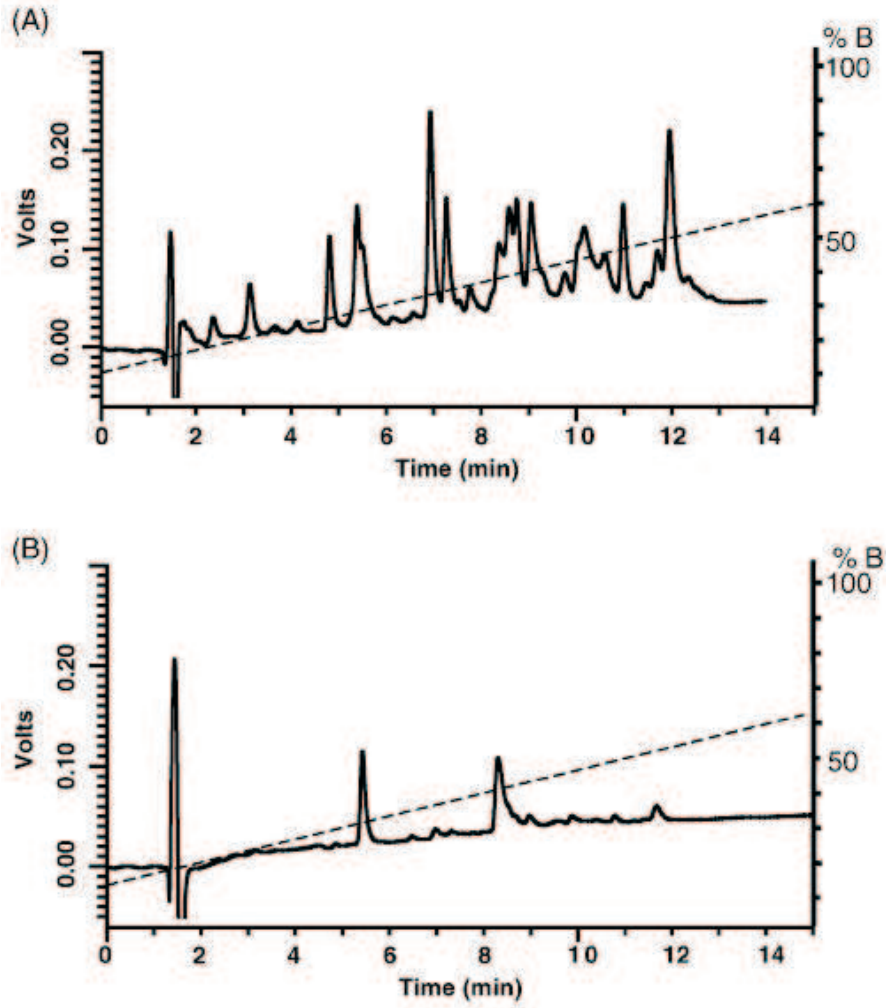

Figure 3.6: Pretreatment of a tryptic digest of β-casein using a titania-coated silica-based monolithic extraction tip to enrich phosphorylated peptides. (A) Chromatogram of sample without pretreatment, (B) Chromatogram of sample with pretreatment. LC analysis took place on a MonoCap silica-based capillary column (0.1 mm ID, 15 cm length). Mobile phases A and B consisted of 0.05% trifluoroacetic acid in water and acetonitrile respectively. (reprinted with permission from Miyazaki S., Morisato K., Ishizuka N., Minakuchi H., Shintani Y., Furuno M., Nakanishi K.; Journal of Chromatography A; 1043, 19; copyright 2004 Elsevier)

3.6 Conclusion

One of the latest developments in column technology is the development of monolithic columns, which overcome some of the limitations associated with packed columns when it comes to throughput and diffusion-limited mass transfer. Monolithic columns were first developed using organic monomers. Several years later, progress in silicium chemistry allowed preparing silica-based monoliths. The bimodal pore structure of silica monoliths exhibits large, interconnected throughpores and smaller mesopores inside the thin skeleton defining the throughpores. This results in high porosity and small distances over which the analytes diffuse. These characteristics allow very efficient separations at low pressures thereby enabling to speed up the analysis of complex samples. Two approaches seem to prevail in HPLC-related research on monoliths. The first is to obtain very efficient separation media by synthesising monoliths with very small throughpores and fine skeletons at the cost of an increased operating pressure. The second is to prepare monoliths with large throughpores requiring very low pressures thereby allowing very long columns to be used. Even though the effects of most synthesis conditions on the morphology of monoliths are understood, more research is needed to design more homogeneous and efficient stationary phases.

3.7 List of abbreviations

APTES:	(3-aminopropyl) triethoxysilane
BAPNA:	N-α-benzoyl-DL-arginine-p-nitroanilide
BET:	Brunauer-Emmett-Teller
BSA:	Bovine serum albumin
CEC:	Capillary electrochromatography
CEOS:	2-Cyanoethyltriethoxysilane
DGS:	Diglycerylsilane
ESI:	Electrospray ionisation
ETMS:	Ethyltrimethoxysilane
HPLC:	High-pressure liquid chromatography
LC:	Liquid chromatography
MALDI:	Matrix assisted laser desorption/ionisation
MS:	Mass spectrometry
MS/MS:	Tandem mass spectrometry
MTMS:	Methyltrimethoxysilane
PEG:	Poly-(ethylene)glycol

pI:	Isoelectric point
RPLC:	Reversed-phase liquid chromatography
SCX:	Strong cation exchange
SEC:	Size exclusion chromatography
SEM:	Scanning electron microscopy
TEM:	Transmission electron microscopy
TEOS:	Tetraethoxysilane
TMOS:	Tetramethoxysilane
TOF:	Time-of-flight
TSC:	Tetrahedral skeleton column
UHPLC:	Ultra high-pressure liquid chromatography
2D-LC:	Two-dimensional liquid chromatography
2D-PAGE:	Two-dimensional polyacrylamide gel electrophoresis

3.8 List of symbols

C_d:	Axial diffusion in the mobile phase
C_e:	Eddy dispersion
C_m:	Mass transfer in the mobile phase
C_{sm}:	Mass transfer in the stationary phase
d_{disp}:	Equivalent dispersion parameter
D_m:	Solute diffusion coefficient in the mobile phase
d_p:	Particle diameter
d_{perm}:	Equivalent permeability parameter
E:	Separation impedance
H:	Plate height
k_{cat}/K_m:	Catalytic efficiency
ηT:	Pore connectivity
P_t:	Pressure of transition
u:	Linear flow velocity

References

[1] P. H. O' Farrell; *Journal of Biological Chemistry* **250**, 4007 (1975)

[2] H. Schagger, G. Von Jagow; *Analytical Biochemistry* **166**, 368 (1987)

[3] M. P. Washburn, D. Wolters, J. R. Yates III; *Nature Biotechnology* **19**, 242 (2001)

[4] M. T. Davis, J. Beierle, E. T. Bures, M. D. McGinley, J. Mort, J. H. Robinson, C. S. Spahr, W. Yu, R. Luethy, S. D. Patterson; *Journal of Chromatography B: Biomedical Applications* **752**, 281 (2001)

[5] P. A. Bristow, J. H. Knox; *Chromatographia* **10**, 279 (1977)

[6] N. Tanaka, H. Kobayashi, K. Nakanishi, H. Minakuchi, N. Ishizuka; *Analytical Chemistry* **72**, 420A (2001)

[7] J. H. Knox; *Journal of Chromatography A* **960**, 7 (2002)

[8] I. Halasz, R. Endele, J. Asshauer; *Journal of Chromatography A* **112**, 37 (1975)

[9] J. E. MacNair, K. D. Patel, J. W. Jorgenson; *Analytical Chemistry* **71**, 700 (1999)

[10] J. E. MacNair, K. C. Lewis, J. W. Jorgenson; *Analytical Chemistry* **69**, 983 (1997)

[11] H. Fu, X. Huang, W. Jin, H. Zou; *Current Opinion in Biotechnology* **14**, 96 (2003)

[12] K. K. Unger, O. Jilge, J. N. Kinkel, M. T. W. Hearn; *Journal of Chromatography A* **359**, 61 (1986)

[13] N. B. Afeyan, N. F. Gordon, I. Mazsaroff, L. Varady, S. P. Fulton, S. B. Yang, F. E. Regnier; *Journal of Chromatography A* **519**, 1 (1990)

[14] T. B. Tennikova, M. Bleha, F. Svec, T. V. Almazova, B. G. Belenkii; *Journal of Chromatography A* **555**, 97 (1991)

[15] T. B. Tennikova, J. Reusch; *Journal of Chromatography A* **1065**, 13 (2005)

[16] E. F. Hilder, F. Svec, J. M. J. Frechet; *Journal of Chromatography A* **1044**, 3 (2004)

[17] N. Tanaka, T. Ebata, K. Hashizume, K. Hosoya, M. Araki; *Journal of Chromatography A* **475**, 195 (1989)

[18] H. Minakuchi, K. Nakanishi, N. Soga, N. Ishizuka, N. Tanaka; *Analytical Chemistry* **68**, 3498 (1996)

[19] P. Gzil, N. Vervoort, G. V. Baron, G. Desmet; *Analytical Chemistry* **76**, 6707 (2004)

[20] L. C. Hansen, R. E. Sievers; *Journal of Chromatography* **99**, 123 (1974)

[21] S. Hjerten, J. L. Liao, R. Zhang; *Journal of Chromatography A* **473**, 273 (1989)

[22] H. Kaji, K. Nakanishi, N. Soga; *Journal of Non-Crystalline Solids* **185**, 18 (1995)

[23] T. N. M. Bernards; *Silicate sol-gel chemistry as studied by hydrolysis-gelation time curves*; Phd thesis; Utrecht University, (1997)

[24] N. Ishizuka, H. Minakuchi, K. Nakanishi, N. Soga, N. Tanaka; *Journal of Chromatography A* **797**, 133 (1998)

[25] C. J. Brinker; *Journal of Non-Crystalline Solids* **100**, 31 (1988)

[26] C. J. Brinker, K. D. Keefer, D. W. Schaefer, C. S. Ashley; *Journal of Non-Crystalline Solids* **48**, 47 (1982)

[27] H. Minakuchi, K. Nakanishi, N. Soga, N. Ishizuka, N. Tanaka; *Journal of Chromatography A* **797**, 121 (1998)

[28] N. Ishizuka, H. Minakuchi, K. Nakanishi, N. Soga, H. Nagayama, K. Hosoya, N. Tanaka; *Analytical Chemistry* **72**, 1275 (2000)

[29] Z. G. Shi, Y. Q. Feng, S. L. Da; *Journal of Liquid Chromatography and Related Technologies* **26**, 2881 (2003)

[30] M. A. Brook, Y. Chen, K. Guo, Z. Zhang, W. Jin, A. Deisingh, J. Cruz Aguado, J. D. Brennan; *Journal of Sol-Gel Science and Technology* **31**, 343 (2004)

[31] N. Ishizuka, H. Kobayashi, H. Minakuchi, K. Nakanishi, K. Hirao, K. Hosoya, T. Ikegami, N. Tanaka; *Journal of Chromatography A* **960**, 85 (2002)

[32] K. Nakanishi, Y. Kobayashi, T. Amatani, K. Hirao, T. Kodaira; *Journal of Materials Chemistry* **16**, 3652 (2004)

[33] D. Goradia, J. Cooney, B. K. Hodnett, E. Magner; *Journal of Molecular Catalysis B: Enzymatic* **32**, 231 (2005)

[34] R. J. Hodfson, Y. Chen, Z. Zhang, D. Tleugabulova, H. Long, X. Zhao, M. Organ, M. A. Brook, J. D. Brennan; *Analytical Chemistry* **76**, 2780 (2004)

[35] J. H. Smith; *Chromatographic properties of silica-based monolithic HPLC columns*; Ph.D. thesis; Virginia State University, Chemistry Department (2002)

[36] M. Motokawa, H. Kobayashi, N. Ishizuka, H. Minakuchi, K. Nakanishi, H. Jinnai, K. Hosoya, T. Ikegami, N. Tanaka; *Journal of Chromatography A* **961**, 53 (2002)

[37] N. Ishizuka, H. Minakuchi, K. Nakanishi, K. Hirao, N. Tanaka; *Colloids and Surfaces A: Physicochemical and Engineering Aspects* **187-188**, 273 (2001)

[38] S. M. Fields; *Analytical Chemistry* **68**, 2709 (1996)

[39] R. Braunrath, M. Cichna; *Journal of Chromatography A* **1062**, 189 (2005)

[40] L. Betancour, F. Lopez Gallego, A. Hidalgo, M. Fuentes, O. Podrasky, G. Kuncova, J. M. Guisan, R. Fernadez Lafuente; *Biomacromolecules* **6**, 1027 (2005)

[41] S. Miyazaki, M. Y. Miah, K. Morisato, Y. Shintani, T. Kuroba, K. Nakanishi; *Journal of Separation Science* **28**, 39 (2005)

[42] Z. G. Shi, Y. Q. Feng, L. Xu, M. Zhang, S. L. Da; *Talanta* **63**, 593 (2004)

[43] Z. G. Shi, Y. Q. Feng, L. Xu, S. L. Da, Y. Y. Ren; *Microporous and Mesoporous Materials* **68**, 55 (2004)

[44] J. B. Laughlin, C. J. Cassidy, J. A. Cox; *Rapid Communications in Mass Spectrometry* **11**, 1505 (1997)

[45] M. C. Breadmore, S. Shrinivasan, K. A. Wolfe, M. E. Power, J. P. Ferrance, B. Hosticka, P. M. Norris, J. P. Landers; *Electrophoresis* **23**, 3487 (2002)

[46] D. Allen, Z. El Rassi; *Electrophoresis* **24**, 408 (2003)

[47] K. Kawakami, Y. Sera, S. Sakai, T. Ono, H. Ijima; *Industrial and Engineering chemistry research* **44**, 236 (2005)

[48] J. D. Badjic, N. M. Kostic; *Journal of Materials Chemistry* **11**, 408 (2001)

[49] T. Salesch, S. Bachmann, S. Brugger, R. Rabelo-Schaefer, K. Albert, S. Steinbrecher, E. Plies, A. Mehdi, C. Reye, R. J. P. Corrin, E. Lindner; *Advanced Functional Materials* **12**, 134 (2002)

[50] K. Nakanishi, H. Minakuchi, N. Soga, N. Tanaka; *Journal of Sol-Gel Science and Technology* **8**, 547 (1997)

[51] N. N. Khimich; *Glass Physics and Chemistry* **30**, 107 (2004)

[52] D. M. Krol, J. G. van Lierop; *Journal of Non-Crystalline Solids* **63**, 131 (1984)

[53] J. G. van Lierop, A. Huizing, W. C. P. M. Meerman, C. A. M. Mulder; *Journal of Non-Crystalline Solids* **82**, 265 (1986)

[54] F. Kirkbir, H. Murata, D. Meyers, S. R. Chaudhuri; *Journal of Non-Crystalline Solids* **225**, 14 (1998)

[55] F. Kirkbir, H. Murata, D. Meyers, S. R. Chowdhury; *Journal of Sol-Gel Science and Technology* **13**, 311 (1998)

[56] S. Dai, Y. H. Ju, H. J. Gao, J. S. Lin, S. J. Pennycook, C. E. Barnes; *Chemical Communications* 243–244 (2000)

[57] E. Calleri, G. Massolini, D. Lubda, C. Temporini, F. Loiodice, G. Caccialanza; *Journal of Chromatography A* **1031**, 93 (2004)

[58] Z. Chen, K. Uchiyama, T. Hobo; *Journal of Chromatography A* **942**, 83 (2002)

[59] E. Calleri, G. Massolini, F. Loiodice, G. Fracchiolla, C. Temporini, G. Felix, P. Tortorella, G. Caccialanza; *Journal of Chromatography A* **958**, 131 (2002)

[60] Z. Liu, K. Otsuka, S. Terabe, M. Motokawa, N. Tanaka; *Electrophoresis* **23**, 2973 (2002)

[61] S. Miyazaki, K. Morisato, N. Ishizuka, H. Minakuchi, Y. Shintani, M. Furuno, K. Nakanishi; *Journal of Chromatography A* **1043**, 19 (2004)

[62] H. Yang, Q. Shi, B. Tian, S. Xie, F. Zhang, Y. Yan, D. Zhao; *Chemistry of Materials* **15**, 536 (2003)

[63] C. G. Goeltner, M. C. Weissenberger; *Acta Polymerica* **49**, 704 (1998)

[64] L. R. Snyder, J. C. Giddings, R. A. Keller; *Principles of adsorption chromatography - The separation of nonionic organic compounds*; Marcel Dekker, New York (1968)

[65] C. Alie, R. Pirard, J. P. Pirard; *Colloids and Surfaces A: Physicochemical and Engineering Aspects* **187-188**, 367 (2001)

[66] J. Nawrocki, M. P. Rigney, A. McCormick, P. W. Carr; *Journal of Chromatography* **657**, 229 (1993)

[67] W. Werner, I. Halasz; *Journal of Chromatographic Science* **18**, 277 (1980)

[68] R. Nikolov, W. Werner, I. Halasz; *Journal of Chromatographic Science* **18**, 207 (1980)

[69] M. Careri, A. Mangia; *Journal of Chromatography A* **1000**, 609 (2003)

[70] H. Minakuchi, N. Ishizuka, K. Nakanishi, N.Soga, N. Tanaka; *Journal of Chromatography A* **828**, 83 (1998)

[71] D. Allen, Z. El Rassi; *Journal of Chromatography A* **1029**, 239 (2004)

[72] T. P. Hennessy, R. I. Boysen, M. I. Huber, K. K. Unger, M. T. W. Hearn; *Journal of Chromatography A* **1009**, 15 (2003)

[73] L. Xiong, R. Zhang, F. E. Regnier; *Journal of Chromatography A* **1030**, 187 (2004)

[74] Q. Tang, N. Wu, M. L. Lee; *Journal of Microcolumn Separation* **12**, 6 (2000)

[75] F. C. Leinweber, D. Lubda, K. Cabrera, U. Tallarek; *Analytical Chemistry* **74**, 2470 (2002)

[76] N. Vervoort, P. Gzil, G. V. Baron, G. Desmet; *journal of chromatography* **1030**, 177 (2004)

[77] A. I. Liapis, J. J. Meyers, O. K. Crosser; *Journal of Chromatography A* **865**, 13 (1999)

[78] J. J. Meyers, A. I. Liapis; *Journal of Chromatography A* **852**, 3 (1999)

[79] B. He, N. Tait, F. E. Regnier; *Analytical Chemistry* **70**, 3790 (1998)

[80] B. Barroso, D. Lubda, R. Bischoff; *Journal of Proteome Research* **2**, 633 (2003)

[81] F. C. Leinweber, D. G. Schmid, D. Lubda, B. Sontheimer, G. Jung, U. Tallarek; *Journal of Mass Spectrometry* **39**, 223 (2004)

[82] T. Koerner, K. Turck, L. Brown, R. D. Oleschuk; *Analytical Chemistry* **76**, 6456 (2004)

[83] L. Spoof, J. Meriluoto; *Journal of Chromatography A* **947**, 237 (2002)

[84] F. C. Leinweber, D. G. S. Schmid, D. Lubda, K. H. Wiesmuller, G. Jung, U. Tallarek; *Rapid Communications in Mass Spectrometry* **17**, 1180 (2003)

[85] N. I. Govorukhina, A. Keizer-Gunnink, A. G. J. van der Zee, S. de Jong, H. W. A. de Bruijn, R. Bischoff; *Journal of Chromatography A* **1009**, 171 (2003)

[86] V. V. Tolstikov, A. Lommen, K. Nakanishi, N. Tanaka, O. Fiehn; *Analytical Chemistry* **75**, 6737 (2003)

[87] H. Kimura, T. Tanigawa, H. Morisaka, T. Ikegami, K. Hosoya, H. Minakuchi, K. Nakanishi, M. Ueda, K. Cabrera, N. Tanaka; *Journal of Separation Science* **27**, 897 (2004)

[88] S. Wienkoop, M. Glinski, N. Tanaka, V. Tolstikov, O. Fiehn, W. Weckwerth; *Rapid Communications in Mass Spectrometry* **18**, 643 (2004)

[89] C. Wang, R. Oleschuk, F. Ouchen, J. Li, P. Thibault, D. J. Harrison; *Rapid Communications in Mass Spectrometry* **14**, 1377 (2000)

[90] M. T. Davis, T. D. Lee, M. Ronk, S. A. Hefta; *Analytical Biochemistry* **224**, 235 (1995)

[91] A. M. Girelli, E. Mattei; *Journal of Chromatography B: Biomedical Applications* **819**, 3 (2005)

[92] B. F. Erlanger, N. Kokowsky, W. Cohen; *Archives of Biochemistry and Biophysics* **95**, 271 (1961)

CHAPTER 4

Fast, High-Efficiency Peptide Separations on a 50-μm Reversed-Phase Silica Monolith in a nanoLC-MS Set-Up

4.1 Introduction

Highly efficient separations are the cornerstone of many analytical methods that deal with extremely complex mixtures. Examples are the analysis of the proteome of a cell, tissue or body fluid, which are currently the focus of many research activities in academic groups and pharmaceutical companies alike. Proteomic studies continue to foster the development of novel technologies able to comprehensively analyse large sets of proteins or peptides. These new analytical tools need to be fast and of sufficient resolving power to detect minute qualitative and quantitative changes in a protein profile. Monitoring such changes could lead to interesting new drug targets or diagnostic tools.

Until recently, two-dimensional polyacrylamide gel electrophoresis (2D-PAGE) [1] has been the method of choice for the analysis of complex protein mixtures. However, 2D-PAGE shows limitations when it comes to analysing proteins with extreme size and pI. Moreover, the dynamic range is often not sufficient to detect low-abundance proteins [2]. Attempts to overcome these limitations have led to the development of two-dimensional liquid chromatography (2D-LC) for protein and peptide analysis. 2D-LC requires less sample handling and can be more easily

automated. In addition, it can be coupled to mass spectrometry either on-line via electrospray ionisation (ESI) [3–5] or off-line after spotting onto a target plate for matrix-assisted laser desorption ionization (MALDI) [6, 7]. In order to increase peak capacity, the separation mechanisms in 2D-LC must be orthogonal, meaning that they must be based on different interaction principles [8]. Whereas many chromatographic retention mechanisms have been used in the first dimension, the favourite mode of separation for the second LC dimension is reversed-phase (RP). In order to make full use of RPLC coupled to MS/MS for peptide sequencing, the so-called shotgun method was developed by Yates and coworkers, which involves digesting a protein mixture with trypsin prior to separation [3, 9, 10]. Especially in its comprehensive form, complex peptide mixtures generated by shotgun proteomics have to be separated by 2D-LC, which often requires a full day of analysis time per sample [4, 11]. Consequently, great efforts continue to be made to optimise the separation efficiency of LC columns to reduce the overall analysis times. Options to improve separation efficiency include porous or non-porous particles of smaller diameter (i.e. 1 μm) [12], which come at the expense of an elevated backpressure. To circumvent the general problems resulting from the need for very high pressures for μm-sized particles and the low capacity of non-porous media, perfusion chromatography, was introduced [13]. Shortly thereafter, a new support for membrane chromatography was developed to achieve the same goal [14]. In these so-called organic monolithic materials, separation takes place on a very short and wide macroporous polymeric membrane characterised by low backpressures. However, organic polymers are often subject to swelling or shrinking in organic solvents and exhibit micropores [15], drastically deteriorating the performance of a column. A silica-based monolith designed for HPLC was synthesised [16] based on the hydrolysis and poly-condensation of alkoxysilanes [17]. It exhibited a bimodal pore structure with μm-sized throughpores and nm-sized mesopores. This structure allowed high-efficiency separations at very low backpressure. First synthesised in 9.0-mm-I.D. polycarbonate molds [16,18,19], silica monoliths have also been prepared in the capillary format [20, 21] and coupled to mass spectrometry for application in proteomics research [21–23]. The study of the proteome often requires high-sensitivity measurements and has thus stimulated further miniaturisation of monolithic chromatography columns. In this study, we present the evaluation of 50-μm-ID reversed-phase silica monoliths which are compatible with nanoelectrospray ionisation, using tryptic digests of standard proteins as well as a real-life sample. The influence of various chromatographic parameters on efficiency, resolution and analysis time was assessed. To demonstrate the capability of such an analytical system for high-resolution, high-speed separations, a tryp-

tic digest of depleted serum from a cervical cancer patient was analysed. The throughput time of this analysis was 30 min per sample, with peak widths of approximately 10 s at half height. High repeatability of retention times (0.5 - 1.6% relative standard deviation (RSD) between columns) and peak heights (<20% RSD without the use of an internal standard) in a nanoLC-MS set-up allowed comparative analyses of complex samples using these reversed-phase silica-based monoliths, as required in biomarker discovery projects.

4.2 Experimental

4.2.1 Chemicals

Formic acid (FA) and hexylbenzene (98-100% pure) were purchased from Merck (Darmstadt, Germany), and acetonitrile (HPLC Supra-Gradient grade) from Biosolve (Valkenswaard, The Netherlands). Horse-heart cytochrome c (CC) (>95% pure), dibutylaniline (DBA) (97% pure), ammonium bicarbonate and ammonium acetate (>98% pure) were purchased from Sigma-Aldrich (Zwijndrecht, The Netherlands). Modified trypsin (sequencing grade) was purchased from Promega (Leiden, The Netherlands).

4.2.2 Equipment

The nanoHPLC system was based on a Series 1100 set-up, consisting of a dynamic nanoflow splitter with flow meter, micro vacuum degasser, thermostated microwell-plate autosampler with a six-port micro switching valve combined with a thermostated column compartment, six-port micro switching valve and ion trap SL mass spectrometer (Agilent Technologies, Waldbronn, Germany) [5]. The nanoelectrospray ion source was modified in-house to minimise post-column dead volumes (<20 nL). Nanoelectrospray tip and analytical column were butt-connected using a teflon sleeve of 360-μm ID, thereby reducing post-column dead volumes by approximately 80% as compared to the original design. The C_{18} trap column was loaded using an ISCO pump model 2350 from Teledyne ISCO, Inc. (Wierde, Belgium).
The loading pump was directly connected to the microwell-plate autosampler, so that the flow passed through the micro switching valve, sample loop and needle. The sample plug was concentrated on a C_{18} trap column, which was mounted between two ports of the switching valve in the thermostated column compartment. The flow was further directed to waste during sample loading. The nanopump

was also connected to this second micro switching valve, in order to direct the flow through the trap column and elute the analytes onto the monolithic (analytical) column in the backflush mode. The analytical column was butt-connected to the gold-coated nanoelectrospray emitter (50-μm fused-silica capillary tapered to 10 μm ID, Nanoseparations, Nieuwkoop, The Netherlands) using a 360-μm-ID Teflon sleeve, and subsequently mounted in front of the nanoelectrospray source entrance.

4.2.3 Liquid chromatography

The following conditions were used for the analysis of tryptic peptides throughout this study, unless otherwise stated:
Analytical column: silica-based reversed-phase (C_{18}) monolith, 560 x 0.05 mm, fabricated for research purposes using a method similar to that reported in [20] (Merck, Darmstadt, Germany). Capillaries prepared following this procedure generally exhibit throughpores of 2-3 μm, a skeleton of 1.0-1.5 μm and mesopores of 18 nm.
Trap column: Zorbax 300 SB C_{18}, 5 μm particle diameter (d_p), 5 x 0.3 mm (Agilent, Waldbronn, Germany)
The loading pump delivered a solution of 0.1% FA in water: acetonitrile (ACN) (97.5:2.5) at 50 μL/min. The trap column was switched on-line with the analytical column after a 5-min loading time.
Gradient elution was performed with 0.1% FA in water as mobile phase A and 0.1% fa in ACN as mobile phase B. Gradient elution, unless otherwise stated, was performed according to the following scheme: 2.5% B from 0 to 5 min, linear increase to 40% B in 25 min, linear increase to 80% B in 5 min, column wash at 80% B for 4 min, return to initial conditions (2.5% B) in 6 min. Equilibration of the column at 2.5% B for 10 min. The flow rate was set as described in the Results section.

4.2.4 Mass spectrometry

The following settings were used throughout this study. Ionisation parameters for nanoelectrospray experiments: drying gas (N_2), 6.0 L/min; temperature, 285°C; capillary exit voltage, 115.0 V (CC experiments) and 106.5 V (DBA experiments); skimmer voltage, 40.0 V. The capillary voltage was set between 1550 and 2650 V, depending on the flow rate and the slope of the gradient. Ionisation parameters for experiments using the standard ESI source: nebulising gas (N_2), 16.0 psi; drying gas (N_2), 6.0 L/min; temperature, 285°C. The capillary voltage was set

at 3200 V, below which no stable signal could be obtained. For peptide analysis, the mass analyser parameters were: octapole 1 DC, 12.0 V; octapole 2 DC, 2.24 V; octapole RF, 150 Vpp; lens 1, -5.0 V; lens 2, -60.0 V; trap drive, 78.6 V. For DBA, the mass analyser parameters were: octapole 1 DC, 12.0 V; octapole 2 DC, 1.70 V; octapole RF, 132.8 Vpp; lens 1, -5.0 V; lens 2, -60.0 V; trap drive 29.5 V. For both types of experiments, the following parameters were kept constant: dampening gas, He; target, 30 000 ions; maximum accumulation time, 30.0 ms; number of averaged scans: 4; rolling average 'ON', number: 2.

4.2.5 Sample preparation

4.2.5.1 Tryptic digest of cytochrome c

0.5 mg CC was dissolved in 50 μL of freshly made 100 mM ammonium bicarbonate (pH $\approx$ 8.0). 50 μL of trypsin (0.4 mg/mL trypsin in 100 mM acetic acid in water), 25 μL $CaCl_2$ (100 mM) and 425 μL NH_4HCO_3 (100 mM) were added to the vial containing the CC solution. The mixture was incubated overnight at 37°C and 350 rpm in an Eppendorf thermomixer. After about 16 h, the solution was diluted 100 times with 0.1% FA in water: ACN (97.5:2.5) to a concentration of 833 fmol/μL. The sequence, molecular weight, m/z and assigned number of the studied peptides are shown in Table 4.1. For a second batch of CC tryptic digest, prepared using the same protocol, peptide 6 was not observed. The more hydrophilic peptide 7 was studied in place of peptide 6.

Peptide Number	Sequence	Molecular Weight	m/z
1	KTGQAPGFSYTDANK	1584.7	529.8 and 793.2
2	TGQAPGFSYTDANK	1456.8	729.3
3	EDLIAY	723.6	723.6
4	MIFAGIK	779.8	390.8 and 779.5
5	TGPNLHGLF	955.5	478.8
6	GITWGEETLMEYLENPK	2010.0	671.0 and 1005.5
7	IFVQKCAQCHTVEK	1633.8	545.7

Table 4.1: Assigned number, amino acid sequence, molecular weight and m/z of selected tryptic peptides of cytochrome c. Peptides 3 & 5 resulted from the digestion of CC by residual chymotryptic activity present in the trypsin stock solution.

4.2.5.2 Preparation of a tryptic digest of human serum

Serum was obtained from the Department of Gynecological Oncology (University Medical Center Groningen, The Netherlands) and depleted of albumin and γ-

globulins as previously described [24]. 1.26 pmol/μL CC were added to the original serum for internal calibration. The depleted serum was subsequently digested with trypsin as described above at an enzyme-to-total protein ratio of 1:20.

4.2.5.3 Preparation of dibutylaniline and hexylbenzene solutions

A solution of 4.4 μM DBA was prepared by making 6 consecutive dilutions of 1 volume of DBA solution in 9 volumes of 10 mM ammonium acetate (pH = 6.86): ACN (1:9), starting from pure liquid DBA (molecular weight = 205.35 g/mol, density = 0.906, m/z = 206.4). A solution of 1.06 mM hexylbenzene was prepared by diluting 20 μL of pure hexylbenzene (molecular weight = 162.28 g/mol, density = 0.861) solution to 100 mL using methanol : water (80:20).

4.2.6 Determination of column and system characteristics

4.2.6.1 Optimum plate height for dibutylaniline and hexylbenzene

For independent determination of the optimum height equivalent of a theoretical plate (HETP) value for the 50-μm-ID monolithic column, a chromatographic system where both the flow and the sample are split before the column was used. Post-column band broadening was minimised using a capillary electrochromatography (CEC) UV detection cell directly connected to the column. The CEC cell was a Knauer K-2501 model (Knauer, Berlin, Germany) fitted with a 100-μm ID/ 360-μm OD capillary with a window for detection. A split ratio between 1:600 and 1:1000 was obtained, depending on the pressure produced by the monolithic column. Column flow rates between 0.1 and 0.2 μL/min were obtained (0.81 to 1.62 mm/s, respectively). A 1.0 μL sample was injected and split before the column to bring a 1.0-to-2.0 nL sample plug onto the column. Separation efficiency was determined under isocratic conditions with 10 mM ammonium acetate (pH 6.86) and ACN, at a ratio of 1:9 (v/v) for a sample containing 4.4 μM DBA in 10 mM ammonium acetate (pH = 6.86): ACN (1:9). For hexylbenzene, isocratic elution conditions were methanol/water at a ratio of 80:20 (v/v). Hexylbenzene was injected as a solution prepared in mobile phase.

4.2.6.2 Van Deemter curve for cytochrome c digest

1 μL of digested 833 nM CC in 0.1% formic acid in water: ACN (97.5:2.5) was injected onto the nanoLC system (trap column + monolithic column) at varying flow rates, from 0.25 to 1.95 μL/min (linear velocities between 2.4 and 18.4 mm/s) at a constant mobile phase composition of 25% ACN in 0.1% aqueous formic

acid. Five injections were made at each flow rate, and the average HETP was determined.
The Van Deemter curve for the monolithic column without the trap column was determined in a similar fashion, by injecting 1.0 μL of a solution of 833 nM CC tryptic digest in 0.1% formic acid in water: ACN (97.5:2.5) directly onto the column under the same chromatographic conditions used above, to focus the peptides at the beginning of the column. This methodology was also applied to assess the linear flow rate dependence for the HETP obtained for DBA. Eluent conditions as described in section "Optimum plate height for dibutylaniline and hexylbenzene".

4.2.6.3 Loadability and capacity for cytochrome c digest

The loadability of the system and the capacity of the monolithic column were evaluated by injecting increasing amounts of a CC tryptic digest ranging from 10 ng (833 fmol) to 8.0 μg (666 pmol).

4.2.6.4 Optimisation of chromatographic parameters for rapid separations

The influence of flow rate on resolution under gradient elution conditions was investigated by injecting 833 fmol of CC tryptic digest 5 times each at flow rates ranging from 0.25 to 1.95 μL/min and a gradient slope of 1.5 %. Similarly, the effect of gradient slope on the separation was examined by injecting 833 fmol of CC tryptic digest 5 times consecutively at each gradient slope, ranging from 0.25 to 9.0 %, at a flow rate of 1.0 μL/min.
To shorten the analysis time of depleted, digested serum from a cervical cancer patient, we used a reduced loading time for the trap column (1 min at 50 μL/min) and increased the flow through the monolithic column to 1.5 μL/min. Gradient slope was 3.0 % between 10 and 40% and 4.0 % up to 80%, a composition that was maintained for 4 min. The column required an equilibration time of 5 min at 1.75 μL/min at the end of the cycle reducing the total cycle time to 30 min.

4.3 Results and Discussion

4.3.1 Chromatographic efficiency of 50 μm reversed-phase silica-based monoliths

Traditionally, low-molecular-weight compounds such as benzene derivatives have been used to characterise silica-based reversed-phase monoliths [25] and RPLC columns in general. Chromatographic performance of the 50 μm silica-based monolith was thus first evaluated by studying the relationship between HETP and the linear flow rate for the analytes DBA and hexylbenzene. To avoid extracolumn contributions to band broadening, a split-flow system was used, and detection was performed by UV absorbance in a CEC detector cell. Isocratic elution gave minimum HETPs between 7 and 9 μm at linear flows between 1 and 2 mm/s for DBA, and 11 μm at 1 mm/s for hexylbenzene. Similar results are reported for other monoliths [19], including a 50-μm-ID-sized silica-based monolith [20].

Monolithic columns have high column permeability and small-sized skeletons that decrease the diffusion pathlength of molecules in the stationary phase, resulting in a reduced contribution of both the A- and C-terms to band broadening. This characteristic is of special interest for molecules having low diffusion coefficients, such as proteins and peptides. Taking this into account, the system efficiency was also evaluated for selected tryptic peptides of CC, mimicking the situation encountered in proteomics applications.
A tryptic digest of CC in 0.1% aqueous FA : ACN (97.5:2.5) was analysed under isocratic conditions of 25% ACN in 0.1% aq. FA over a linear flow range of 2 to 18 mm/s (0.25 to 1.95 μL/min). Direct injections were made onto the monolithic column (no trap column), and detection was by nanoelectrospray MS. Figure 4.1 shows that minimum HETP of 5 to 10 μm were obtained at a linear flow velocity of 2.4 mm/s. HETP increased to approximately 140 μm at the upper end of the linear flow range, a region that cannot be studied in conventional packed columns. It should be noted that even the use of more than 4000 bars in UltraHigh Pressure Liquid Chromatography (UHPLC) [26] does not allow linear flows of this magnitude. Thus, HETP values for a low-molecular-weight analyte (DBA) and tryptic peptides from CC were comparable under similar flow conditions.
In order to evaluate performance under conditions usually employed for proteomics samples, the peptide mixture was injected onto a nanoLC-MS system containing a trap column. The analyses showed that the contribution of the trap

column to the overall efficiency was negligible. Omission of a trap column in the system led to slightly reduced performance for the most hydrophilic peptides. For example, peptide 2 (see Table 4.1) had a peak width at half height ($w_{0.5}^{-}$) of 5.2s (RSD = 22.7%) without a trap column, while $w_{0.5}^{-}$ was 4.8s (RSD = 15.3%) with the trap column (based on extracted-ion chromatograms). This was likely due to band broadening induced by the rather large injection volume. Since omission of a trap column is not practical for proteomics applications, we pursued evaluation of the complete system, including the trap column.

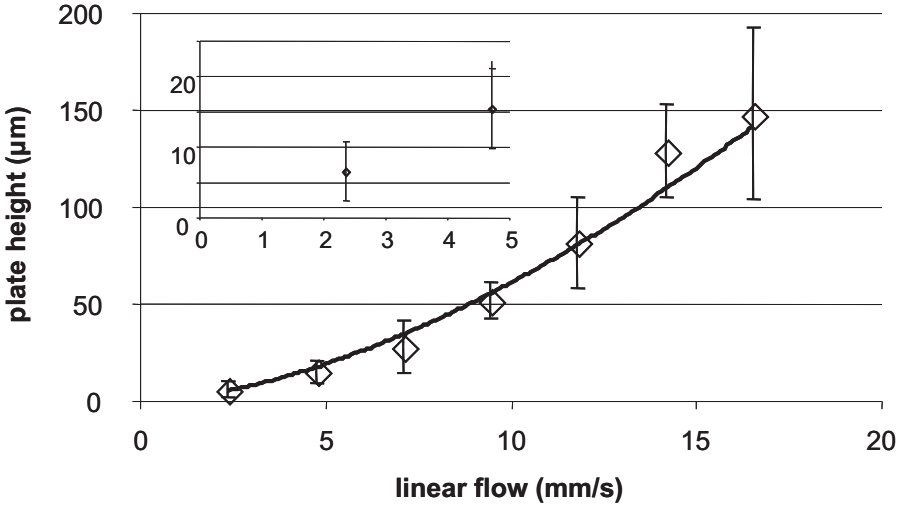

Figure 4.1: Van Deemter curves for a 50-μm-ID silica-based reversed-phase monolith for a tryptic digest of CC (diamonds) (isocratic in 0.1% FA in water: ACN (3:1)). Each point is the average of 5 determinations for the 6 different CC peptides and standard deviations are shown as error bars. Flow rate was varied between 0.25μL/min and 1.75 μL/min (average plate height of 6 peptides) corresponding to a linear flow range of 2.0 to16.5 mm/s.

4.3.2 Repeatability

Comparative proteomics analyses require that separations be highly reproducible, notably with respect to retention times. To evaluate the repeatability of separations on 50-μm silica-based reversed-phase monoliths, a tryptic digest of CC was injected 24 consecutive times onto two different monolithic columns on different days and analysed by nanoLC-MS. The separations were performed using gradient elution at 1.5 %. Separation showed an intra-column repeatability of <0.5% relative standard deviation (RSD) for retention times and <15% for peak widths

at half height. The MS signal intensity showed a RSD of <35%. Inter-column reproducibility proved to be very high, with RSDs of the corrected retention times between 0.5 and 1.6%. Inter-column reproducibility for peak width at half height showed RSDs between 13 and 30%. This relatively large variation in peak width originates primarily from spray instability rather than from differences in separation efficiency between columns. The results obtained for reproducibility of retention time agree well with the findings of Kele et al., who reported RSD values inferior to 0.2% for retention times and between 1 and 4% for peak width at half height in a long-term reproducibility experiment [27]. Instability of the nanoelectrospray signal was the main cause for the lower repeatability in peak width or intensity in the nanoLC-MS system as compared to UV detection (Figure 4.2 and Table 4.2). Even though repeatability is negatively affected by some instability of the nanoelectrospray, it was our intention to evaluate the system under conditions normally required for high-sensitivity proteomics work. The retention time repeatability and stability over time for the evaluated silica monoliths is promising with respect to their future use in comparative biomarker studies and for proteomics in general.

	Retention times (min)		Peak width at half height (min)		Peak height (counts)	
	Average	RSD (%)	Average	RSD (%)	Average	RSD (%)
Peptide 1	18.96	0.49	0.16	6.89	591445	10.59
Peptide 2	19.94	0.48	0.16	8.34	7451711	9.74
Peptide 3	22.77	0.35	0.19	8.28	3152229	17.51
Peptide 4	22.97	0.36	0.20	13.97	4577364	19.71
Peptide 5	24.69	0.28	0.20	9.87	5065457	12.95
Peptide 7	27.83	0.10	0.14	9.39	1789507	35.43

Table 4.2: Repeatability of retention times, peak widths at half height and peak heights for a silica-based monolith (50 μm ID) as assessed by 24 consecutive injections of a cytochrome c tryptic digest in the course of one day. Peptide 6 was not observed due to a missed cleavage, peptide 7 was the most hydrophobic peptide in this case (see Table 1 for peptide identities).

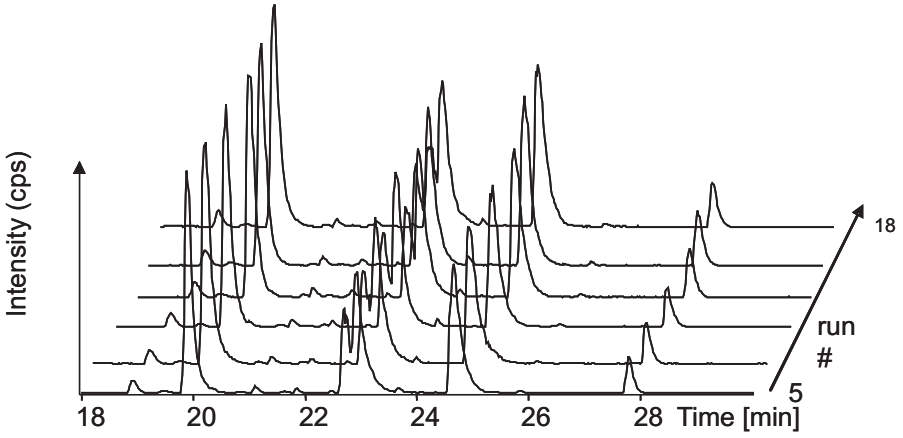

Figure 4.2: Repeatability of the separation of selected tryptic peptides (peptides 1 to 7 except peptide 6, cf. Table 4.1) of CC with 1.5% gradient slope and a flow rate of 1.0 μL/min. Runs were performed over 24 h. Not all chromatograms are shown. The lowest chromatogram corresponds to run number 5, while the highest chromatogram corresponds to run number 18. Combined extracted ion chromatograms corresponding to the m/z values reported in Table 4.1.

4.3.3 System loadability

Monolithic stationary phases attempt to combine high efficiencies at relatively low pressures with sample loadabilities comparable to porous silica particles. This is achieved through a bimodal pore size distribution [28]. Sample loadability is of great importance in proteomics studies, since many peptides of interest occur at low relative abundances in the sample.

Loadability of a column can be determined by either injection of increasing amounts of sample (elution chromatography) or by continuous infusion of sample until it appears in the breakthrough (frontal chromatography) [29]. In a nanoLC system consisting of a trap and an analytical column, it is important to evaluate the loadability for both columns. The trap column serves to quantitatively retain analytes, and can be almost saturated with peptides, as long as the monolithic (analytical) column has sufficient loading capacity and a stronger hydrophobicity than the trap column to refocus the analytes. The loadability of the trap column was first determined by applying increasing amounts of a CC tryptic digest ranging from 10 ng (833 fmol) to 8.0 μg (666 pmol). Elution was performed with a gradient slope of 1.5 % and a flow rate of 1.0 μL/min. The peak area for each peptide was chosen as an indicator of overloading of the trap column, due to loss

of peptides to waste as a result of breakthrough during loading and washing. Injections of increasing amounts of a tryptic CC digest resulted in an increase in peak area up to approximately 1.0 μg (83.3 pmol). For larger amounts, the peak area of the early eluting peptides started to decrease while the peak area kept on increasing for the more hydrophobic peptides (Figure 4.3). This shows that competition for the stationary phase occurred on the trap column, and that the most hydrophilic peptides started breaking through due to displacement by the more hydrophobic peptides. There was no indication of peptides in the flow-through of the monolithic column at a loaded amount of 1.0 μg, showing that overloading occurred on the trap column and not on the monolith. Therefore, it is important that the amount of sample injected onto this system remains smaller than 1.0 μg for a trap column of 5 $\times$ 0.3 mm (void volume $\approx$ 1.0 μL) in order not to perturb the original composition of the sample by selectively losing the more hydrophilic peptides to waste.

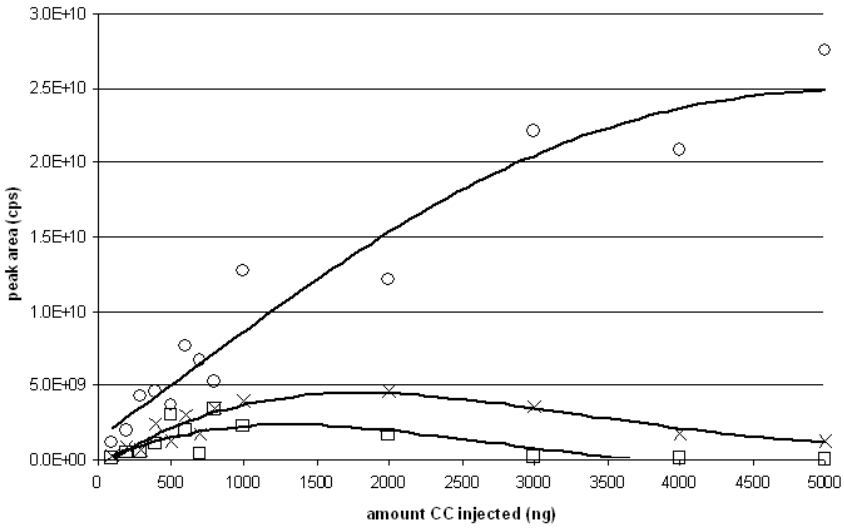

Figure 4.3: Capacity of the nanoLC-MS system with respect to a tryptic digest of CC. Increasing amounts of a CC digest were loaded at 50 μL/min onto a trap column with 0.1% FA in water: ACN (97.5:2.5). Separation was performed with a 1.5% gradient slope at a flow rate of 1.0 μL/min. (peptide 2, squares; peptide 4, crosses; peptide 6, circles). For peptide identities, see Table 4.1.

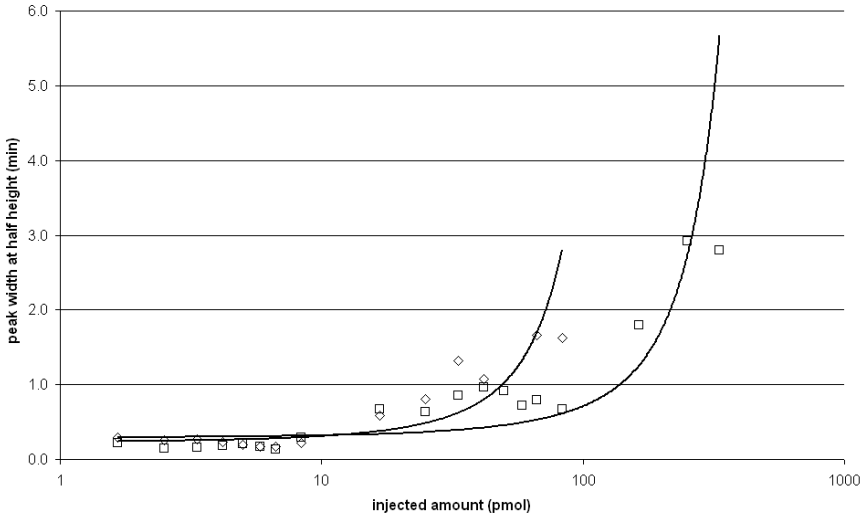

Figure 4.4: Evaluation of the capacity of the 50 μm monolithic reversed-phase column by measuring the peak width at half height versus the amount of loaded tryptic CC digest. Increasing amounts of the CC digest were loaded in 1 μL of 0.1% FA in water: ACN (97.5:2.5) and the separation was performed with a 1.5% gradient slope at a flow rate of 1.0 μL/min. The column is considered to be overloaded when the peak width increased by 20% or more compared to its original value. Points above the breakthrough point on the trap were not included. (peptide 3, diamonds (early eluting); peptide 6, squares (late eluting)). See Table 4.1 for peptide identities.

To evaluate the loading capacity of the monolithic column in a nanoLC-MS set-up, increasing amounts of a CC digest were loaded. An analytical column is considered overloaded with respect to a given component when the retention time of the analyte diminishes, the resolution between two compounds in a mixture decreases (increasing peak widths) and peak fronting appears, leading to an increase in the HETP. We chose to measure the peak width at half height as a sensitive indicator of overloading. The column was considered to be overloaded when the peak width increased by 20 % [26]. Overloading became apparent above 8.3 pmol (100 ng) CC digest (Figure 4.4), although this amount is well below the total loading capacity of the monolith. Larger amounts of tryptic digest resulted in excessive peak broadening, dramatically lower plate numbers and thus a much reduced resolution. For amounts greater than 1.0 μg of proteolytic digest, displacement effects on the monolith became visible, as exemplified for peptide 4

(Figure 4.5). A marked peak sharpening due to displacement of peptide 4 by the more hydrophobic peptide 6 on the analytical column was observed.

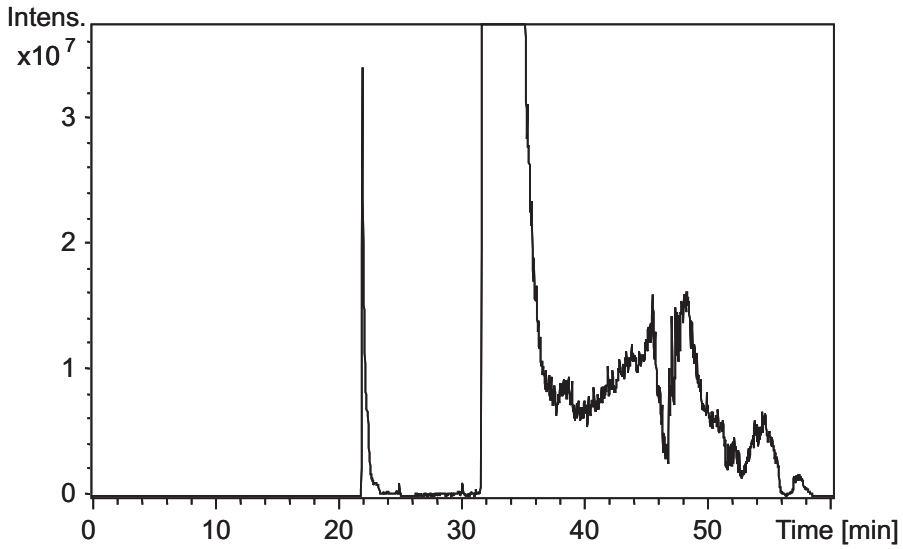

Figure 4.5: Example of displacement of peptide 4 (appr. 22 min) by a larger amount of the more hydrophobic peptide 6 (appr. 32 min) at a sample load of 3.0 μg (appr. 250 pmol). Separation with a 1.5% gradient slope at a flow rate of 1.0 μL/min. Combined extracted ion chromatograms of tryptic peptides 4 and 6 of CC (cf. Table 4.1).

The capacity of a column is related to its accessible surface area. Leinweber et al. [30] showed that silica monoliths have a specific surface area comparable to that of a capillary of similar dimensions packed with 5-μm porous silica particles. 1.5-μm ethyl-bridged hybrid silica porous particles [26] exhibit a specific surface area comparable to that of both monolith and conventional porous silica particles. To compare the capacity of columns of different dimensions filled with different materials, it is easier to refer to the capacity (in mol or g) divided by the capillary volume (in μL). From the data reported by Jorgenson and coworkers [26], ratios of 0.45 to 0.9 pmol/μL and 14 to 19 pmol/μL were calculated for 1.0-μm non-porous silica particles and 1.5-μm ethyl-bridged hybrid silica porous particles, respectively. Smith et al. [31] reported a capacity between 0.15 and 1.5 μg for a complex peptide mixture, depending on the experimental conditions for a 150-μm-ID capillary packed with 5-μm porous silica particles. This yielded capacity-to-

column volume ratios of 8.5 to 85 ng/μL. The monolith used in this study showed good resolution up to about 10 pmol/μL or 100 ng/μL and therefore exhibits a capacity comparable to porous silica particles and highly superior to non-porous particles.

4.3.4 Optimisation of chromatographic parameters for rapid separations

An important aspect of high-performance separations is the reduction of separation time to a minimum, especially in proteomics studies, where large numbers of samples need to be compared. In the following, we have investigated how the overall analysis time can be shortened for complex biological samples by exploiting the unique properties of silica-based monoliths.

4.3.4.1 Influence of flow rate and gradient slope on chromatographic resolution

Except for peptides 3 and 4, which were very difficult to separate, resolution decreased marginally up to a maximum flow rate of 1.95 μL/min under gradient elution conditions (data not shown). This flow rate is 10 times higher than for columns of similar internal diameter packed with 5-μm beads, and makes it possible to regenerate and re-equilibrate the monolith-based capillary column much faster than regular columns. These flow rates are also much larger than those achieved in UltraHigh-Pressure Liquid Chromatography (UHPLC), but are generated at a fraction of the column pressure [26].
In order to shorten analysis time, we investigated the effect of increased gradient slope on resolution in the 50 μm monolith. Gradient slopes ranging from 0.25 to 9.0 % were investigated for the separation of a tryptic digest of CC (Figure 4.6). All peptides, except the closely eluting peptides 3 and 4, were adequately separated (resolution >1.25) within a time window of 3 min at 9% and a flowrate of 1 μL/min (Figure 4.6, lower trace). The use of a gradient as steep as 15% was investigated, but the time saved on the analysis was not large enough to compensate for the long time required by the pump to generate a stable flow.
In practice, sample complexity and the required sensitivity in MS detection dictate the maximum gradient slope and flow rate that can be employed. A relatively simple separation could be performed at 2.0 μL/min and a gradient of 9%. More complex mixtures may have to be analysed at lower flow rates with flatter gradients to increase resolution and especially to facilitate high-sensitivity nanoelectrospray.

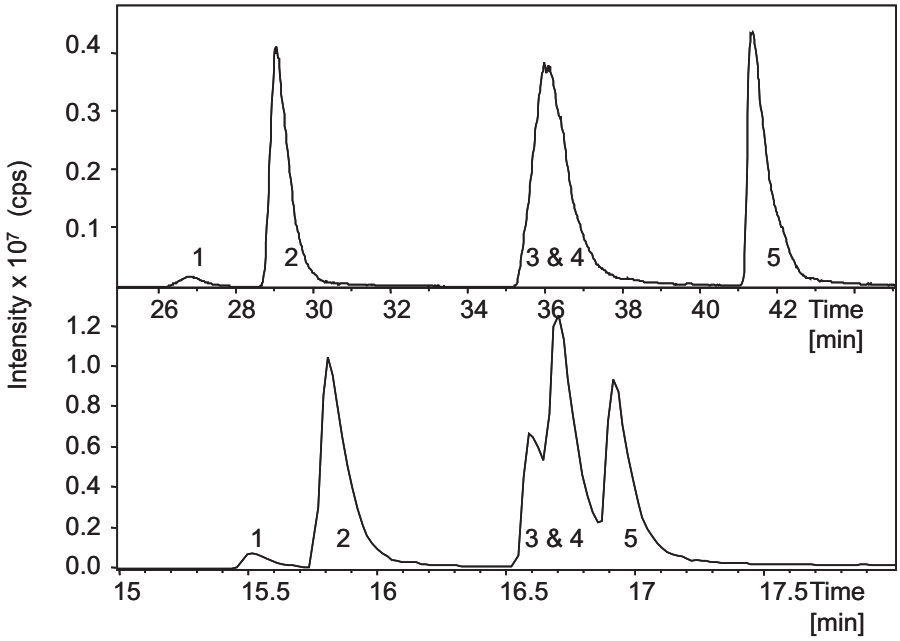

Figure 4.6: Effect of gradient slope on resolution between selected tryptic peptides of CC (cf. Table 4.1) at 0.25 (upper trace) and 9.0 % (lower trace) at a flow rate of 1.0 μL/min. Combined extracted ion chromatogram of peptides 1 through 5 (see Table 4.1 for m/z ratios).

4.3.4.2 Application of high-speed separations to a tryptic digest of serum from a cervical cancer patient

The study of diseased states by monitoring biomarkers is an increasingly important field in proteomics research. Serum is a highly complex biofluid often used in clinical studies for this purpose. In order to enhance the capability of analytical methods to detect proteins of lower abundance, it may be advantageous to first deplete the serum of high-abundance proteins [24, 32, 33] followed by tryptic digestion of the remaining proteins. This generates extremely complex mixtures of peptides. Analytical methods have been developed to study the serum proteome of cervical cancer patients by LC-MS with chromatographic separation times on the order of 3 h per run (unpublished results). In a field where samples from many patients have to be analysed, such run times contribute significantly to the overall analysis time and make larger clinical studies extremely time-consuming. Using the 50-μm-ID monolithic capillary column described, we attempted to in-

crease sample throughput for nanoLC-MS. This was done by using short loading times (1 min) for the trap column at 50 μL/min, as well as a high flow rate and a steep gradient on the analytical column. Using this approach, the total cycle time was reduced by a factor of 6 to a total of 30 min while retaining good chromatographic resolution. Peak widths at half height were on the order of 10 s, as shown for the extracted ion chromatogram of an endogenous peptide (Figure 4.7).

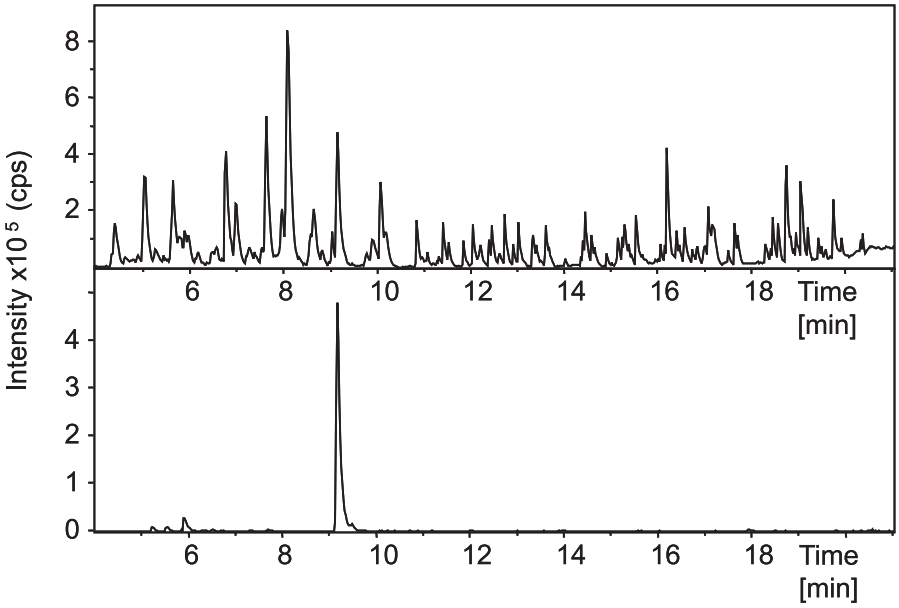

Figure 4.7: Analysis of a tryptic digest of depleted serum from a cervical cancer patient showing short analysis time and narrow peaks. (upper trace: base peak chromatogram; lower trace: extracted ion chromatogram of a peptide fragment at m/z = 694.4). 1.0 μL of depleted serum spiked with CC for internal standardisation ($\approx$1.25 pmol serum calculated on the basis of an average molecular weight of 50000 Da and 1.26 pmol of CC) was digested with trypsin. Separation was performed with a 3.0% gradient slope at a flow rate of 1.5 μL/min.

The use of small (1.5 μm dp), non-porous particles in 150-μm-ID capillaries has resulted in comparable run times as described here for the analysis of proteolytic digests, but at the expense of a sharply decreased loading capacity. Long (up to 80 cm) 150-μm-ID columns packed with 3.0-μm-dp porous particles were also able to resolve very complex peptide mixtures in about 30 min but at significantly higher column pressures [34, 35]. Recently, Jorgenson [26] investigated the use of even

smaller, hybrid porous silica particles (1.5-μm-dp ethyl-bridged silica) that can withstand pressures up to about 5000 bars in 30-μm-ID and 15-cm-long capillaries. It proved possible to separate small compounds very efficiently (h_{min} = 2.5-3.0 μm at 1.5 mm/s). However, the use of small particles in conjunction with relatively long capillaries requires the purchase of special UHPLC systems that can operate at pressures greater than 1000 bars [26]. Monolithic columns are a compromise in this area, in that they allow very fast separations at pressures that can be handled by any conventional HPLC system, while maintaining acceptable loading capacities. Our investigation of a 50-μm silica-based reversed-phase monolith for nanoLC-MS of peptide mixtures shows that very efficient separations can be achieved in a total analysis time of less than 30 min without requiring more than 300 bars pressure. When sample complexity can be reduced, for example by introducing a first-dimension pre-fractionation, even shorter throughput times ($\approx$ 4 min) can be obtained using very short monoliths at high flow rates and gradient slopes [36].

4.4 Conclusion

A 50-μm reversed-phase silica-based monolith was chromatographically characterised by nanoLC-MS with special emphasis on proteomics applications. The high efficiency of this material and its low resistance to flow allowed separation of highly complex mixtures in a fraction of the analysis time usually achieved with porous particle-packed columns. Peak widths at half height were on the order of 10 s. A wide range of flow rates, up to 1.95 μL/min, and gradient slopes, from a conventional 0.5 % to an unusually fast 9%, could be efficiently used. Depending on the complexity of the separation, a large increase in flow rate and/or gradient slope resulted in only a limited loss in resolution. Separations showed very high repeatability over time, which will be a great asset for future comparative biomarker studies and for proteomics in general. Two measures for loadability were determined during the evaluation of the nanoLC-MS system. The loadability of the trap column was large, with up to 1.0 μg sample retained. The capacity of the monolith, which accounts for the amount of analyte that can be loaded onto the column without deteriorating the quality of the separation, was equal to $\approx$ 10 pmole (or 100 ng in the case of a tryptic digest of CC).
Use of monoliths to their full extent is limited by nanoLC instrumentation, with which it is difficult to generate very steep gradients (15 %). In addition, nanoelectrospray interfaces function best at flow rates below 1 μL/min [37] and the relatively large peak volume at high flow rates does not favour high sensitivity

analyses.
For fast, high-resolution separations of complex samples, the 50-μm-ID reversed-phase monolith investigated in this study appears to be a viable alternative to the recently introduced UHPLC systems We expect that rapid separations by nanoLC-MS on columns based on silica monoliths will extend the possibilities for proteomics, notably for the comparative analysis of larger sets of samples. The good repeatability in terms of retention times is encouraging in this respect.

References

[1] P. H. O' Farrell; *Journal of Biological Chemistry* **250**, 4007 (1975)

[2] S. P. Gygi, G. L. Corthals, Y. Zhang, Y. Rochon, R. Aebersold; *PNAS* **97**, 9390 (2000)

[3] M. P. Washburn, D. Wolters, J. R. Yates III; *Nature Biotechnology* **19**, 242 (2001)

[4] M. T. Davis, J. Beierle, E. T. Bures, M. D. McGinley, J. Mort, J. H. Robinson, C. S. Spahr, W. Yu, R. Luethy, S. D. Patterson; *Journal of Chromatography B: Biomedical Applications* **752**, 281 (2001)

[5] E. Nagele, M. Vollmer, P. Horth; *Journal of Chromatography A* **1009**, 197 (2003)

[6] E. Machtejevas, H. John, K. Wagner, L. Standker, G. Marko-Varga, W. G. Forssmann, R. Bischoff, K. K. Unger; *Journal of Chromatography B: Biomedical Applications* **803**, 121 (2004)

[7] K. Wagner, t. miliotis, G. Marko-Varga, R. Bischoff, K. K. Unger; *Analytical Chemistry* **74**, 809 (2002)

[8] G. Guiochon, L. A. Beaver, M. F. Gonnord, A. M. Siouffi, M. Zakaria; *Journal of Chromatography A* **255**, 415 (1983)

[9] W. H. McDonald, J. R. Yates III; *Disease Markers* **18**, 99 (2002)

[10] D. A. Wolters, M. P. Washburn, J. R. Yates III; *Analytical Chemistry* **73**, 5683 (2001)

[11] M. P. Washburn, R. R. Ulaszek, C. Deciu, D. M. Schieltz, J. R. Yates III; *Analytical Chemistry* **74**, 1650 (2002)

[12] I. Halasz, R. Endele, J. Asshauer; *Journal of Chromatography A* **112**, 37 (1975)

[13] N. B. Afeyan, N. F. Gordon, I. Mazsaroff, L. Varady, S. P. Fulton, S. B. Yang, F. E. Regnier; *Journal of Chromatography A* **519**, 1 (1990)

[14] T. B. Tennikova, M. Bleha, F. Svec, T. V. Almazova, B. G. Belenkii; *Journal of Chromatography A* **555**, 97 (1991)

[15] N. Tanaka, T. Ebata, K. Hashizume, K. Hosoya, M. Araki; *Journal of Chromatography A* **475**, 195 (1989)

[16] H. Minakuchi, K. Nakanishi, N. Soga, N. Ishizuka, N. Tanaka; *analytical chemistry* **68**, 3498 (1996)

[17] H. Kaji, K. Nakanishi, N. Soga; *Journal of Non-Crystalline Solids* **185**, 18 (1995)

[18] H. Minakuchi, K. Nakanishi, N. Soga, N. Ishizuka, N. Tanaka; *Journal of Chromatography A* **797**, 121 (1998)

[19] H. Minakuchi, N. Ishizuka, K. Nakanishi, N.Soga, N. Tanaka; *Journal of Chromatography A* **828**, 83 (1998)

[20] N. Ishizuka, H. Kobayashi, H. Minakuchi, K. Nakanishi, K. Hirao, K. Hosoya, T. Ikegami, N. Tanaka; *Journal of Chromatography A* **960**, 85 (2002)

[21] F. C. Leinweber, D. G. S. Schmid, D. Lubda, K. H. Wiesmuller, G. Jung, U. Tallarek; *Rapid Communications in Mass Spectrometry* **17**, 1180 (2003)

[22] B. Barroso, D. Lubda, R. Bischoff; *Journal of Proteome Research* **2**, 633 (2003)

[23] F. C. Leinweber, D. G. Schmid, D. Lubda, B. Sontheimer, G. Jung, U. Tallarek; *Journal of Mass Spectrometry* **39**, 223 (2004)

[24] N. I. Govorukhina, A. Keizer-Gunnink, A. G. J. van der Zee, S. de Jong, H. W. A. de Bruijn, R. Bischoff; *Journal of Chromatography A* **1009**, 171 (2003)

[25] A. M. Siouffi; *Journal of Chromatography A* **1000**, 801 (2003)

[26] J. S. Mellos, J. W. Jorgenson; *Analytical Chemistry* **76**, 5441 (2004)

[27] M. Kele, G. Guiochon; *Journal of Chromatography A* **960**, 19 (2002)

[28] F. C. Leinweber, D. Lubda, K. Cabrera, U. Tallarek; *Analytical Chemistry* **74**, 2470 (2002)

[29] R. Hahn, R. Schlegel, A. Jungbauer; *Journal of Chromatography B: Biomedical Applications* **790**, 35 (2003)

[30] F. C. Leinweber, U. Tallarek; *Journal of Chromatography A* **1006**, 207 (2003)

[31] Y. Shen, R. Zhao, M. E. Belov, T. P. Conrads, G. A. Anderson, L. Pasa Tolic, T. D. Veenstra, M. S. Lipton, H. R. Udseth, R. D. Smith; *Analytical Chemistry* **73**, 1766 (2001)

[32] M. Fountoulakis, J. F. Juranville, L. Jiang, D. Avila, D. Roder, P. Jakob, P. Berndt, S. Evers, H. Langen; *Amino Acids* **27**, 249 (2004)

[33] C. Greenough, R. E. Jenkins, N. R. Kitteringham, M. Pirmohamed, B. K. Park, S. R. Pennington; *Proteomics* **4**, 3107 (2004)

[34] L. Tolley, J. W. Jorgenson, M. A. Moseley; *Analytical Chemistry* **73**, 2985 (2001)

[35] J. E. MacNair, G. J. Opiteck, J. W. Jorgenson, M. A. Moseley; *Rapid Communications in Mass Spectrometry* **11**, 1279 (1997)

[36] H. Kimura, T. Tanigawa, H. Morisaka, T. Ikegami, K. Hosoya, H. Minakuchi, K. Nakanishi, M. Ueda, K. Cabrera, N. Tanaka; *Journal of Separation Science* **27**, 897 (2004)

[37] M. S. Wilm, M. Mann; *International Journal of Mass Spectrometry and Ion Processes* **136**, 167 (1994)

CHAPTER 5

RAM-based albumin depletion coupled on-line to nanoLC-MS for the analysis of complex proteomics samples

5.1 Introduction

Liquid chromatography-mass spectrometry (LC-MS) is an important analysis technique in proteomics. In order to increase the concentration sensitivity of LC-MS for low-molecular-weight peptides, it is often necessary to enrich them prior to analysis and to remove high-abundance proteins like albumin. Notably, body fluids like serum [1] or cerebrospinal fluid (CSF) [2] often contain considerable amounts of albumin, making the analysis of constituents at nM concentrations or below difficult. Removal of albumin and other high-abundance proteins is often achieved by immunoaffinity chromatography based on a panel of immobilised antibodies [1–3]. However, highly abundant proteins can bind lower-abundance proteins or peptides, which leads to the loss of the less-abundant species upon removal of the high-abundance species. This is especially true when non-denaturing conditions have to be used as in the case of immunoaffinity chromatography [4]. Consequently, improved methodology based on efficient sample pretreatment is often necessary to study the low-abundance peptides in complex biological samples containing albumin.
Restricted access material (RAM) are porous silica materials used in chromatogra-

phy for the separation of low-molecular-weight analytes from matrix components like albumin by a combination of size exclusion and conventional adsorptive chromatography. Though the applicability of RAM for the analysis of peptides has been demonstrated [5], RAM chromatography is seldom used in proteomics [6]. It has been applied to the analysis of cyanobacterial peptides after off-line sample preparation [7] and for the quantitation of neuropeptide Y in porcine plasma. In the latter case, the RAM column was coupled to reversed-phase LC-MS in a forward-flush system, enabling a limit of detection (LOD) of 5 μM [8]. Unfortunately, no data about the efficiency of albumin removal were provided [5, 8]. A more complex set-up for the analysis of highly complex biofluids was described by Wagner et al. [9]. This multidimensional system made use of RAM, coupled on-line with ion-exchange and reversed-phase chromatography. All the columns were connected in a back-flush fashion. Using this system, 92% of albumin was depleted from the sample matrix.

In this study, a novel set-up for multidimensional nanoLC-MS featuring three columns coupled on-line was developed and characterised. In particular, we were concerned with the analysis of Substance P (SP) in albumin-rich matrices. The columns were coupled using a single gradient pump and switching valve to minimise extracolumn dead volumes. Though the flow direction was controlled by a switching valve, the analytes never flowed through valves except during injection. For the first time, a RAM cartridge was coupled to nanoLC-MS in a forward-flush mode and used for the analysis of microdialysis perfusates as model matrix and SP as model peptide. BSA, which was added to reduce non-specific peptide adsorption to the microdialysis membrane and connecting silica capillaries, could be removed efficiently with the RAM cartridge while SP was quantitatively retained. The set-up described here can be used reproducibly with fast gradients (RSD of retention time $\approx$ 3% over a week), without requiring an extensive time period to stabilise the flow or the pressure. Separation efficiency was high (peak width at half-height of 10s) and samples up to 100 μL could be injected. Perfusates containing up to 4.0 μM BSA were analysed without any off-line sample pretreatment. The total cycle time, including sample pre-treatment, separation, washing and equilibration, was about 40 min. Such rapid, reproducible and robust separations by nanoLC-MS are expected to be of interest for the comparative analysis of complex biofluids.

5.2 Materials and methods

5.2.1 Materials

Formic acid (FA) (98-100% pure), formamide, sodium chloride, potassium chloride (all >99.5% pure) and magnesium chloride hexahydrate (99-102% pure) were purchased from Merck KGaA (Darmstadt, Germany), and acetonitrile (ACN) (HPLC Supra-Gradient grade) from Biosolve B.V. (Valkenswaard, The Netherlands). Ethyl acetate (99.9% pure) and 1/16" stainless steel blank nuts were obtained from VWR International B.V. (Amsterdam, The Netherlands) and electrodag PF-407A (carbon ink) from Acheson Industries Europe Ltd. (Scheemda, The Netherlands). Substance P acetate salt (SP) (>98% pure), bovine serum albumin (BSA) (>96% electrophoretically pure) and calcium chloride dihydrate (>99% pure) were obtained from Sigma-Aldrich (Zwijndrecht, The Netherlands), D(+)-glucose anhydrous from J.T. Baker Chemicals B.V. (Deventer, The Netherlands) and dimethyl sulfoxide (DMSO) ($\geq$ 99.5% pure) from Fluka (Zwijndrecht, The Netherlands). Fused-silica capillaries (50-200 μm ID, 360 μm OD) were purchased from Composite Metal Service (Ilkley, UK) and microtight PEEK sleeve (0.0155" ID, 0.025" OD) and microT PEEK assembly (0.25" bore) from Upchurch Scientific (Oak Harbor, WA, USA). PEEK cartridges and their stainless steel holder were obtained from SPARK Holland (Emmen, The Netherlands). Restricted-access chromatographic media of varying selectivity, C_{18}, C_8 and GFF-II (glycine-phenylalanine-phenylalanine-based material) (C_{18}-RAM, C_8-RAM & GFF), were a gift from Regis Technologies (Morton Grove, IL, USA) and the potassium silicate solution (Kasil 1) a gift from PQ Europe (Winschoten, The Netherlands).

5.2.2 Preparation of frits, columns and cartridges

Column frits were prepared based on a method described by Meiring et al. [10], which involves polymerisation of potassium silicate in the solution at the end of the capillary. Briefly, 50 μL of formamide were pipetted into a 1.5-mL Eppendorf vial and 150 μL of Kasil 1 were added. Promptly after, the mixture was briefly vortexed, and 10-to-15-cm long silica capillaries were immersed in the polymerising mixture at a right angle with the surface of the liquid to a depth of approximately 5 mm. In this way, the silicate solution was passively introduced to the ends of the capillaries by capillary forces. Typically, 10 frits were prepared at the same time. Polymerisation was completed by heating the capillaries at 100°C in an oven for 4h. The resulting frits were cut to a length of approximately

0.5 mm.
Trap columns and cartridges were packed using a pneumatic pump (Knauer K-1900, Berlin, Germany) able to deliver flows at pressures up to 1000 bar. The pump was connected to an empty 3-mm-ID stainless steel LC column acting as a reservoir for the slurry of packing material.
The capillary to be packed was connected to the 3-mm-ID column by the end opposite to the frit. The slurry (10 mg/mL in acetone) was introduced in the empty reservoir and the pump was turned on until the chromatographic bed had the desired length.
Cartridges with a stainless-steel frit at one end were prepared according to the same procedure. They were positioned in a cartridge holder during both packing and chromatographic separation.

5.2.3 NanoLC-MS set-ups

All experiments were performed using an 1100 LC system consisting of a vacuum degasser and a high pressure-mixing binary pump without static mixer (Agilent Technologies, Waldbronn, Germany). The damper was positioned in-line between one of the pump heads and the T-piece used to mix the solvents. This set-up minimised delay in gradient delivery. 0.1% formic acid (FA) in water and 0.1% FA in acetonitrile (ACN) were the two solvents (respectively solvents A & B) making up the mobile phase. A Midas autosampler (SPARK Holland, Emmen, The Netherlands) equipped with a 250-μL syringe and either a 10- or 100-μL injection loop was used in conjunction with an LCQ Classic ion trap mass spectrometer (Thermo Electron Corporation, San Jose, CA, USA). The nanoelectrospray ion source was built in-house. The gold-coated nanoelectrospray tip and the analytical column were butt-connected using a Teflon sleeve of 360-μm-ID to minimise post-column dead volumes (3-4 nL), and placed in the stainless steel holder on the source table to ensure electrical contact. The nanospray tip was positioned 1 mm away from the opening of the heated MS capillary. The spray voltage was normally set at 1.6 or 1.7 kV.
Two nanoLC-MS set-ups were evaluated. These are schematically presented in Figure 5.1. One consisted of a 50-μm-ID analytical column (15 cm long) and a 100- or 200-μm-ID trap column (2 or 5 cm long). This set-up will be referred to as Set-up 1. The other set-up is based on Set-up 1, but contained an additional 1-mm-ID cartridge (1 cm long) between the injection assembly and the trap column and is referred to as Set-up 2. The analytical column was packed with Biosphere C_{18} material (5 μm d_p, 100 Åpore size). The trap column was either packed with a

regular RP stationary phase (Biosphere C_{18}, 5 μm d_p, 100 Åpore size), or a RAM phase (Regis C_8, C_{18} or GFF-II; 5 μm d_p, 100 Åpore size). The cartridge was only used with Regis C_8 RAM packing material. Columns packed with Biosphere C_{18} were purchased from Nanoseparations (Nieuwkoop, The Netherlands). In both set-ups, the 6-port switching valve of the MS was used to control the flow direction.

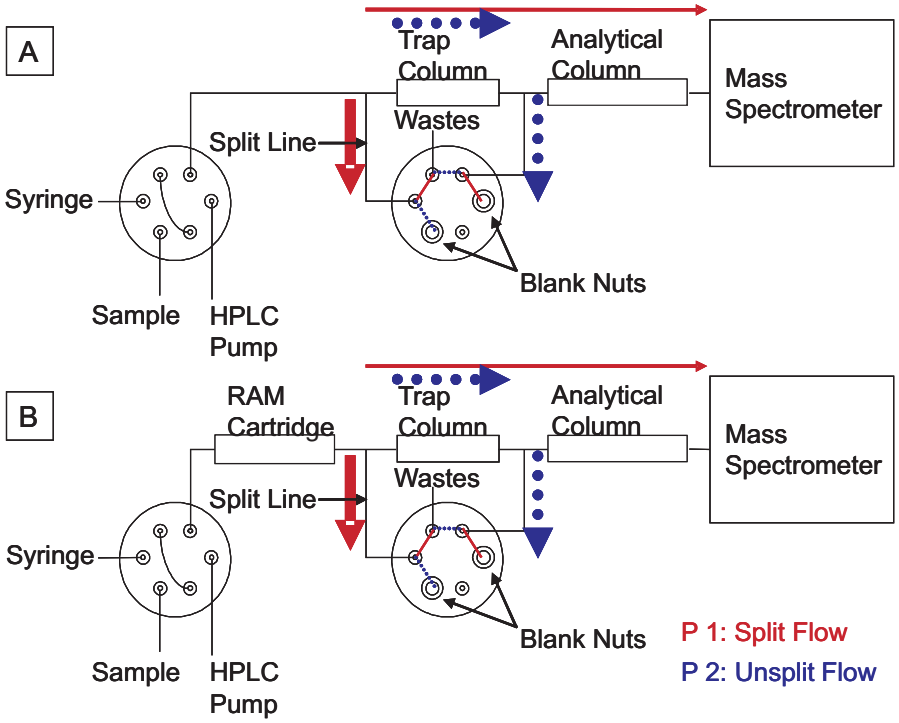

Figure 5.1: Schematic representation of the nanoLC-MS set-ups. A: Set-up 1. The trap column was either packed with C_{18} or different RAMs (C_8, C_{18} or GFF) (20-50 mm long, 0.1-0.2-mm ID, 5 μm d_p, 100 Åpore size). B: Set-up 2. The RAM cartridge was packed with C_8-RAM particles (10*1.0 mm ID, 5 μm d_p, 100 Åpore size) and the trap column consisted of a bed of C_{18} particles (20*0.1-mm ID, 5 μm d_p, 100 Åpore size). The arrows indicate the direction of the LC eluent in the system depending on the position of the switching valve (P1: split flow & P2: unsplit flow). The full arrows indicate how the flow is split in front of the trap column. Only a small portion (1:3000 to 1:4000 depending on mobile phase composition) of the eluent flows through the trap and analytical columns. The dotted arrows show the path of the flow prior to splitting that is directed through the trap column to waste.

5.2.4 NanoLC Procedures

Set-up 1 has been extensively described by Meiring et al. [10]. Briefly, the sample plug was concentrated on either a C_{18} (20 * 0.1-mm-ID) or a RAM (50 * 0.2-mm-ID) trap column. The flow (10 to 50 μL/min, 1 to 10% ACN) was directed through the trap column by switching the valve so as to connect the split line (300 * 0.05 mm ID) to a blank nut. Elution of the analytes from the trap column onto the analytical column was performed by switching the valve so as to connect the split line to the waste line. The flowrate was concomitantly raised to 400 μL/min, which was split down to 100-150 nL/min, and the gradient was started. The gradient ran up to 65% ACN at 3%/min. Subsequently, the solvent composition was returned to the starting composition and the system was equilibrated for 10 min. Set-up 2 is based on Set-up 1 and Figure 5.1 illustrates its operation. An additional RAM C_8 cartridge, in a cartridge holder, was positioned between the injection assembly and the split line. Programming of both the gradient pump and the switching valve is described in Table 5.1. Briefly, the principle of the set-up is the following. During the first 10 minutes, the flow was split between the RAM cartridge and the nanoLC part of the system discarding the BSA that is not retained on the RAM to waste. The transfer of SP from the RAM cartridge to the trap column of the nanoLC was performed by directing the flow through the trap column without splitting it. After loading of the trap column, the valve was switched back to its original position, thereby splitting the flow again. At the same time, the flow was raised and the gradient started, simultaneously washing the RAM cartridge of the remaining BSA to waste and eluting SP off the nanoLC. In the following discussion, the term "trap" refers to the type of column used in Set-up 1 (100- or 200-μm ID). The term "cartridge" applies to the column (1-mm ID) at the front-end of Set-up 2.

5.2.5 Sample preparation

The perfusate was composed of 140 mM NaCl, 3 mM KCl, 1.25 mM $CaCl_2$, 1 mM $MgCl_2$, 3 mM glucose and either 0.025 or 0.0025% BSA (w/v) ($\approx$ 4.0 or 0.4 μM).

The perfusate was used, pure or as a mixture with 0.1% FA in DMSO in the following ratios, perfusate: DMSO (19:1, 3:1 and 1:1), to dilute standards [11]. SP standards were also prepared in 0.1% FA in water:DMSO at the same ratios. Concentrations ranged from 0.5 up to 50 nM. The volumes injected were either 10 or 100 μL depending on the experiment.

Valve		LC pump		
T (min)	Position	T (min)	% B	Flow (μL/min)
0		0	1	50
	P1	5	1	50
10		5.01	10	50
10.01		15	10	50
	P2			
15		15.01	10	400
15.01		32.2	65	400
	P1	32.21	1	400
42.2		42.2	1	400

Table 5.1: Programming of both the gradient pump and the switching valve in Set-up 2. The terms split flow and unsplit flow are related to the position of the switching valve (P1 & P2) and its action on the flow (see Figure 5.1). During loading of the sample and elution of the nanoLC, the flow is split (P1) in front of the trap column with a large fraction going to waste and a small one flowing through the trap and the analytical columns. The split ratio is 1:3000 to 1:4000, depending on the mobile phase composition. Conversely, the flow is unsplit (P2) when the switching valve directs the flow through the trap column to waste (during transfer of the analytes from the RAM cartridge to the trap column) (cf. Figure 5.1)

.

5.3 Results and discussion

5.3.1 NanoLC-MS: Set-up 1

Initially, Set-up 1 was used to analyse microdialysis perfusates containing large amounts of BSA. The need for adding BSA to the perfusate to increase recovery of SP has a three-fold negative effect on the analysis by nanoLC-MS. First, the elution peak of SP overlaps with a very large peak of BSA (Figure 5.2) causing severe ionisation suppression. Moreover, an excess of BSA overloads the system and its only partial elution from the trap column makes the enrichment of SP difficult if not impossible after a few runs. Additionally, BSA eluting off the column crystallises at the inlet of the MS and obstructs it. Though SP could be analysed in the presence of a large excess of BSA, retention time varied greatly. After only 3 injections, the retention time already varied by almost 6%. Altogether, this resulted in a non-robust nanoLC-MS system that cannot be used for the routine analysis of microdialysis perfusates.

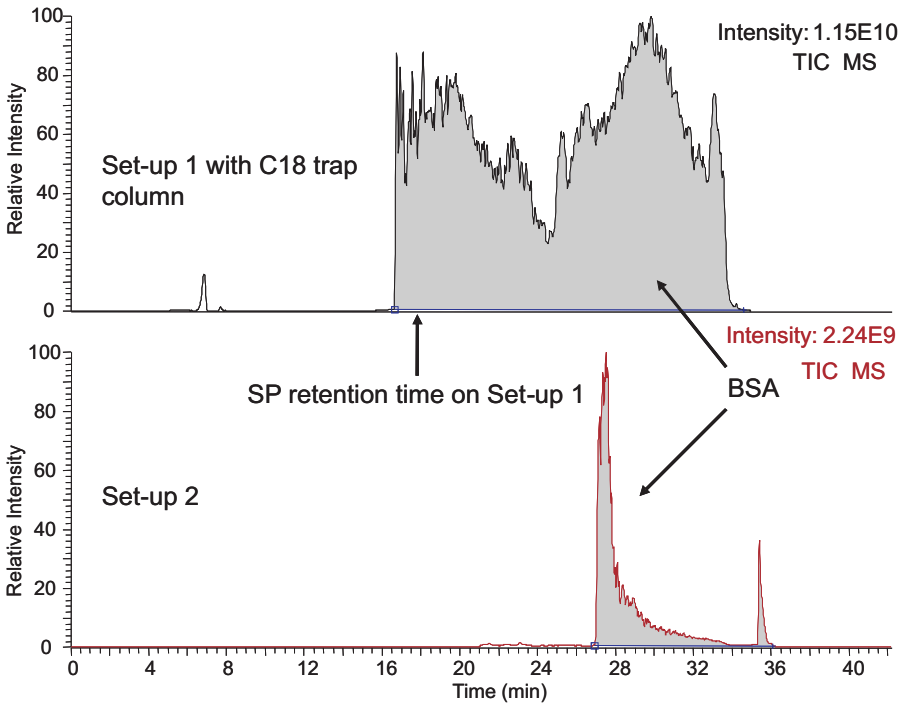

Figure 5.2: Evaluation of the efficiency of the albumin depletion step by RAM chromatography (TIC chromatograms obtained in full scan mode between m/z 300 and 1500). Top: 10 μL of perfusate on Set-up 1 equipped with a C_{18}-trap column. The flow (10 μL/min, 1% ACN) was directed through the trap column for 5 min. Elution of the analytes was performed using a gradient that increased to 65% ACN in 20 min. The solvent composition was returned to 1% ACN and the system was equilibrated for 10 min. Bottom: 100 μL of perfusate on Set-up 2 after approximately 750 injections. Programming of the gradient pump and MS valve as indicated in Table 5.1.

To reduce the load of albumin on the nanoLC-MS system, the C_{18} trap column was replaced by trap columns packed with C_{18}-RAM, C_8-RAM or GFF-RAM. The quality of the resulting chromatographic separations was assessed by injecting (in triplicate) 10 μL of solutions of increasing concentrations of SP in different matrices (i.e. containing 25 or 50% DMSO to increase recovery [11]). The results showed no significant differences in selectivity and signal intensity between the different trap columns (data not shown). Peak shapes were comparable for all restricted-access packing materials, though it was expected that peak focusing on the C_{18} analytical column would provide narrower peaks in combination with the C_8-RAM as compared to the C_{18}-RAM.

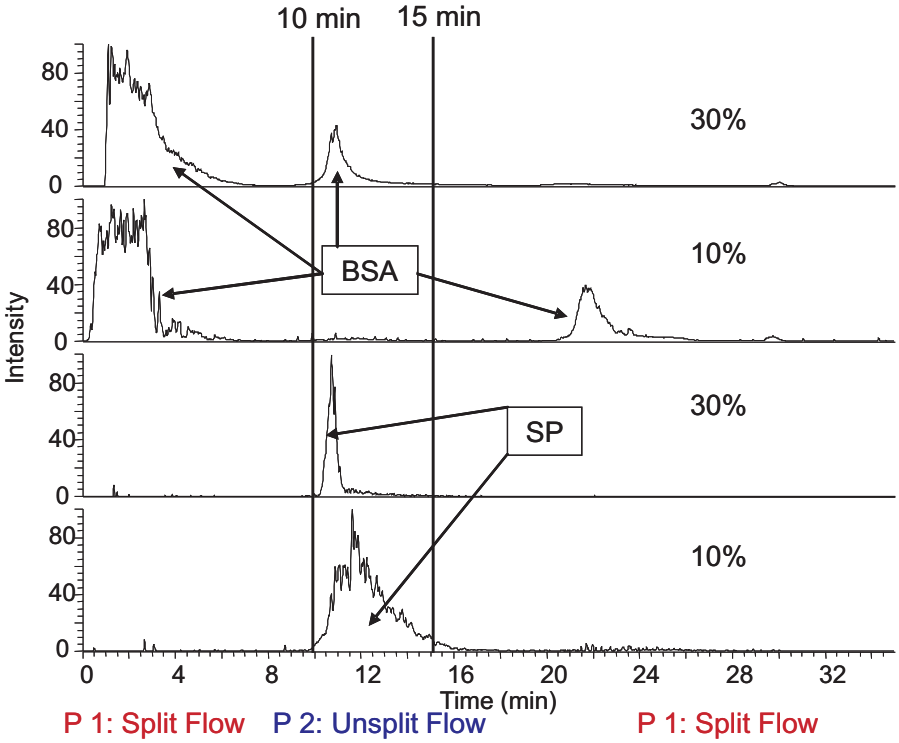

Figure 5.3: Evaluation of the influence of varying the mobile phase composition from 10 to 30% ACN during the step elution on the resolution between SP and BSA. 10-μL samples (4.0 μM BSA:0.1%FA in DMSO (3:1)) were injected on a C_8-RAM cartridge directly coupled to the MS. The sample was loaded on the C_8-RAM cartridge using 1% ACN for 5 min, then the gradient was stepped up to either 10 or 30% ACN for 5 min before going up to 95% ACN in 15 min. The cartridge was reequilibrated at 1% ACN for 10 min. Separation was performed at a flow of 50 μL/min. The two lines at 10 and 15 min indicate the moment at which the switching valve of the MS is switched with the C_8-RAM cartridge mounted in Set-up 2. The same code as in Figure 5.1 (P1 and P2) is used to indicate when the flow is split (P1) or not (P2) and to easily relate to the functioning of Set-up 2.

The use of a trap column packed with RAM not only improved the reproducibility of retention time (1.5 <RSD (%) <4.3 depending on sample matrix) but also increased the period during which the system could be operated reproducibly. However, this system still did not enable the analysis of both unknown samples and standard solutions under routine conditions. BSA was still found

to crystallise at the MS opening, so the system had to be cleaned on a daily basis. The presence of BSA crystals on the MS endplate indicated that a significant portion of the injected BSA was not eliminated by the RAM column. To better characterise BSA retention in the system, the C_8-RAM trap column was coupled directly to the ion trap using a 10-μm-ID gold coated nanospray emitter mounted on the nanospray interface and 10-μL injections of SP in perfusate were performed. Interestingly, BSA eluted in two fractions, the first one in the flowthrough and the second after the elution of SP (Figure 5.3). Preliminary experiments showed that linear flowrate and mobile phase composition were factors of major importance for efficient removal of BSA and retention of SP. As much as 80% of BSA remained on the RAM trap at higher flowrates (10-20 μL/min) during sample loading (data not shown). Using a C_8-RAM trap column (20*0.1-mm ID) and a flow of 2.5μL/min, improved BSA depletion was observed; 75% BSA could be discarded in the flowthrough. Lower flowrates were expected to result in even more efficient depletion of BSA. However, such low flowrates are highly impractical with the system used. Firstly, such low flows are very unstable if delivered without flow splitting. Moreover, sample volumes as large as 100 μL were expected to be brought onto the trap column, which would result in extremely long loading times. As an alternative, 0.2-mm-ID trap columns were considered but, when coupled to a 50-μm ID analytical column, this resulted in broad chromatographic peaks. Therefore, a change in set-up was necessary, incorporating an on-line albumin depletion step using a larger ID C_8-RAM cartridge coupled to the original reversed-phase nanoLC system.

5.3.2 Set-up 2: RAM cartridge coupled to nanoLC-MS

In order to remove BSA prior to nanoLC-MS in a more efficient manner, Set-up 2 was used (Figure 5.1). In this set-up, a RAM cartridge (10 * 1.0-mm-ID) was positioned in-between the injection valve and the trap column. During the first 10 minutes, the flow was split between the RAM cartridge and the nanoLC part of the system, discarding the BSA that was not retained on the RAM to waste. The transfer of SP from the RAM cartridge to the trap column of the nanoLC was performed by directing the flow through the trap column without splitting. After loading of the trap column, the valve was switched back to its original position, thereby splitting the flow again. At the same time, the flow was raised and the gradient started, simultaneously washing the RAM cartridge of the remaining BSA to waste and eluting SP off the nanoLC. In this set-up a RAM cartridge was coupled to nanoLC-MS in a forward-flush mode, an approach

that has, to our knowledge, not been described before. This set-up has the advantage that no additional switching valve or pump are required, whereas most nanoLC designs making use of a trapping column do require a second "loading" pump [12, 13]. Commonly, in the elution step, the sample is back-flushed off the RAM cartridge and flows through the switching valve before reaching the analytical column. Back-flush set-ups minimise the contact time between analyte and trap column. However, positioning the switching valve on the sample path increases non-specific interactions between analytes and metal parts of the valve. The set-up described here can be used reproducibly with very fast gradients and without requiring an extensive period to stabilise both the flow and the pressure [13]. Moreover, the use of fewer parts is likely to reduce down-times of the instrumental set-up, though this remains to be seen in further long-term studies. Additionally, large sample volumes (10 to 100 μL) could be injected at high flowrates (50 μL/min) on Set-up 2. Haskins described a sensitive nanoLC-MS system for the analysis of neuropeptides in microdialysates in the absence of BSA in which no trap column was used. 5 min were necessary to inject 1.8 μL of sample on a 25-μm-ID column [14]. On-line coupling of trap and analytical columns enabled faster loading (<2 min) of larger sample volumes (10 μL) while separation was performed at nL/min flowrates [12]. The design of the nanoLC set-up described here allows for even larger sample volumes (up to 100 μL) to be loaded in a short time. Moreover, analytes can be efficiently separated from the BSA-containing sample matrix during loading before being further separated on the nanoLC-MS part of the system.
This set-up has great potential for on-line sample preparation coupled to nanoLC-MS. Its selectivity can be tailored to suit the needs of a particular application by varying the selectivity of the cartridge and/or of the trap column. To demonstrate the feasibility for on-line albumin depletion coupled to nanoLC-MS, a C_8-RAM cartridge was characterised and coupled on-line with a C_{18} nanoLC system.

5.3.3 Characterisation of RAM material

Using Set-up 2, it is of great importance to avoid that SP elutes in the flowthrough containing the majority of BSA and to maximise resolution between SP and the remainder of BSA that is retained on the RAM cartridge. To this end, loading and elution conditions and the %DMSO in the sample were optimised. A cartridge (10*1 mm) packed with C_8 RAM was coupled directly to the ion trap mass spectrometer using a commercially available interface.

5.3.3.1 Sample loading conditions

The impact of the mobile phase composition (1 to 15%ACN) during loading of the sample was investigated. In addition, the influence of the flowrate during loading of the RAM cartridge was investigated (50 to 250 μL/min). The influence of the ACN percentage was investigated at a flow of 250 μL/min, while for the investigation of flowrate an ACN percentage of 1% during loading of the sample was used. Prior to injection, the RAM cartridge was equilibrated for 2 min (at 250 μL/min) at the mobile phase composition used for sample loading. After sample loading, the gradient was started at this percentage. The ACN percentage increased to 95%, the change in volume fraction of acetonitrile per gradient volume was held constant, i.e., the volume of the column effluent from the start to the end of the gradient was constant. Every experiment was performed with perfusates containing 0.1%FA in DMSO at the following ratios (19:1, 3:1 and 1:1).
Two BSA fractions were observed, one in the flowthrough and the other resulting from retention of a part of BSA on the RAM column. Retention of BSA on the RAM may have resulted from either one or a combination of three distinct phenomena. First, BSA may interact with the polyethylene glycol chains present on the outer surface of the RAM silica particles in a hydrophilic interaction chromatography (HILIC) retention mode. However, HILIC using the C_8-RAM cartridge was only observed for SP at very high percentages of ACN (>60 %ACN. data not shown). HILIC can therefore be ruled out at the mobile phase composition (1 %ACN) used during loading of the sample on the trap column. Second, BSA may bind to the remaining silanol groups at the surface of the RAM as suggested by Wagner et al. who used cation-exchange RAM particles [9]. Most likely, however, is that some of the BSA passes through the polyethylene glycol network and enters the pores, where it interacts with the C_8 groups.
SP eluted between the two BSA fractions. 30 to 60% BSA were retained on the C_8-RAM cartridge depending on the mobile phase composition and the %DMSO in the sample. Increasing the %ACN in the mobile phase during loading from 1 to 15% resulted in an increase of 5 to 10% of BSA (at fixed %DMSO in the sample) in the flowthrough. It indicated that, indeed, BSA apparently interacts with the octyl groups inside the pores of the silica particles. As expected, retention of SP was also negatively influenced by an increased %ACN in the loading buffer. Loading at 1% ACN offered the best compromise. SP was strongly retained on the RAM phase and well separated from the second BSA fraction.
Increasing the flowrate only resulted in minor changes. Resolution between SP and the second BSA fraction and the %BSA in the flowthrough were barely in-

fluenced. However, the time window to switch the valve and direct BSA to waste and SP to the nanoLC logically decreased with increasing flowrate.
Increasing the %DMSO in the sample increased the intensity of the MS signal for SP indicating that DMSO probably prevents interactions between SP and BSA. It also resulted in a greater proportion of BSA in the flowthrough on the RAM. However, the SP peaks showed a better reproducibility in terms of peak shape and peak width when the samples contained only a limited amount of DMSO. Therefore, the flowrate was set at 50 μL/min and 25% DMSO in the sample and 1% ACN in the loading buffer were selected as the best compromise in terms of signal intensity, reproducibility (MS signal and retention time) and depletion of BSA.

5.3.3.2 Percentage ACN during elution of the RAM cartridge

To attain efficient elution of SP from the RAM cartridge while avoiding co-elution with the fraction of BSA also retained on the RAM cartridge, the %ACN during the elution step was investigated. The sample (containing 25% DMSO) was loaded on the RAM cartridge at 1%ACN. After 5 min, SP was eluted applying a step gradient up to 10 or 30%ACN for 5 min. The gradient was then linearly increased up to 95% ACN at a flow of 50 μL/min. The RAM cartridge was equilibrated at 1 %ACN for 10 min prior to the next injection.
Increasing the %ACN during step elution barely influenced the retention time of SP as 10% ACN was already sufficient for SP to start eluting. However, the retention of the retained BSA fraction was strongly influenced by the higher percentage of ACN during elution (Figure 5.3).
Step elution of SP using 10% ACN ensured baseline resolution between SP and the BSA fraction retained on the cartridge whereas step elution using 30% ACN resulted in co-elution of SP and BSA. The principle of Set-up 2 ensures complete albumin depletion while SP was retained on the cartridge and chromatographically well-resolved from the second BSA fraction. Therefore elution of SP was performed by step elution using 10% ACN.

5.3.3.3 Recovery

%ACN and flowrate during loading and %DMSO in the sample were expected to affect SP recovery. However, with respect to flowrate, no decrease in recovery was observed over the range of flowrates investigated. Breakthrough of SP was observed when more than 5%ACN were used during loading of the sample on the RAM cartridge or when the sample contained more than 25% DMSO.

Additionally, the recovery of SP was expected to be influenced by the presence of BSA and the time for which the RAM column was washed. The recovery of SP in the presence (or absence) of BSA and with varying loading/washing times (1 or 10 min) of the RAM cartridge was investigated by injecting 100 μL of sample. Loading was performed using 1% ACN during either 1 or 10 min. Subsequently, the gradient went up to 95% ACN in 6 min at a flowrate of 250 μL/min. Finally, the cartridge was subsequently re-equilibrated for 2 min at the loading buffer composition (1% ACN). The sample solvent was either perfusate (4.0μM BSA):0.1% FA in DMSO (3:1) or 0.1% FA in water:DMSO (3:1). Samples containing 14.8, 148 & 1480 nM SP were sequentially injected onto the system. The resulting calibration curves showed different sensitivities that can be directly related to the respective recovery. The four different experiments showed decreasing recovery in the following order: samples without BSA and 1 min wash >samples with BSA and 1 min wash >samples without BSA and 10 min wash >samples with BSA and 10 min wash. The washing time of the RAM cartridge clearly led to great losses of SP. Recovery decreased by as much as 50% when the washing time was increased from 1 to 10 min. Part of the SP was probably washed away by the large excess of mobile phase used to wash the RAM cartridge. Sensitivity was a few percent lower in the presence than in the absence of BSA, indicating that only a small percentage of SP remained bound to BSA and was discarded to waste together with the eliminated BSA. Though only repeated gel filtration could dissociate the complex formed between SP and the high-molecular weight plasma components [15], it was possible with our set-up to efficiently enrich SP and discard BSA using a short RAM cartridge and a relatively high flowrate.

5.3.4 Set-up 2 under optimised conditions

The optimised chromatographic conditions for coupling the RAM cartridge with nanoLC-MS in Set-up 2 (Figure 5.1, Table 5.1) were the following.
100 μL of perfusate (containing 0.4 or 4.0μM BSA and 25% acidified DMSO) was loaded on the RAM cartridge using 1 %ACN at 50μL/min. A 50μL/min flowrate during elution made it possible to couple the RAM cartridge directly to the reversed-phase trap column without operating pressures exceeding 160 bar. A step gradient to 10% ACN allowed the transfer of SP from the RAM cartridge to the C_{18} trap column. No breakthrough of SP on the C_{18} trap column (20 * 0.1-mm ID) was observed even up to an ACN concentration of 30 %ACN in the elution step (data not shown). The RAM cartridge was washed during elution of SP over the nanoLC system using a linear gradient up to 65% ACN. The programming of

the gradient pump and switching valve is described in Table 5.1.
Separations were very efficient with peak widths of 10s at half height. Such peak widths are consistent with other high-efficiency nanoLC systems [12, 14]. These set-ups, however, did not integrate an on-line sample pretreatment step. The total analysis time including sample pretreatment, separation of the analytes, washing and equilibration of the system, was about 40 min.
As a control of the efficiency of BSA removal by RAM sample pretreatment using Set-up 2, 100 μL of perfusate (containing 4.0μM BSA) were injected on Set-up 2 and the eluent of the nanoLC was monitored by full-scan mass spectrometry. The area of the BSA peak was compared to the area of the BSA peak resulting from the injection of 10 μL of perfusate on Set-up 1 equipped with a C_{18}-trap column. The peak area due to remaining BSA on Set-up 2 was estimated to be approximately 2-3% of that resulting from a ten-time smaller direct injection on the C_{18}-nanoLC system (Set-up 1). Therefore, only about 0.2-0.3% of the injected BSA on Set-up 2 reached the MS (Figure 5.2). With the system described by Wagner et al., as much as 8% of the original albumin content remained on the system after the RAM step [9]. Although antibody-based depletion approaches were specifically designed to selectively remove albumin and other high-abundance proteins [3], depletion did not reach the level achieved by our system. In the same study, other depletion (antibody- or dye-based) columns apparently achieved better results than our system but were not tested with a system as sensitive as a nanoLC-MS. Moreover, anti-HSA columns require exchanging solvents before LC-MS analysis. An advantage of RAM materials over antibody-based columns is that non-specific binding of SP to BSA was reduced by adding 25% acidified DMSO (0.1% FA) to the sample, which is not possible for antibody-based systems.
Based on the optimised conditions, Set-up 2 was operated for more than a week ($\approx$ 250 injections) without the need for washing either the nanoLC or the MS endplate. Retention times were much more reproducible (RSD $\approx$ 3% over a week) than for Set-up 1 (RSD $\approx$ 6% over 3 runs) even though samples with two different matrices (0.4 or 4.0μM BSA) were injected. After approximately 750 injections of perfusate (0.4 or 4.0μM BSA:0.1%FA in DMSO (3:1)) on Set-up 2, 100 μL of perfusate were injected and the elution of BSA followed by full scan mass spectrometry. The peak area of BSA was comparable to the area observed after only a few injections. We therefore conclude that the system still operated reproducibly after 750 injections.

5.4 Conclusion

In this study, a novel set-up for multidimensional nanoLC-MS featuring three columns coupled on-line was developed and characterised. For the first time, a RAM cartridge was coupled on-line to nanoLC-MS in the forward-flush mode. No additional switching valve or pump are required to couple the three different columns. The set-up described here can be used reproducibly with very fast gradients without requiring an extensive period to stabilise either flow or pressure [13]. Moreover, its simplicity makes it very robust and cheap. After optimisation, all SP in the perfusate was brought on the nanoLC part and virtually all BSA (99.7-99.8%) was discarded. While analysing the sample by nanoLC-MS, the RAM cartridge was washed using the eluent of the nanoLC. The RAM cartridge and the nanoLC were re-equilibrated using the same mobile phase. Separations were very efficient with peak widths (at half height) of 10s. The total analysis time including sample pretreatment, separation of the analytes, washing and re-equilibration of the system, was about 40 min. Moreover, the separation was highly reproducible (RSD on retention time $\approx$ 3% over a week) and robust (750 injections without any change of RAM cartridge or nanoLC columns) compared to a trap-nanoLC system such as Set-up 1. It was used almost continuously for a couple of months before the different columns and the RAM cartridge were exchanged as a precautionary measure. The set-up is particularly suitable for peptides and other low-molecular weight analytes in matrices containing large amounts of high-molecular weight proteins like BSA. Importantly, it can be used for the analysis of relatively large volumes (10-100 μL) for nanoLC-MS.
Our rapid, reproducible and robust RAM-nanoLC-MS set-up is expected to be of great interest for comparative analysis of large sets of samples. Further developments of this modular system involve the use of stationary phases of different selectivity and the coupling to a more sensitive triple quadrupole or linear ion trap mass spectrometer. We consider that this system holds promise in the field of biomarker discovery, where limited sample is available (e.g. CSF from animal studies) and concentrations of interesting molecules is rather low.

References

[1] N. I. Govorukhina, A. Keizer-Gunnink, A. G. J. van der Zee, S. de Jong, H. W. A. de Bruijn, R. Bischoff; *Journal of Chromatography A* **1009**, 171 (2003)

[2] C. Li, K. H. Lee; *Analytical Biochemistry* **333**, 381 (2004)

[3] K. Bjrhall, T. Miliotis, P. Davidsson; *Proteomics* **5**, 307 (2005)

[4] Y. Li, J. W. Cooper, C. S. Lee; *Journal of Chromatography A* **979**, 241 (2002)

[5] T. C. Pinkerton, K. A. Koeplinger; *Journal of Chromatography A* **458**, 129 (1988)

[6] S. Souverain, S. Rudaz, J. L. Veuthey; *journal of chromatography B* **801**, 141 (2004)

[7] J. A. O. Meriluoto, K. Isaksson, H. Soini, E. Nygard, J. E. Eriksson; *Chromatographia* **30**, 301 (1990)

[8] K. Racaityte, E. S. M. Lutz, K. K. Unger, D. Lubda, K. S. Boos; *Journal of Chromatography A* **890**, 135 (2000)

[9] K. Wagner, T. Miliotis, G. Marko-Varga, R. Bischoff, K. K. Unger; *Analytical Chemistry* **74**, 809 (2002)

[10] H. D. Meiring, E. van der Heeft, G. J. ten Hove, A. P. J. M. de Jong; *Journal of Separation Sciences* **25**, 557 (2002)

[11] P. van Midwoud, L. Rieux, R. Bischoff, E. Verpoorte, H. A. G. Niederlander; *Journal of Proteome Research* **In preparation** (2006)

[12] Y. Shen, N. Tolic, C. Masselon, L. Pasa-Tolic, D. G. Camp, K. K. Hixson, R. Zhao, G. A. Anderson, R. D. Smith; *Analytical Chemistry* **76**, 144 (2004)

[13] L. Rieux, D. Lubda, H. A. G. Niederlander, E. Verpoorte, R. Bischoff; *Journal of Chromatography A* **1120**, 165 (2006)

[14] W. E. Haskins, Z. Wang, C. J. Watson, R. R. Rostand, S. R. Witowski, D. H. Powell, R. T. Kennedy; *Analytical Chemistry* **73**, 5005 (2001)

[15] N. Corbally, D. Powell, K. F. Tipton; *Biochemical Pharmacology* **39**, 1161 (1990)

CHAPTER 6

Improvement of Recovery and Repeatability in Peptide Analysis

6.1 Introduction

Nowadays (two-dimensional) liquid chromatography coupled to (tandem) mass spectrometry (2D-LC-MS/MS) is one of the main techniques applied for proteomics analysis. Briefly, proteins are first digested with an enzyme to yield proteolytic peptides. The resulting complex peptide sample is chromatographically separated and the eluting peptides are detected and characterised with mass spectrometry. 2D-LC-MS/MS systems have proven their capability for qualitative analysis of proteins in proteomics; however, quantitative analysis is still a challenge due to the considerable variation in absolute peak intensities or peak areas. In the experiments described in this study, relative standard deviations (RSD) of as much as 80-90% were observed. Labeling techniques or addition of internal standards may alleviate the problem [1,2]. Most of these methods rely on relative quantification, by means of either differential labeling [3, 4] or standard addition with a well characterised peptide mixture [5]. However, these techniques require additional sample handling and increase sample complexity and the risk of ionisation suppression. Furthermore, in the case of standard addition, peptides and standards may still differ sufficiently in their characteristics to impair good

normalisation for every single peptide in a sample. Last but not least, none of these techniques addresses the sensitivity issue related to limited solubility, which may often underlie the variability problem observed.

For proteins it is well known that hydrophobic hydration [6] and interaction with surfaces can give rise to their loss from solution through adsorption and / or aggregation [7–9]. However, the adsorptive behavior of poly- and oligopeptides at low concentrations, as often encountered in proteomics research, is less well studied and documented. For Calcitonin, a 32-amino-acid hormone, adsorption from solutions in the μM range to glass and polypropylene has been shown to be significant [10,11]. The influence of pH, container material and surfactants on adsorptive behavior has been studied [10,11]. The use of surfactants as a pharmaceutical excipient to reduce adsorptive losses of this polypeptide in pharmaceutical formulations was suggested. For the analysis of Calcitonin in serum using LC-MS, however, surfactants may not be used, as these compounds are not compatible with MS measurements. A water / acetonitrile (ACN) reconstitution solvent was suggested instead [12], with a 57%-ACN-in-water mixture proving effective for preventing adsorption to container surfaces at 50 nM concentrations. When not applying MS detection, a surfactant may be safely applied to avoid container adsorption, as shown for the quantification of a 36-amino-acid inhibitor of HIV-1 membrane fusion by LC down to a concentration level of about 50 nM [13].

Adsorption has also been shown to play an important role in the quantitative analysis of individual oligopeptides at the μM-concentration level [14–16]. A detailed study of the adsorption process and options to avoid adsorption were separately published for the decapeptide, Cetrorelix [17], and the cyclic heptapeptide, microcystin-LR [18]. For Cetrorelix, adsorptive losses to vial surfaces was studied as a function of analyte concentration down to the μM level, vial type, dissolution medium and pH, as well as surfactant additives. Adsorption was observed to follow a Langmuir isotherm, and reducing adsorption by addition of modifiers (ethanol, acetic acid, surfactants) was accompanied by a decrease in response variability. For mycrocystin-LR, investigation of adsorptive losses during laboratory manipulation of the sample showed that processes like repeated pipetting led to cumulative losses. In addition, losses in microcentrifuge tubes could be significant, depending on the tube material, but could be avoided when using a dissolution medium containing >25% methanol (MeOH).

For the quantitative analysis of mixtures of proteolytic peptides at the low concentrations often encountered in proteomics studies (nM), systematic studies concerning the effect of adsorptive losses have, to the best of our knowledge, not yet been performed. Detection and quantification of proteolytic peptides at this con-

centration level can be of utmost importance in finding biomarkers for disease pathology or metabolic activity, for example. Losses and variability resulting from adsorption to the surfaces of vials or other analytical components can be detrimental in such studies.
This publication focuses on methodology for improving repeatability and recovery in the analysis of a model mixture of proteolytic peptides at the nM concentration level using LC-MS. As repeatability and recovery issues were already apparent when applying 1D-LC-MS, a simple LC-MS system was used for all experiments. The system was miniaturised using a capillary monolithic reversed-phase (RP) column, since nanoLC-MS is often required in proteomics to achieve adequate sensitivity. Using this system, it is demonstrated that poor recovery of peptides from the sample vials at the nM concentration level is the primary cause for the quantification problems observed.
Peptide interactions with solvents and surfaces will differ, depending on the side chains of the amino acids making up a peptide. Whether a peptide remains in solution or not depends on these interactions. The influence of both solvent composition and vial surface on peptide solubility in a model sample has been studied. Fundamental physico-chemical aspects influencing solubility are considered in specific cases.

6.2 Experimental

6.2.1 Chemical reagents

Acetonitrile (ACN, Supra gradient) and methanol (MeOH, HPLC grade) were purchased from BioSolve B.V. (Valkenswaard, The Netherlands). HPLC-grade water was prepared by passing demineralised water through an Elgastat Maxima ultrapure water system (ELGA, High Wycombe, UK). Formic acid (FA, ultrapure, 98-100%), acetic acid (HAc, 100%), acetone (ACT, 99.5%) and potassium chloride (KCl, 99.5%) were purchased from Merck KGaA (Darmstadt, Germany). Dimethyl sulfoxide (DMSO, 99.5%) was purchased from Fluka (Buchs, Switzerland). Bovine-heart cytochrome c, trypsin, calcium chloride ($CaCl_2$ 99.0%), ammonium bicarbonate (NH_4HCO_3, 99.5%) and ammonium formate (NH_4OOCH, 99.995+%) were purchased from Sigma (St. Louis, MO, USA).

6.2.2 Materials

Fused-silica capillaries (50-100 μm ID, 360 μm OD) were obtained from Composite Metal Services Ltd. (Ilkley, UK). Capillary tubing connections to the HPLC pump and the injection and switching valves were made with 1/16-inch Valco connections with short 0.020-inch ID PEEK sleeves (Houston, TX, USA). The Teflon tubing (1/16-inch OD and 0.3-mm ID) for butt-connecting the analytical column and the ESI emitter was from Supelco (Bellefonte, PA, USA). The tubing connections between the trap column and the analytical column were made with MicroTight fittings and tees purchased from Upchurch Scientific (Oak Harbor, WA, USA). The trap column (50 * 0.2 mm) and the analytical column (500 * 0.050 mm) were both monolithic C18 columns and were fabricated by Merck (Darmstadt, Germany) for research purposes using a similar method to that reported in [19]. The gold-coated ESI emitter (50-μm ID * 360-μm OD), tapered to 10 ± 0.5 μm, was obtained from NanoSeparations (Nieuwkoop, The Netherlands). Class A borosilicate glass vials, deactivated class A borosilicate glass vials, and polypropylene vials were purchased from Waters (Milford, MA, USA). The deactivated glass vials have been treated with a gas-phase reactive organosilane to produce a hydrophobic glass surface. The volume of the glass vials is 1.5 mL, whereas the volume of the polypropylene vials is 350 μL.

6.2.3 Instrumentation

The automated LC-MS system consisted of an Agilent 1100 Series LC system with low-pressure mixing (Palo Alto, CA, USA), an Endurance autosampler (Spark Holland, Emmen, The Netherlands) and an API 2000 triple quadrupole mass spectrometer (Sciex, Toronto, Canada). The autosampler was equipped with a 250-μL Kloehn syringe and a 10-μL injection loop. For all experiments, the sample was injected in full-loop injection mode and tray cooling was set at 4°C. Detection was performed on the API 2000 triple quadrupole mass spectrometer, using a microelectrospray ionisation interface (micro-ESI, Figure 6.1) based on the commercially available MicroIonSpray interface from Sciex (Toronto, Canada) and modified in-house to render it suitable for the API 2000. Particular attention was paid to the reduction of post-column dead volume introduced by the interface.
The commercial interface contains a micro volume union to connect the column to the spray tip and requires a relatively long spray-tip (5 cm) (Figure 6.1). The dead volume introduced by the micro volume union and the spray-tip resulted in extra peak broadening at the flow rate applied (800 nL/min). To minimise post-column dead volume, the column was butt-connected to a gold-coated tip 1 to 1.5 cm long

(50 μm ID tapered to 10 μm), using a Teflon sleeve. For this purpose, the hole in the micro volume union was increased to 400 μm to allow the analytical column to be guided through it. The voltage is directly applied to the gold-coated tip via a cogwheel-shaped metal spacer. The spacer was slid over the tip on the inside of the metal holder, and carbon paste was applied to ensure a good electrical connection. The resulting microESI is suitable for low-nanoliter-per-minute up to microliter-per-minute flow rates. The cogwheel shape of the spacer allows for the pneumatic assistance option of the commercial interface to remain available. At low-nanoliter-per-minute flows, the interface is operated without pneumatic assistance. At the column flow rate applied (800 nL/min), signal intensity for the sample peptides increased up to a nebuliser gas pressure of 3 psi. Increasing the pressure of the nebuliser gas above 3 psi did not result in any further increase in signal. The term "nanoESI" is used throughout this publication to describe this specific interface. For all the experiments described in this report, the ESI tip was positioned slightly off-axis with respect to the orifice.

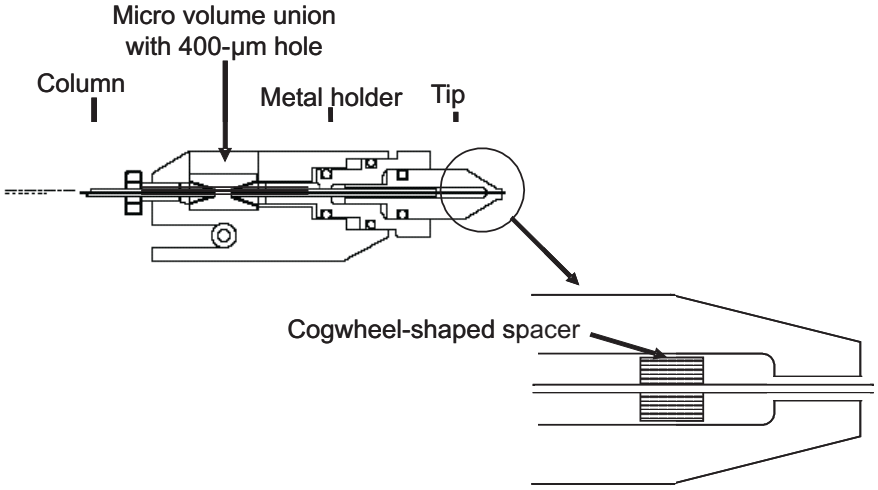

Figure 6.1: Sciex MicroIonSpray modified in-house for nanoflow conditions.

6.2.4 LC-system configuration

Figure 6.2 presents the LC system configuration, as previously presented by Meiring et al. [20] and used for peptide analysis in this study. A restriction of 1500 * 0.075-mm fused-silica capillary is placed before the trap column to split the flow at a ratio of 500-to-1. The six-port valve is used to control both the flow direc-

tion after the trap column and the on/off switching of the flow restriction before the trap column. The tubing connections from the LC pump to the autosampler were made with 100-μm-ID fused-silica capillary, and the connections between the autosampler and the column were made with 75-μm-ID fused-silica capillaries.

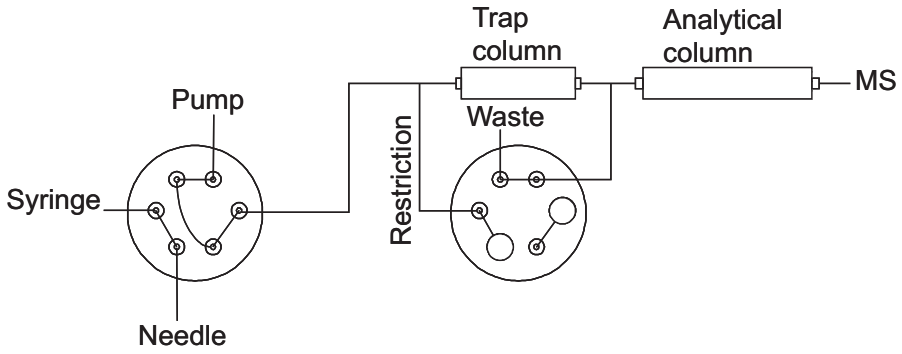

Figure 6.2: LC-system configuration used in this study. This set-up has been extensively described by Meiring et al. [20].

6.2.5 MS and MS/MS parameters

MS source parameters were set to achieve optimised peptide signal intensity when a 3-μM proteolytic peptide mixture in water: ACN: FA (95:5:0.1; v/v/v) was directly infused into the MS. The flow rate was set at 800 nL/min.
Curtain gas was set at 25 psi, nebuliser gas (GS 1) at 2 psi and the ion spray voltage at 3500 - 4200 volts. The settings for ion optics, declustering potential (DP), focusing potential (FP), entrance potential (EP) and collision cell entrance potential (CEP) depend on the m/z for the peptides monitored and were set as in Table 6.1. Parameters for peptide fragmentation, collision energy (CE) and collision cell exit potential (CXP) also depend on the initial m/z of the peptide monitored and are included in the table. The collision gas (N_2) pressure was set at 2 psi.

6.2.6 Procedures

The wash solvent used to rinse the injection needle and buffer tubing of the autosampler after an injection was 10 % ACN, 10 % DMSO, 10 % FA and 70 % water.
For all experiments described, full-loop injection (10 μL) of a cytochrome c digest

Peptide	m/z Q1	m/z Q3	DP	FP	EP	CEP	CE	CXP
A	678.27	402.10	141.00	230.00	-10.50	26.00	37.00	10.00
B	634.33	374.10	126.00	260.00	-11.00	28.00	35.00	10.00
C	529.08	548.10	46.00	320.00	-11.00	18.00	23.00	12.00
D	729.05	1099.30	76.00	130.00	-9.00	34.00	29.00	28.00
E	779.31	520.00	136.00	200.00	-11.00	26.00	39.00	14.00
F	584.93	506.00	96.00	310.00	-8.00	26.00	25.00	12.00
G	482.87	494.10	36.00	290.00	-9.00	32.00	21.00	12.00
H	545.23	616.20	81.00	300.00	-9.50	16.00	29.00	16.00
J	713.67	841.20	61.00	300.00	-11.00	26.00	29.00	22.00
K	673.00	358.30	81.00	210.00	-11.50	32.00	23.00	8.00

Table 6.1: Ion optics and fragmentation parameters.

(CC digest) was performed. In total, 55 μL of sample was removed from the vial for each injection, in order to flush the injection assembly thoroughly with sample. Loading the sample onto the trap column is performed as described by Meiring et al. [20]. Briefly, the splitter restriction is switched off and the flow is directed through the trap column and further to wastes. The sample is loaded at 10 μL/min (loading time, 2.5 min). The loading buffer consisted of 0.1% FA in water: ACN (99 : 1 v/v, pH $\approx$ 3). After loading the sample, the valve is switched back, splitting the flow before the trap column at a ratio of about 500:1. The pump flow is increased to 400 μL/min and the resulting flow through the column is 800 nL/min. The sample is eluted from the trap column onto the analytical column where chromatographic separation takes place. In this configuration, the trap column is operated in forward-flush mode [20]. Gradient elution of the analytical column is performed, using 0.1% (v/v) FA in water (solvent A) and 0.1% (v/v) FA in ACN (solvent B). A gradient starting at 3% solvent B and increasing to 55% solvent B over 45 minutes is employed. Before the next sample is injected, both the trapping column and the analytical column are equilibrated at 1% solvent B for 10 minutes.

6.2.7 Sample preparation

A CC digest was chosen because it contains peptides with a wide range of polarities and isoelectric points (pI, from 4 to 9.5).
CC was digested with trypsin. A 50-μL volume of CC protein (10 mg/mL) was mixed with 12.5μL of trypsin (1 mg/mL in 50 mM HAc), 25 μL $CaCl_2$ (100 mM

in water) and 412.5μL ammonium bicarbonate (100 mM in water, pH 8). The solution was incubated at 37°C overnight with slight vortexing at 300 rpm in an Eppendorf thermomixer. The digestion was stopped by diluting the solution 10 times with 0.1% FA in water.
Assuming complete digestion, a tryptic digest concentration of 83.3μM of each peptide was obtained, which was used to calculate the peptide concentrations of the injected samples. Sample peptide concentrations of 1.67, 8.33 and 16.7 nM were prepared by stepwise dilution with the sample matrix. The composition of the sample matrix was varied throughout this study and is presented in the sections and figure captions below. Trypsin specifically cleaves peptide bonds on the carboxyl end of arginine and lysine [21]. The peptides observed in this study are presented in Table 6.2 and cover 80% of the amino acid sequence of bovine-heart CC.

Peptide	Sequence	m/z	Charge	Retention (min)	pI
A	YIPGTK	678.3	1+	11,16	8,59
B	IFVQK	634.3	1+	12,29	8,75
C	KTGQAPGFSYTDANK	529.1	3+	16,01	8,50
D	TGQAPGFSYTDANK	729.0	2+	17,43	5,50
E	MIFAGIK	779.3	1+	21,63	8,50
F	TGPNLHGLFGR	584.9	2+	22,02	9,44
G	EDLIAYLK	482.9	2+	25,08	4,34
H	IFVQKCAQCHTVEK	545.2	3+	27,86	8,06
J	GITWGEETLMEYLENPKK	713.6	3+	30,68	4,49
K	GITWGEETLMEYLENPK	1005.7	2+	32,41	4,09

Table 6.2: Peptides observed for a CC digest. Note that peptides C, H and J have a missed cleavage.

6.3 Results and discussion

Repeatability for the instrumental set-up was assessed using five sequential injections of 167 femtomoles in 10μL (16.7 nM) of the CC digest in mobile phase (0.1% FA in water) from the same sample vial. RSD values observed for absolute peak area of the individual peptides ranged from 15 to almost 90%. As RSD is especially poor for the late eluting peptides (peptides H, J and K), there appears to be a correlation with hydrophobicity.

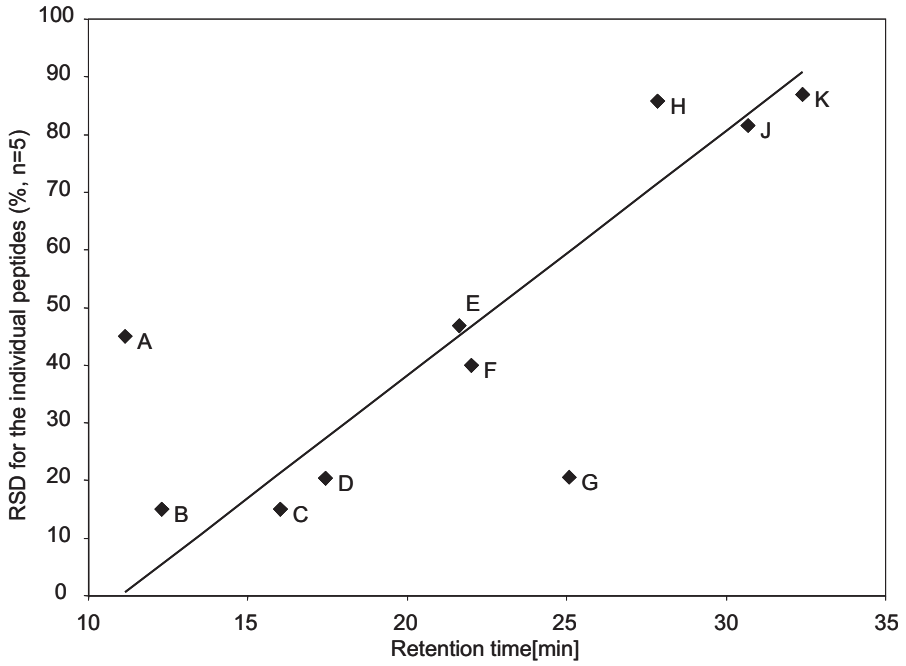

Figure 6.3: Relative standard deviation (RSD) for peak areas for the individual peptides (see Table 6.2) for repeated (n=5) injections of CC digest (167 femtomole in 10μL) as a function of retention time. Sample matrix: 0.1% formic acid in water.

As originally established by Cowan and Whittaker [22], the average hydrophobicity of peptides is adequately expressed by retention time in reversed-phase chromatography. Therefore, retention time is used as a measure of hydrophobicity throughout this study. RSD as a function of retention time is presented in Figure 6.3. As can be seen, there is a clear correlation of RSD with retention time, with the exception of peptides A and G. For peptide A, it should be noted that breakthrough on the C_{18} trap column was observed at ACN percentages of the sample loading solvent as low as 2 - 3%. Therefore, the relatively high RSD for this peptide is probably due to variable losses during sample loading. For peptide G, no obvious causes can be given for the deviation from the correlation between RSD and retention time. In general, it can be concluded from Figure 6.3 that the RSD for absolute peak area increased with the hydrophobicity of the peptides, up to RSD values exceeding 80%. Especially at these high RSD values, it would be impossible to perform quantitative analyses without using an internal standard

or a stable-isotope labeling technique. Without normalising against an internal standard, LOD values of about 30 to 40 femtomole (3 - 4 nM in 10 μL) for the hydrophilic peptides to about 100 to 200 femtomole (10 - 20 nM in 10 μL) for the hydrophobic peptides were obtained. It was postulated that the large variability in peak areas observed might be due to limited peptide solubility in the sample, loading buffer, or eluent, leading to losses, especially for the more hydrophobic peptides. Alternatively, ion evaporation in the electrospray process interfacing LC with MS can be influenced by compound hydrophobicity [23, 24], leading to variability in the MS signal. Both possibilities were investigated.

6.3.1 Electrospray stability and variable ionisation efficiency

It is well known that organic modifiers exhibit a positive influence on spray stability and ion evaporation when coupling liquid chromatography with mass spectrometry through ESI interfacing [23–25]. Since gradient elution is applied for chromatographic separation of the CC peptides, the late eluting hydrophobic peptides enter the ESI interface at a relatively high organic modifier percentage ($\approx$ 40% ACN), which should in fact favor solvent- and ion evaporation. Given that RSD values for these peptides are very high, increasing the modifier percentage even further is not expected to provide a very significant improvement in RSD. Changing the modifier type is an interesting option, however. Recently, Borges and Henion [25] and Szabo and Kele [26] obtained improved results when adding DMSO for direct-infusion ESI-MS of hydrophobic compounds, including a synthetic hydrophobic peptide. Szabo and Kele observed an improvement in signal intensity at the m/z values for the protonated and sodiated analytes when solutions in pure DMSO were electrosprayed by direct infusion. They attribute the signal intensity improvements observed to improved solubility of the compounds studied. In addition, Borges and Henion found that sensitivity and spray stability are adequate when applying DMSO as the solvent for direct-infusion ESI-MS of some hydrophobic basic drugs. Furthermore, sensitivity was enhanced when applying DMSO in combination with water and formic acid.
We studied the effect of DMSO in direct-infusion nanoESI-MS of an 8.3-μM CC digest. The CC digest was dissolved in water containing 0.1% formic acid (v/v) and 0, 1, 2.5, 5 or 10% DMSO (v/v). Signal intensity and the RSD thereof did not improve over this range of DMSO concentrations. On average, signal intensity decreased with increasing DMSO concentration, an effect that was more pronounced for the hydrophobic than the hydrophilic peptides. The RSD of the signal intensity (i.e. spray stability) remained largely unaffected. Adding a small

percentage of DMSO (0.1%) to the mobile phase for LC-ESI-MS also did not improve repeatability for the CC peptides in LC-ESI-MS (data not shown).
Hence, solubility issues during the electrospraying and / or ionisation process as observed by Szabo and Kele [26] do not apply for the model sample of proteolytic peptides used in this study. In agreement with Borges and Henion [25], spray stability remained adequate when applying DMSO, but sensitivity improved with a decreasing percentage of DMSO in the electrospraying solvent. As the RSD on signal intensity remained largely unaffected by the DMSO percentage, it was concluded that the large RSD values for observed peak area for our model sample of proteolytic peptides must originate from solubility issues prior to interfacing LC with MS.

6.3.2 Improving solubility to decrease adsorption

DMSO, along with some other polar aprotic solvents, has the unique property that it efficiently dissolves both polar and apolar compounds. It is frequently applied for solubilisation of peptides and proteins for biological and biochemical studies [27], synthesis and isolation [28–31], (conformational) studies with NMR [32], spectrophotometric [33] or other techniques [34], as well as for pharmaceutical formulations [35]. Solubility is also a known issue in proteomics analysis of hydrophobic proteins and peptides with ESI-MS [36]. However, to our knowledge, only the direct-infusion study by Szabo and Kele [26] demonstrates the applicability of DMSO for solubilisation of a hydrophobic peptide for LC-MS analysis [26]. DMSO-water mixtures show a good peptide-solvent interaction. DMSO promotes hydrogen bonding with water molecules, while efficiently solvating hydrophobic parts of solutes, thus creating a favorable network with water for dissolving peptides [31].
Dissolving the CC digest in water: FA: DMSO (90:5:5, v/v/v, pH $\approx$ 2) showed an improvement in RSD of peak area for each of the CC peptides monitored. Experiments were performed at three concentration levels (1.67, 8.33 and 16.7 nM CC digest), each analysed in triplicate. For every peptide, at each concentration level, RSD of peak area improved by a factor of 3 to 10, with a few exceptions where the improvement was even bigger. With the exception of the peptides eluting last (peptides H, J and K), the RSD of peak area was now at about or below 10%. For peptides H, J and K, the improvement was generally best, but RSD values were still on the order of 10 to 20%. When using the data obtained to fit calibration curves, an improvement of the regression coefficient (R^2) was also observed. This

improvement was limited for early-eluting peptides, with a sensitivity gain[1] of a factor of ≈ 1.35 peptides C and D. However, a factor of up to 2.5 improvement was obtained for peptides F, H, J and K. The R^2 was between 0.97 and 0.999 for all peptides monitored, with an exception for peptides J and K (R^2 was 0.89 and 0.83, respectively).
Some improvement in the RSD of peak area was also observed when only increasing the FA percentage to 5% (pH ≈ 2), without addition of DMSO, or when only adding 5% DMSO, but keeping the FA percentage at 0.1% (pH ≈ 3). However, the observed effect was limited as compared to the situation where both the FA percentage was increased to 5% and 5% DMSO was added to the sample. Especially for peptides J and K, the separate effects of increasing the FA percentage or adding DMSO was almost negligible.
The beneficial effect of increasing the FA percentage in the sample from 0.1 to 5% may well be due to the accompanying decrease in pH from ≈3 to ≈2, which in turn results in reduced electrostatic interactions between the peptides and the vial wall (silanol groups). However, an FA percentage of 5% is sufficiently high to have a direct effect on peptide solvation as well.

6.3.3 Adsorption to different vial materials

To evaluate how remaining adsorptive effects depend on the vial surface material, three different vial types were evaluated. In previous experiments, only glass vials were used. In addition to these, organosilane deactivated glass vials and polypropylene vials were tested in the following experiments. An 83-femtomole CC digest sample (10 μL, 8.33 nM), diluted in 5% DMSO and 5% FA, was injected from each of these vial types (n=10, from a different vial for each repetition). For all but the late-eluting, most hydrophobic peptides (peptides H, J and K), peak area was essentially independent of vial type. The results for one of the early-eluting peptides (peptide C) and peptide J are presented in Figure 6.4. For the more hydrophilic peptide C, hardly any effect of vial surface material was observed. Only for the most hydrophobic vial type, a very limited decrease in peak area as compared to the other two vial types might exist. However, peak area for peptide J decreases with increasing hydrophobicity of the vial surface (Peak area: glass >organosilane deactivated glass >polypropylene). Thus, adsorption to the vial surface results from hydrophobic interactions, which are much more pronounced for the hydrophobic than for the hydrophilic peptides in the model sample of proteolytic peptides.

[1] Increase in the slope of the calibration curve.

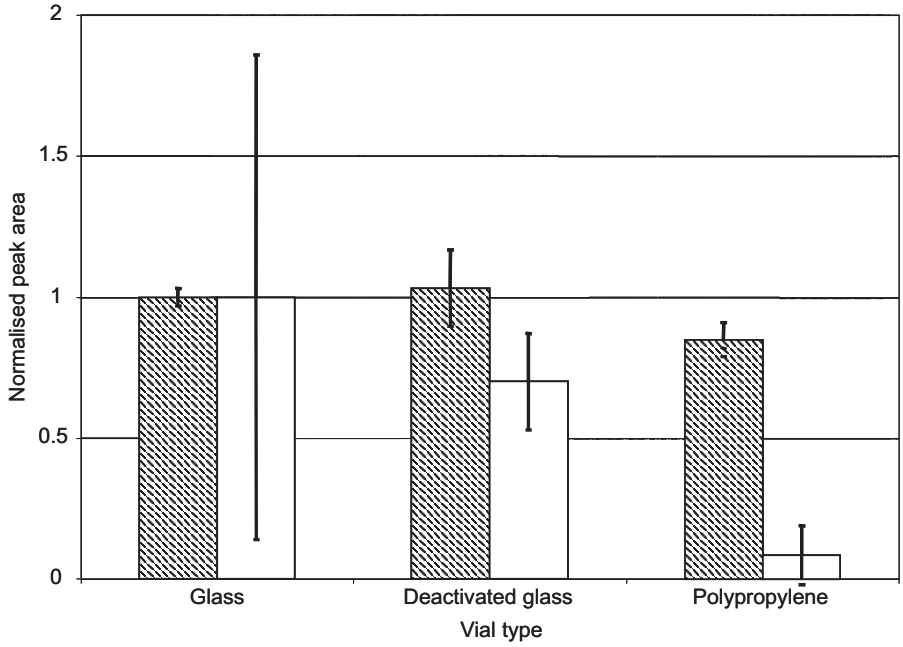

Figure 6.4: Effect of vial type on peak area for repeated (n=10) CC digest injections (83.3 femtomoles in 10 μL), normalised to the situation for glass vials. Peptide C: shaded bars; peptide J: blank bars. Sample matrix: 5% FA and 5% DMSO in water.

For peptide J, the standard deviation on peak area is exceptionally large when using glass vials. The effect is also observed for the other two most hydrophobic peptides, H and K. This variability is perhaps due to vial-to-vial differences in surface characteristics. Given the effect on average peak area for the most hydrophobic peptides, glass vials were selected for all further experiments. To obtain a further decrease in RSD values for these peptides, a higher percentage of DMSO in the sample, rather than a more hydrophobic vial type, was considered. A further increase in FA percentage, thereby lowering pH below $\approx$2, was not expected to have a further positive effect on decreasing electrostatic interactions with silanol groups. Moreover, DMSO is a more logical choice for a further improvement of peptide solvation, aimed at decreasing hydrophobic adsorption to the vial surface.

6.3.4 Effect of surface-to-volume ratio

Limited solvation of hydrophobic peptides leading to adsorption to surfaces also leads to a correlation between peak area and surface-to-volume ratio for the sample in the vials. Such a correlation proved to be especially evident for the more hydrophobic peptides.

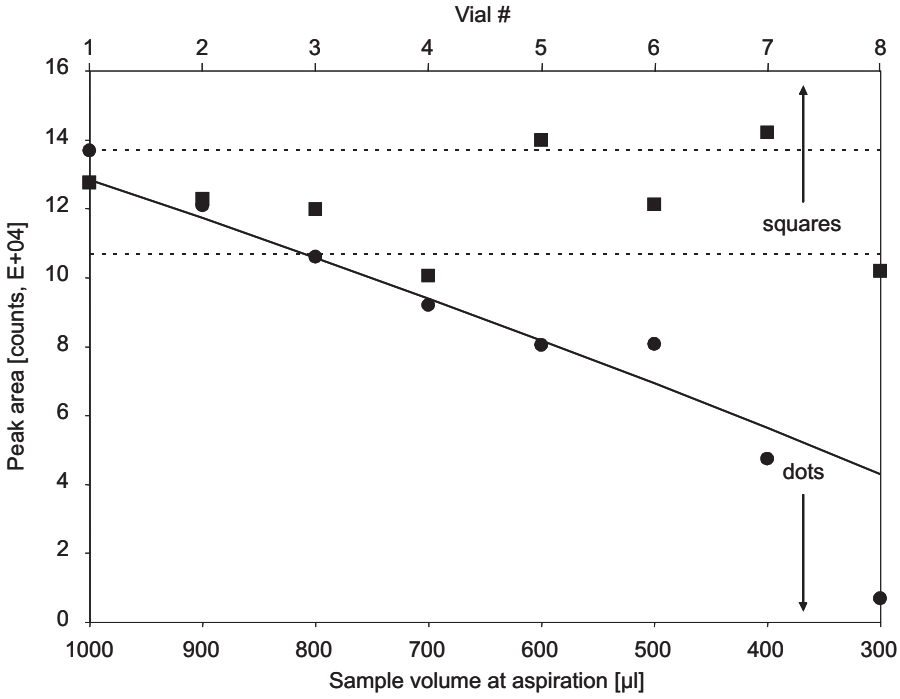

Figure 6.5: The effect of increasing surface-to-volume ratio on peak area for peptide K (surface-to-volume ratio increases with decreasing volume). Eight injections of 83.3 femtomole in 10 μL were made from individual vials with a decreasing volume (dots) or from individual vials with a constant volume (1000 μL; squares). The continuous line represents the fit of the theoretical expression for recovery to the data obtained (Vial ID = 1 cm, Kpept.-K $\approx$ 7.5 cm). The standard deviation interval on the injections from the 1000 μL samples is indicated by the broken lines. Sample matrix: 5% FA and 5% DMSO in water.

When repeated injections were performed from a single sample vial, peak area for the most hydrophobic peptides (peptides J and K) decreased with every subsequent injection. This indicated a continuous decrease in peptide concentration upon repeated injection from a single vial. The same effect was observed when

injections were made from individual vials containing decreasing initial sample volumes (Figure 6.5). Figure 6.5 also shows that, when injecting from different vials, each containing 1000 μL sample, this effect is not observed.

The observed effect follows directly from a simple expression for thermodynamic equilibration of peptides between the sample and the vial surface, as a function of surface-to-volume ratio. The equilibrium constant for equilibration of a compound between a solution phase and a solid surface (K_X) can be expressed as:

$$K_X = \frac{C_{XA}}{C_X} = \frac{n_{XA}}{n_X}\frac{V_S}{A_V} = \frac{n_X^0 - n_X}{n_X}\frac{1}{SVR} = \frac{1 - \%R}{\%R}\frac{1}{SVR} \tag{6.1}$$

Where: $C_{XA}$is the concentration (moles.m^{-2}) of compound X adsorbed to the vial surface, C_X the concentration (moles.m^{-3}) of compound X in solution, n_{XA} the amount (moles) of compound X adsorbed to the vial wall, n_X the amount (moles) of compound X in solution, n_{X0} the amount (moles) of compound X in solution before adsorption took place, V_S the sample volume (m^3), A_V the surface area (m^2) of the vial in contact with the sample solution, SVR the surface-to-volume ratio, and $\%R = n_X/n_{X0}$ the percentage of compound X recovered in solution. Rewriting this expression for recovery yields:

$$\%R = \frac{1}{1 + K_X SVR} \tag{6.2}$$

Equation 6.2 shows that the percentage compound recovered in solution is inversely proportional to the surface-to-volume ratio. When sample volume decreases in a vial, the absolute contact area between the sample and the wall of the vial decreases. However, the surface-to-volume ratio increases, and the observed effect occurs. Recovery reaches a (theoretical) maximum at infinite sample volume where SVR converges to a value determined by the inner diameter of the vial. Taking this limiting case into account, the fit of the data obtained for this expression is shown in Figure 6.5. In addition to surface-to-volume ratio, recovery is also inversely proportional to the equilibrium constant for equilibration of the peptides between the solution phase and the vial surface. Recovery from the sample matrix applied was anticipated to be less than 20% for peptide K (see Figure 6.6). An estimate of the equilibrium constant can then be obtained upon fitting the model to the data (see Figure 6.5). Since the equilibrium constant increases with increasing adsorption behavior of peptides, the effect of surface-to-volume ratio will be more pronounced for peptides adsorbing strongly. For the hydrophobic peptides in the model sample, shifting the equilibrium towards the soluble phase should therefore lead to improved recovery and a reduced effect of

the SVR on recovery. For peptides C and D, the observed increase in sensitivity upon addition of 5% FA and 5% DMSO, as highlighted in section 6.3.2 above, is most probably due to this effect.

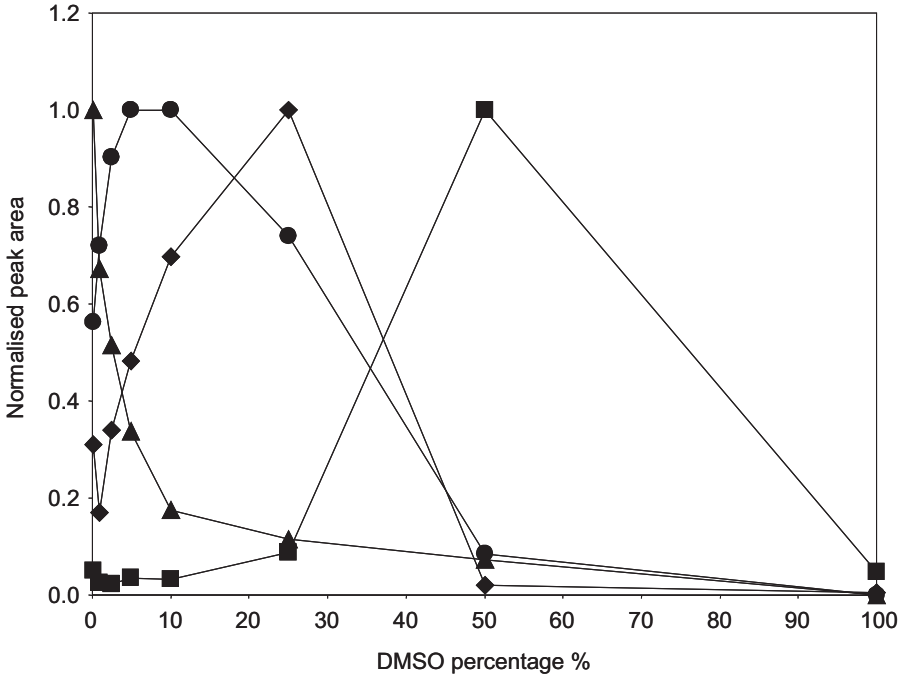

Figure 6.6: Peak area, normalised with respect to the optimum value for the individual peptides, as a function of DMSO percentage in the sample matrix for 10-μL injections of a 16.7-nM CC digest (167 femtomole injected). Peptide B (triangles), peptide E (dots), peptide H (diamonds) and peptide K (squares) are shown.

6.3.5 Optimal DMSO percentage for individual peptides

Increasing the percentage of DMSO in the sample should lead to improved solvation, and thus to a decrease of the equilibrium constant for adsorption to the vial surface and thereby to improved recovery. The effect of increasing percentages of DMSO on peak area was therefore studied for individual peptides.

As expected, the equilibrium constant for equilibration of peptides in solution and adsorbed to the vial surface is also influenced by sample temperature. Whenever samples were not allowed to reach the temperature of the autosampler tray (4°C) before the first injection, peak areas for this first injection were significantly larger than for subsequent injections. This problem could be overcome by

preparing samples at 4 °C or by allowing them to reach the temperature of the autosampler. In addition, to avoid a superimposed effect of surface-to-volume ratio, only single injections were made from individual sample vials.
Typical profiles for changing peak area with DMSO percentage are presented in Figure 6.6 for peptides B, E, H, and K. Increasing the percentage of DMSO in the sample at a fixed FA percentage of 5% has a dramatic effect on peak area for all the peptides monitored. For early-eluting peptides (A, B, C and D), peak area decreases rapidly with increasing DMSO percentage over the range from 0 to 10%. For peptide A, peak area decreases upon the addition of as little as 1% DMSO to the sample. For peptides B, C and D, peak area remains constant, or even increases a little up to a DMSO percentage of 2.5%, but decreases rapidly at higher percentages. For late-eluting peptides (J and K), peak area remains almost constant up to a DMSO percentage of 25%. However, a substantial gain in peak area of a factor of about 20 is obtained upon increasing the DMSO percentage from 25 to 50%. Upon increasing the DMSO percentage even further (from 50 to 100%), peak area decreases again. The other peptides (E, F, G and H) show intermediate behavior. An increase in peak area can be attributed to improved solvation of the corresponding peptide and thus a decrease in adsorption. The subsequent decline in peak area at higher DMSO percentages is the result of breakthrough of the corresponding peptide on the trap column. As a result, every (group of) peptide(s) has its own optimal DMSO percentage, as can be seen from Figure 6.6. For peptides F and G a less pronounced effect of the DMSO percentage on peak area is observed. For these two peptides, peak area decreased slowly with increasing DMSO percentage up to 25 and 50 % DMSO, respectively. Subsequently, at higher DMSO percentages, peak area decreased very rapidly due to breakthrough on the trap column.
The optimal DMSO percentage for the individual peptides as a function of retention time is presented in Figure 6.7. The DMSO percentage for optimal solubility of the peptides is related to hydrophobicity of the peptides in an exponential manner. Assuming that the optimal values correspond to quantitative recovery of the peptides from the sample vial (i.e. no adsorption), the adsorbed amounts for samples giving incomplete peptide solubility can be estimated from the respective peak areas as follows:

$$n_{XA} = \frac{PA_{optimal} - PA_{DMSO\%}}{PA_{optimal}} C_X^0 V_S \tag{6.3}$$

Where: n_{XA} is the amount (moles) of compound X adsorbed to the vial wall, C_X^0 the concentration (moles/L) of peptide X in solution before adsorption,

$PA_{optimal}$ is the peak area for C_X^0 under optimal solubility conditions, $PA_{DMSO\%}$ is the peak area for C_X^0 under conditions less favorable for solubility, and V_S is the sample volume.

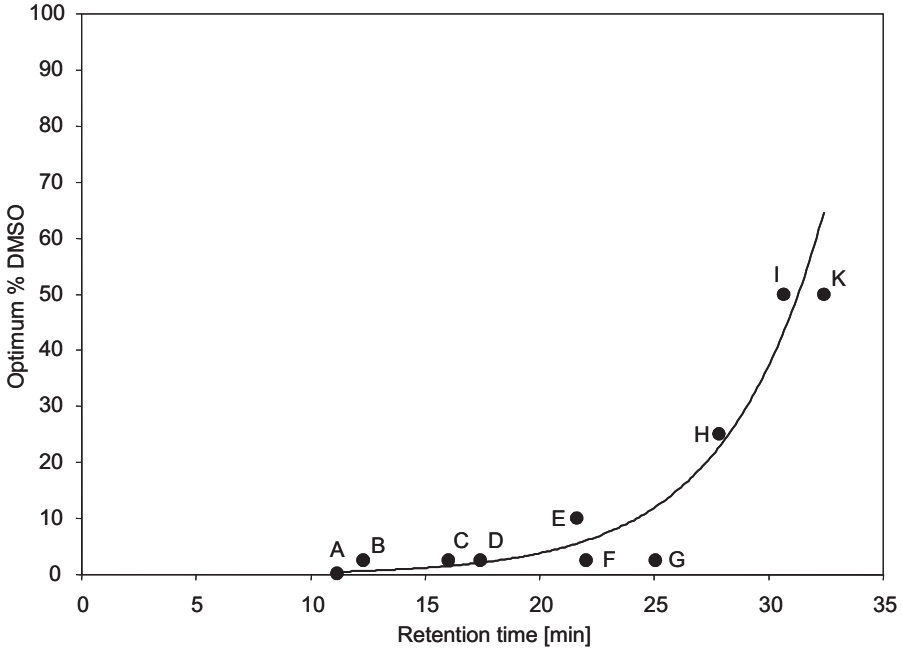

Figure 6.7: Optimal DMSO percentages for recovery of individual peptides as a function of retention time (hydrophobicity). The optimal values presented are independent of sample concentration.

For samples containing 5% FA and 0 - 5% DMSO, a linear dependence of the calculated adsorbed amount (n_{XA}) on sample peptide concentration ($C^0{}_X$) is obtained for the hydrophobic peptides (data not shown). The amount adsorbed per concentration-unit increase is related to peptide hydrophobicity (i.e. the slope increases with hydrophobicity). Given their limited adsorption, any trend in concentration dependence for the hydrophilic peptides (A, B, C and D) is largely obscured by variability. As the peptide concentrations are very small ($\leq$16.7 nM), an adsorption plateau is not reached for any of the peptides studied. For Cetrorelix, Grohganz et al. found that adsorption only reached a plateau at a concentration of 0.4 μg.mL^{-1} ($\approx$ 300 nM) [17], which is at least an order of magnitude higher.

In addition to DMSO, methanol (MeOH), acetonitrile (ACN) and acetone (ACT) were considered for improved peptide solubility in the sample. The difference in selectivity for these three solvents, DMSO and water in Snyder's solvent selectivity classification system was the primary reason for their selection [37]. The trends observed for peak area as a function of the percentage organic modifier in the sample was similar to that observed with DMSO for the individual peptides (data not shown). The only difference is a shift of the optimum value for all the peptides to a lower percentage organic modifier. For MeOH, ACN and ACT, the optimum for peptide K, the most hydrophobic peptide, is 25% as compared to 50% when using DMSO. The observed shift is a direct consequence of the difference in polar characteristics of the different organic solvents. Applying Snyder's solvent polarity index [37], the polarity index for DMSO (7.2) is much closer to that of water (10.2) than is the case for MeOH (5.1), ACN (5.8) or ACT (5.1). Retention of the peptides during sample loading on the trap column is therefore negatively influenced with the latter three solvents [38]. As no additional selectivity differences were observed, solvents other than DMSO were not considered for further experiments.

6.3.6 Needle adsorption

In addition to adsorption and solubility issues in the sample vial, adsorption of peptides to the stainless steel autosampler needle can also lead to losses. Adsorption of peptides on the needle was examined by placing the injection needle in the sample vial without any further action for five minutes. Subsequently, the needle was taken out of the vial and washed with 750 μL wash solvent using a standard wash program. The wash solvent consisted of 10% ACN, 10% DMSO, 10% FA and 70% water. This procedure was repeated five times to accumulate possible losses of the peptides due to adsorption. After these steps the sample was injected and the resulting peak area was compared with the peak area for a sample that did not undergo this procedure.
Losses were observed for six of the ten peptides in the model sample (sample matrix 5% FA and 5% DMSO in water). Losses are on the order of 40% (peptides E, J, and K) to 60% (peptides A, B, and H). The effect for peptide J is somewhat obscured by the relatively large standard deviation for this peptide. As no correlation with peptide hydrophobicity could be established, adsorption on the stainless steel needle through interactions other than hydrophobic interactions is proposed. Interestingly, peptides E, H, J and K are the only peptides in the model sample containing one or more amino acids with a sulfur atom in the

side chain. As no oxidation products were found for these peptides, the losses are attributed to adsorption to the stainless steel needle via the sulfur atom. This is supported by the fact that alkylthiols are applied for the coating of stainless steel. The thiol group binds to the reduced surface of the stainless steel to form a so-called self-assembled monolayer [39]. An explanation for the losses of the two polar peptides (A and B) remains elusive.

6.3.7 Repeatability under Optimised Conditions

Taking all the parameters with respect to the sample matrix and injection routine into account, repeatability was assessed again. All samples were analysed twice, applying two different sample matrices. A sample containing 5% DMSO and 5% FA was applied to avoid loss of the hydrophilic peptides from the trap column, while a second sample, containing 25% DMSO and 5% FA, was applied for improved recovery of the hydrophobic peptides. Samples were prepared at 4°C in glass vials, with a separate vial for each injection. The samples were analysed over a period of 40 h. In Figure 6.8, the RSD values for the different peptides are presented. The figure includes the RSD values for the situation before optimisation of sample matrix and injection routine.
As a result of breakthrough on the trap column, no RSD values could be determined for peptides A and B diluted in 25% DMSO and 5% FA. In addition, variable losses of peptides C, D, E, F and G during sample loading are also the most probable cause of the higher RSD values for these peptides when the sample was diluted in 25% DMSO as compared to 5% DMSO. However, the RSD values for the most hydrophobic peptides (peptides H, J and K) are much lower when the sample was diluted in 25% DMSO. Compared with the original situation, where the sample matrix consisted of 0.1% FA in water and repeated injections were made from a single vial, the improvement for the most hydrophobic peptides is even greater. Improvements for the hydrophilic peptides are limited, due to the fact that the solubility of these peptides is already adequate in an almost purely aqueous environment.

With respect especially to the hydrophobic peptides (F, G, H, J and K), a significant decrease in the limit of detection (LOD) results from the improved recovery and RSD when applying 25% DMSO. For all the peptides in the model sample, LOD values on the order of or below 10 femtomoles in 10 μL (1 nM) can be obtained. For the hydrophilic peptides, the improvement is only a factor of 3 to 4 as compared with the original situation where a sample matrix of 0.1% FA

in water was applied (second paragraph of Results and Discussion). For the most hydrophobic peptides, however, (peptides H, J, and K), the improvement is at least an order of magnitude.

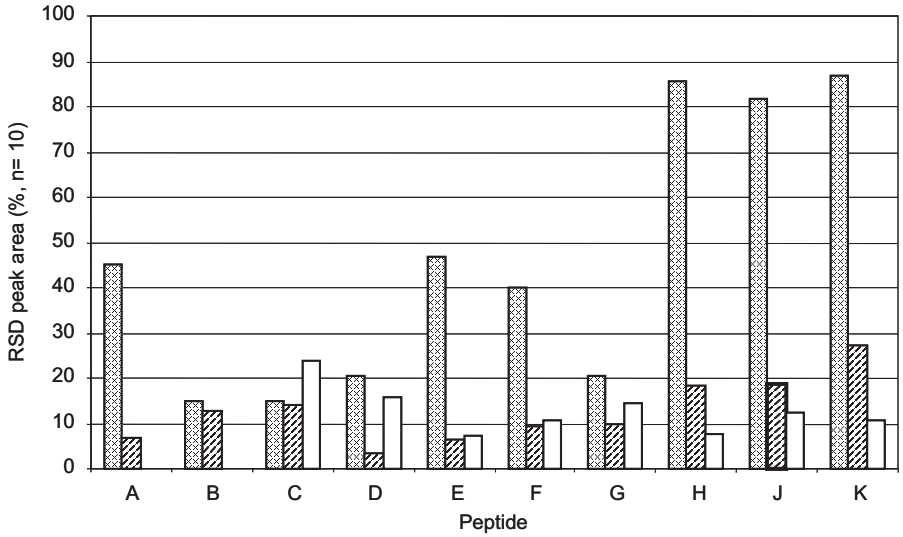

Figure 6.8: Repeatability test (n=10) of 83-femtomole injections of CC digest diluted in 5% DMSO / 5% FA (striped) or 25% DMSO / 5% FA (blank) measured over 40 h. Peptides A and B were not observed in the presence of 25% DMSO, due to lack of binding to the reversed-phase trap column. The RSD values originally obtained for the samples diluted in mobile phase (0.1% FA) are shown for comparison (hatched).

6.4 Conclusion

It has been shown that adsorption of proteolytic peptides to vial surfaces is the cause of repeatability problems in quantitative analysis of these peptides at the nM concentration level. An inverse dependence of recovery and repeatability with peptide - and vial hydrophobicity is demonstrated. The positive influence of applying an organic sample modifier on recovery and repeatability suggests that hydrophobic hydration is an important driving force for adsorptive losses of hydrophobic peptides. As a direct result of the improved recovery when an organic sample modifier is used, repeatability increases and LOD decreases. For the most hydrophobic peptides, a gain in LOD of at least an order of magnitude is obtained. In an aqueous sample containing 0.1% formic acid (FA), it is possible

to detect 100 to 200 femtomoles of peptide, whereas ± 10 femtomoles can be detected in a sample containing 5% FA and 25% DMSO (10 μl injections).
For quantitative analysis of peptides in proteomics samples, preparation of at least two samples in different sample matrices for each peptide mixture is recommended. One sample should consist of the peptide mixture diluted in a significantly high percentage organic modifier to achieve good recovery for hydrophobic peptides. The other sample should consist of the peptide mixture diluted in a solution of low-percentage organic modifier, to avoid breakthrough of hydrophilic peptides on the trap column. DMSO is especially suited as an organic modifier, as it solubilises hydrophobic peptides very well but is not a very strong eluent in reversed-phase chromatography, thereby reducing the risk of breakthrough on the trap column.
Furthermore, it was shown that some peptides, including all sulfur-containing peptides, adsorb on the stainless steel injection needle. To overcome this problem, unnecessary contact of the sample with the autosampler injection needle should be avoided. With many autosamplers, standard procedure sees the injection needle already inserted in the next sample vial in anticipation of the next injection before the previous analysis is finished. This gives the peptides ample time to adsorb on the needle surface. However, this issue could be easily resolved by a change in instrument programming. Our experiments also indicate that only one injection should be made from each individual vial, in order to avoid changes in the surface-to-volume ratio upon repetitive injections from the same vial. A changing surface-to-volume ratio influences the adsorption equilibrium for the peptides between the solution phase and the vial surface. Though surface-to-volume ratio effects are less variable with more hydrophobic vial types than with glass, the equilibrium is shifted further towards peptide adsorption on the vial surface, leading to a decrease in peak area.

References

[1] M. P. Washburn, R. R. Ulaszek, C. Deciu, D. M. Schieltz, J. R. Yates III; *analytical chemistry* **74**, 1650 (2002)

[2] M. Hamdan, P. G. Righetti; *mass spectrometry reviews* **21**, 287 (2002)

[3] S. Sechi, Y. Oda; *Current Opinion in Chemical Biology* **7**, 70 (2003)

[4] M. B. Goshe, r. d. smith; *Current Opinion in Biotechnology* **14**, 101 (2003)

[5] P. V. Bondarenko, D. Chelius, T. A. Shaler; *Anal.Chem.* **74**, 4741 (2002)

[6] V. V. Yaminsky, E. A. Vogler; *Current Opinion in Colloid & Interface Science* **6**, 342 (2001)

[7] C. H. Suelter, M. DeLuca; *analytical biochemistry* **135**, 112 (1983)

[8] D. J. Kirkland, N. N. Kim; *Mutagenesis* **10**, 393 (1995)

[9] W. Norde; *Advances in Colloid and Interface Science* **25**, 267 (1986)

[10] S. Law, C. Shih; *Drug Development and Industrial Pharmacy* **25**, 253 (1999)

[11] M. R. Duncan, J. M. Lee, M. P. Warchol; *International Journal of Pharmaceutics* **120**, 179 (1995)

[12] K. H. Song, H. M. An, H. J. Kim, S. H. Ahn, S. J. Chung, C. K. Shim; *journal of chromatography B* **775**, 247 (2002)

[13] M. K. Lawless, S. Hopkins, M. K. Anwer; *Journal of Chromatography B: Biomedical Sciences and Applications* **707**, 213 (1998)

[14] P. Hyenstrand, J. S. Metcalf, K. A. Beattie, G. A. Codd; *Water Research* **35**, 3508 (2001)

[15] H. Grohganz, O. Schlafli, M. Rischer, M. Brandl; *journal of pharmaceutical and biomedical analysis* **34**, 963 (2004)

[16] H. John, M. Walden, S. Schafer, S. Genz, W. G. Forsmann; *Analytical and Bioanalytical Chemistry* **378**, 883 (2004)

[17] H. Grohganz, M. Rischer, M. Brandl; *European Journal of Pharmaceutical Sciences* **21**, 191 (2004)

[18] P. Hyenstrand, J. S. Metcalf, K. A. Beattie, G. A. Codd; *Toxicon* **39**, 589 (2001)

[19] N. Ishizuka, H. Kobayashi, H. Minakuchi, K. Nakanishi, K. Hirao, K. Hosoya, T. Ikegami, N. Tanaka; *Journal of Chromatography A* **960**, 85 (2002)

[20] H. D. Meiring, E. van der Heeft, G. J. ten Hove, A. P. J. M. de Jong; *Journal of Separation Sciences* **25**, 557 (2002)

[21] J. V. Olsen, S. E. Ong, M. Mann; *Mol Cell Proteomics* **3**, 608 (2004)

[22] R. Cowan, R. G. Whittaker; *Peptide Research* **3**, 75 (1990)

[23] P. Kebarle, L. Tang; *analytical chemistry* **65**, 972A (1993)

[24] A. P. Bruins; *Journal of Chromatography A* **794**, 345 (2002)

[25] V. Borges, J. D. Henion; *Rapid Communications in Mass Spectrometry* **19**, 415 (2005)

[26] P. T. Szab, Z. Kele; *Rapid Communications in Mass Spectrometry* **15**, 2415 (2001)

[27] B. W. Schwab, C. S. G. Davis, P. H. Miller, R. J. Richardson; *Biochemical and Biophysical Research Communications* **132**, 81 (1985)

[28] N. Chang, S. J. Hen, A. M. Klibanov; *Biochemical and Biophysical Research Communications* **176**, 1462 (1991)

[29] H. Kuroda, Y. N. Chen, T. Kimura, S. Sakakibara; *International journal of peptide and protein research* **40**, 294 (1992)

[30] C. K. Taylor, P. W. Abel, M. Hulce, D. D. Smith; *Journal of Peptide Research* **65**, 84 (2005)

[31] L. Malavolta, C. R. Nakaie; *Tetrahedron* **60**, 9417 (2004)

[32] S. Bhattacharjya, P. Balaram; *Proteins: Structure, Function, and Genetics* **29**, 492 (1997)

[33] N. Hirota-Nakaoka, K. Hasegawa, H. Naiki, Y. Goto; *J Biochem (Tokyo)* **134**, 159 (2003)

[34] M. Vauhkonen, P. K. J. Kinnunen, H. Rauvala; *analytical biochemistry* **148**, 357 (1985)

[35] R. G. Strickley; *pharmaceutical research* **21**, 201 (2004)

[36] J. Schaller, B. Christian, P. Urs, P. Schlunegger; *Rapid Communications in Mass Spectrometry* **11**, 418 (1997)

[37] C. F. Poole, S. K. Poole; *Chromatography today*; 5th edition; Elsevier, Amsterdam, The Netherlands (1997)

[38] M. A. D. R. Silva, D. C. da Silva, V. G. Machado, E. Longhinotti, V. L. A. Frescura; *J.Phys.Chem.A* **106**, 8820 (2002)

[39] C. M. Ruan, T. Bayer, S. Meth, C. N. Sukenik; *Thin Solid Films* **419**, 95 (2002)

CHAPTER 7

Conclusion

NanoLC-MS-based platforms present interesting features for the study of the biochemical processes underlying biomedical events. This thesis reports on several studies in which various aspects and components of such a nanoLC-MS system have been optimised, with the aim to rapidly, precisely and accurately quantify peptides in complex matrices. Limitations such as low signal reproducibility, lengthy analysis times and poor system robustness were overcome. Though much progress has been made generally in the field, nanoLC-MS is not yet a user-friendly technique and still requires dexterity. Nevertheless, the latest technological developments have started to make the use of nanoLC-MS more straightforward for inexperienced researchers.

7.1 Nanospray interface

A nanoESI interface was built in-house and the different parameters likely to influence the quality of the spray and the spectra were investigated. The position and dimensions of the nanospray, as well as the composition and flow rate of the mobile phase, were shown to greatly influence the spray and the resulting spectra. Positioning the nanospray tip at a 20°angle with respect to the heated capillary provided the best S/N, whereas signal intensity was highest when the interface was positioned axially and close to the heated capillary. While a larger %ACN

in the mobile phase required a lower spray voltage to obtain a stable spray, the spray voltage had to be carefully adjusted at low % ACN (i.e. 10%). Varying the FA concentration had a clear impact on both signal intensity and the charge envelop. An increase in the %FA in the mobile phase resulted in a shift toward lower m/z. 1% FA, though, led to a strong reduction in signal intensity. Larger intensities were found for coated needles with a small-ID tip.

7.1.1 Perspectives

Ideally, sprays should be stable at every flow rate, under every mobile phase composition and at every analyte concentration. Such a situation has yet to be accomplished, however. For example, it has been demonstrated by Schmidt et al. [1] that there was no ionisation suppression when using very small ID (1 μm) tapered emitters at very low flow rates (<20 nL/min). Emitters allowing the unsuppressed ionisation of analytes at larger flow rates would thus be an attractive addition for these systems. To this end, multiple emitters should be built following the principle described by Tang et al. [2] As already stated, the flow rate through the individual emitters should not be larger than 20 nL/min and the emitter opening should be approximately 1μm. Therefore, the flow rate to be used determines the number of emitters on the multiple-emitter interface. As an example, to optimally couple a 50-μm-ID packed column used at a flow of 100 nL/min to MS would thus require an emitter with 5 openings of approximately 1m ID. The distance between each emitter is likely to strongly influence the sprays formed at each emitter. If the emitters are too close, the sprays formed could (partially) overlap and result in the collision of the small droplets emitted, thereby producing larger droplets and reducing ionisation efficiency. Chip technology is the most amenable way to tackle this problem. The design of the masks used for photopatterning can easily be changed to vary the distance between pairs of emitters. Additionally, the chip could be (partially) made of a conductive polymer that would not require coating of the emitter with gold or other metal, thereby ensuring greater durability of the emitters.

7.2 Column technology

Silica-based monoliths allow high-efficiency separation of complex samples in a fraction of the analysis time required with particle-packed columns. The bimodal pore structure of silica monoliths exhibits large, interconnected throughpores and smaller mesopores inside a thin silica skeleton, resulting in high porosity and only

small distances over which analytes must diffuse. There are two main approaches to preparing monoliths. Monoliths either exhibit large throughpores, offering very low flow resistance at the cost of separation efficiency, or small throughpores and a relatively thick skeleton, allowing very efficient separations though at the cost of higher operating pressures. The monolith we characterised exhibited throughpores of 2-3 μm, a skeleton of 1.0-1.5 μm and mesopores of 18 nm, and appears to be a compromise between the two aforementioned synthesis approaches. Its high efficiency and low flow resistance allowed the separation of very complex mixtures in a much shorter time than what is usually achieved with packed columns. Peak widths at half height were on the order of 10 s and separations were very repeatable. A wide range of flow rates (up to $\approx$ 20 times the flow used with packed columns) and gradient slopes (up to 9% ACN /min) could be used, depending on the complexity of the separation. Moreover, the specific surface area was sufficient to load large sample volumes and achieve good detectability of low-level analytes.

7.2.1 Perspectives

Though silica-based monoliths allow high-efficiency separation at a fraction of the analysis time required with particle-packed columns, several improvements still remain to be achieved. Even more efficient and faster separations could be attained by optimising the synthesis of silica monoliths.
Ideally, the skeletal porosity should be very high to achieve very fast separations. Our monolith had a 1.0-to-1.5-μm thick skeleton and was 90 to 95% porous. Monoliths with "paper-thin" skeletons should thus be more porous and allow faster separations. Moreover, computer simulations predict that an increased porosity should result in more efficient separations [3]. Smaller throughpores were shown to result in more efficient separations, due to the limited distance over which analytes have to diffuse to interact with the stationary phase. Additionally, mesopores should be interconnected and large enough not to hinder the passage of molecules in and out of the pore and to allow convective transport inside the pores. Our monolith had mesopores of 18 nm, which is comparable to the pore size of porous silica beads, which do not exhibit convective transport inside their pores. Thus, we can assume that separations on our monoliths were still limited by the diffusion of analytes in and out of mesopores. Monoliths with large mesopores (>400 nm) have been reported [4], but did not fulfill the promise of more efficient separations. Since separation efficiency is strongly correlated with homogeneity of the chromatographic bed, it is safe to assume that the large mesopore size distribution observed was underlying the fact that separation effi-

ciency did not improve. Therefore, novel monoliths allowing more efficient and faster separations should have well-interconnected pores in the sub-micron range and skeletons as thin as possible. There might be only one type of pore and not two as is the case now. Moreover, both the pore and skeleton size distribution should be as narrow as possible. Such structural characteristics would allow the use of very long LC columns much like GC columns in conjunction with UHPLC equipment to achieve plate numbers of several hundreds of thousands. However, a very thin silica skeleton might not be strong enough to withstand the pressures generated in UHPLC, in which case the use of oxides other than silica might lead to the synthesis of stronger monoliths. The limited stability of silica at extreme pHs presents another reason to turn to alternative monolith materials. Moreover, such monoliths could exhibit a selectivity different from that of silica. For example, metal oxide-based (e.g. TiO_2) stationary phases show great affinity for phosphorylated analytes. Additionally, TiO_2 is much more resistant to extreme pHs than silica and would offer more flexibility in chosing the conditions under which a column can be operated.
Chromatographic beds with very well defined structures, which can be compared to that of monoliths, were prepared by microfabrication [5]. However, though channels (that we can compare to the throughpores of a monolith) were only a few μm wide and deep, the pillars (the equivalent of the skeleton in monoliths) were still too thick to allow very fast separations. Following the idea developed by Regnier, monolith-like chips could be prepared with greater permeability in order to speed up analysis. However, the fabrication of a chip with structural features similar to that of the ideal monolith will require technologies developed for nanotechnologies, such as e.g. e-beam writters.

7.3 Multidimensional chromatography

Due to the great complexity of the proteome of an organism, multiple-step analyses are required in order not to lose a considerable amount of information. Very abundant proteins (e.g. albumin) often mask proteins and peptides of lower abundance and thus interfere with their detection and identification. Therefore, samples must be effectively depleted of these very abundant proteins. For this purpose, three columns were coupled on-line in a novel, though simple, and robust set-up for multidimensional nanoLC-MS (Chapter 5). No additional switching valve or pump was required to couple the three different columns. A RAM cartridge was coupled to nanoLC-MS for the analysis of a neuropeptide and, after optimisation, virtually all BSA was discarded (Chapter 5). Separations were very

efficient with peak widths at half height of 10s. Such narrow chromatographic peaks were rather unexpected due to the large size difference between the RAM cartridge and the nanoLC trap column, introducing significant pre-trap-column dead volume. The total cycle time including albumin depletion, separation of the analytes, washing and re-equilibration of the system, was about 40 min.

7.3.1 Perspectives

Further developments of this modular system would involve the use of stationary phases of different selectivity in the cartridge and the trap column. RAM particles derivatised with strong cation-exchange functionalities would reduce the risk for peptides breaking through on the RP trap column. Additionally, the sample could be more easily fractionated using salt concentration steps, thereby reducing the complexity of the sample and increasing the system peak capacity. Alternatively, an immobilised-enzyme reactor (IMER) could be coupled on-line with set-ups similar to those described in Chapter 5 and Chapter 6. The use of IMERs reduces the digestion time and allows automation of the digestion step. Improvements of digestion rates and sequence coverage can be obtained by derivatising the immobilised enzymes according to the concept presented by Freije [6],using a range of derivatives. Digestions are often performed in mixed aqueous-organic media in order to increase sequence coverage and speed up the digestion step. However, such samples cannot be directly injected onto an RPLC system because peptides are likely to break through the trap column. A multidimensional nanoLC system, based on the set-up described in Chapter 6, would benefit from a mixed-mode trap column containing both HILIC and RP stationary phases, to allow every peptide to be trapped.
The set-up described in Chapter 5 does not contain an additional switching valve or pump, and is therefore amenable to the implementation of multidimensional chromatography on a chip. On-chip sample manipulation would benefit from the implementation of novel microfluidic concepts like that of the use of recirculating flows in microchannels to trap large molecules or particles [7]. Recirculating flows could be used for sample preconcentration before and/or after albumin depletion as well as for digestion. Recirculating flows are likely to improve digestion rates and increase sequence coverage by dragging the proteins to be digested repeatedly along the protease-coated microchannel.

7.4 Non-specific interactions

It has been shown that adsorption of proteolytic peptides to the vial surface is the underlying cause of repeatability problems in the quantitative analysis of peptides. Improved peptide recovery and greater signal repeatability are obtained by improving peptide solubility, which directly influences the adsorption equilibrium for the peptides between the solution phase and the vial surface. Addition of varying amounts of DMSO to the sample vial reduced peptide adsorption by up to 80%, consequently leading to greater repeatability and lower LOD.

7.4.1 Perspectives

Adsorption of peptides to system surfaces is underlying repeatability problems in quantitative analysis. As in vials and in CE, peptides and proteins are also likely to adsorb non-specifically to the capillary or channel walls used in miniaturised analytical systems. Based on the work by Righetti, derivatisation of the capillary walls with non-ionic and zwitterionic [8] surfactants or large polymers [9, 10] led to a reduction in protein adsorption of more than 90%. The same principle is applicable to vials, capillary walls in LC analysis and microchannels in chip-based analysis. Alternatively, novel hydrophilic polymers could be developed to serve as substrate materials for microfluidic device fabrication.

References

[1] A. Schmidt, M. Karas, T. Dulcks; *Journal of the American Society for Mass Spectrometry* **14**, 492 (2003)

[2] K. Tang, Y. Liu, D. W. Matson, T. Kim, r. d. smith; *analytical chemistry* **73**, 1658 (2001)

[3] P. Gzil, N. Vervoort, G. V. Baron, G. Desmet; *analytical chemistry* **76**, 6707 (2004)

[4] N. Ishizuka, H. Minakuchi, K. Nakanishi, K. Hirao, N. Tanaka; *Colloids and Surfaces A: Physicochemical and Engineering Aspects* **187-188**, 273 (2001)

[5] B. He, N. Tait, f. e. regnier; *analytical chemistry* **70**, 3790 (1998)

[6] J. R. Freije, P. P. Mulder, W. Werkman, L. Rieux, H. A. Niederlander, E. Verpoorte, r. bischoff; *Journal of proteome research* **4**, 1805 (2005)

[7] G. L. Lettieri, A. Dodge, G. Boer, N. F. de Rooij, E. Verpoorte; *Lab on a Chip* **3**, 34 (2003)

[8] L. Castelletti, B. Verzola, C. Gelfi, A. Stoyanov, P. G. Righetti; *Journal of Chromatography A* **894**, 281 (2000)

[9] B. Verzola, C. Gelfi, P. G. Righetti; *Journal of Chromatography A* **874**, 293 (2000)

[10] E. Olivieri, R. Sebastiano, A. Citterio, C. Gelfi, P. G. Righetti; *Journal of Chromatography A* **894**, 273 (2000)

Summary

In order to study the complex biochemical processes underlying pharmacological and medical events, sensitive and selective analytical methods are necessary.
Liquid chromatography (LC) is a very versatile and highly selective technique in which separation is achieved through a partitioning or adsorption equilibrium between a liquid mobile phase and a stationary phase. In its multidimensional forms, LC offers potential to achieve separation efficiencies approaching those of two-dimensional polyacrylamide gel electrophoresis (2D-PAGE). It is easily automated and sample pre-treatment steps can be included in the automated analytical set-up. Unlike capillary electrophoresis (CE), on-line coupling of LC to mass spectrometry (MS) is relatively easily achieved by electrospray ionisation (ESI). Moreover, the miniaturisation of LC-MS allows the detection of very-low-level analytes (zmol to amol). NanoLC-MS systems are potentially even more sensitive. However, selectivity, reproduciblity and robustness as well as speed of analysis and ease of use require due attention when turning to such miniaturised systems. In this thesis, several studies are presented in which various aspects and parts of a nanoLC-ESI-MS system have been optimised, with the aim to overcome the aforementioned limitations.
In Chapter 2, the characterisation of our in-house-built nanoESI interface is presented. Aiming at the quantitative analysis of peptides using nanoLC-MS, it is necessary to know how our nanoESI interface responds to variations in the mobile

phase composition, spray voltage and morphology and position of the nanoESI emitter.

Positioning the nanospray tip at a 20˚angle with respect to the heated capillary provides the best signal-to-noise ratios, but signal intensity is highest when the interface is positioned axially and close to the heated capillary. While a larger percentage of acetonitrile (ACN) in the mobile phase requires a lower spray voltage to obtain a stable spray, the spray voltage has to be carefully adjusted at low % ACN (i.e. 10%). Varying the formic acid (FA) concentration has a clear impact on both signal intensity and the charge envelop. An increase in the %FA in the mobile phase results in a shift toward lower m/z. 1% FA, though, leads to a strong reduction in signal intensity. Larger intensities are found for coated needles with a small-ID tip.

Most traditional chromatographic stationary phases are prepared from naturally-occurring organic polymers for the analysis of proteins, and silica beads in the LC-MS analysis of peptides. The smaller the silica beads, the higher the back-pressure. The larger the beads, the lower the separation efficiency and flow resistance. Moreover, highly porous beads have a higher capacity. Thus, the structure of a stationary phase will be of paramount importance to achieve efficient, rapid and sensitive separation. Silica-based monolithic phases are a relatively recent innovation in the area of chromatographic stationary phases, one which we have also considered in this research in conjunction with peptide separations. Silica-based monolith synthesis, characterisation and applications are reviewed in Chapter 3, while the chromatographic performance of a new 50-μm-ID monolithic column are evaluated and its application to peptide analysis demonstrated in Chapter 4. The bimodal pore structure of silica monoliths exhibits large, interconnected throughpores and smaller mesopores inside a thin silica skeleton, resulting in high porosity and only small distances over which analytes must diffuse. There are two main approaches to preparing monoliths. Monoliths either exhibit large throughpores, offering very low flow resistance at the cost of separation efficiency, or small throughpores and a relatively thick skeleton, allowing very efficient separations though at the cost of higher operating pressures. The monolith we characterised exhibits throughpores of 2-3 μm, a skeleton of 1.0-1.5 m and mesopores of 18 nm, and appears to be a compromise between the two aforementioned synthesis approaches. Its high efficiency and low flow resistance allow the separation of very complex mixtures in a much shorter time than what is usually achieved with packed columns. Peak widths at half height are on the order of 10 s and separations are very repeatable. A wide range of flow rates (up to $\approx$ 20 times the flow used with packed columns) and gradient slopes (up to 9% ACN /min) can be

used, depending on the complexity of the separation. Moreover, the specific surface area is sufficient to load large sample volumes and achieve good detectability of low-level analytes.
In Chapter 5, a novel set-up allowing on-line coupling of albumin depletion and sample fractionation with nanoLC-MS is presented. By increasing the efficiency, selectivity and loading capacity of an analytical system, multidimensional approaches increase the number of peptides that can be analysed in a complex sample.
Very abundant proteins (e.g. albumin) often mask proteins and peptides of lower abundance and thus interfere with their detection and identification. Therefore, samples must be effectively depleted of these abundant proteins. To this end, three columns are coupled on-line in a novel, though simple and robust, set-up for multidimensional nanoLC-MS. No additional switching valve or pump is required to couple the three different columns. A cartridge filled with restricted-access material (RAM) was coupled to nanoLC-MS to remove bovine serum albumin (BSA) from a sample containing a neuropeptide. After optimisation, virtually all the BSA is discarded. Separations were very efficient, with peak widths at a half height of 10s. The total cycle time, including albumin depletion, separation of the analytes, washing and re-equilibration of the system, is about 40 min.
In Chapter 6, a study of the repeatability issues in LC-MS is presented. Poor repeatability of peak areas is a problem frequently encountered in peptide analysis with nanoLC-MS. As a result, quantitative analysis is difficult, unless the observed signal variability can be corrected for. Labelling techniques or addition of internal standards can be applied to this end. However, these procedures are often elaborate and error prone and do not always improve repeatability.
Adsorption of proteolytic peptides to the vial surface is shown to be the underlying cause of repeatability problems in the quantitative analysis of peptides by nanoLC-MS. Improved peptide recovery and greater signal repeatability are obtained by improving peptide solubility, which directly influences the adsorption equilibrium for the peptides between the solution phase and the vial surface. Addition of varying amounts of DMSO to the sample vial reduces peptide adsorption by up to more than 90% in some cases, consequently leading to greater repeatability and lower LOD.
In conclusion, in order to achieve the very high throughput and ease necessary in routine comparative proteomic studies, several limitations of nanoLC-MS such as low signal reproducibility, lengthy analysis times and poor system robustness have been overcome. Though much progress has been made generally in the field, nanoLC-MS is not yet a user-friendly technique and still requires dexterity. Nev-

ertheless, the latest technological developments have started to make the use of nanoLC-MS more straightforward for inexperienced researchers.

Samenvatting

Voor het bestuderen van de complexe biochemische processen die een rol spelen in farmacologische en medische processen, is het gebruik van gevoelige en selectieve analytische methodes noodzakelijk.
Vloeistof chromatografie (LC) is een zeer veelzijdige en uitermate selectieve techniek waarin scheiding wordt verkregen door een verdelings- of adsorptie-evenwicht tussen een vloeibare mobiele fase en een stationaire vaste fase. Met multidimensionale LC vormen, is het mogelijk de scheidingsefficintie van tweedimensionale polyacrylamidegel elektroforese (2D-PAGE) te benaderen. Het is gemakkelijk te automatiseren en monstervoorbewerkingsstappen kunnen in de geautomatiseerde analytische opstelling gentegreerd worden. In tegenstelling tot capillaire elektroforese (CE), kan LC vrij gemakkelijk on-line worden gekoppeld aan massaspectrometrie (MS) met behulp van electrospray ionisatie (ESI). Bovendien maakt miniaturisatie van LC-MS de detectie van analieten op een laag concentratieniveau (zmol tot amol) mogelijk. NanoLC-MS systemen zijn in potentie zelfs nog gevoeliger. De selectiviteit, reproduceerbaarheid en de robuustheid en ook de snelheid van analyse evenals het gebruiksgemak van deze geminiaturiseerde systemen vereisen echter aandacht. Dit proefschrift, beschrijft verschillende studies waarin verschillende aspecten en delen van een nanoLC-ESI-MS systeem zijn geoptimaliseerd, met als doel de eerder genoemde beperkingen te overwinnen. In Hoofdstuk 2, wordt de karakterisering van de zelfgebouwde nanoESI-interface

beschreven. Met het oog op de kwantitatieve analyse van peptiden met nanoLC-MS, is het noodzakelijk om te weten hoe deze nanoESI interface zich gedraagt bij variaties in de mobiele fase samenstelling, het spray voltage en de morfologie, evenals de positie van de nanoESI-emitter.
Het positioneren van de nanospray-emitter in een hoek van 20°ten opzichte van de 'heated capillary' levert de beste signaal-ruis verhoudingen. De signaalintensiteit is echter het hoogst wanneer de interface axiaal en dicht bij het heated capillary wordt geplaatst. Terwijl een hoog acetonitrile (ACN) percentage in de mobiele fase een lager spray voltage vereist om een stabiele spray te krijgen, moet het spray voltage bij een laag percentage ACN (b.v. 10%) zorgvuldig worden gekozen. Het variren van de mierezuur (FA) concentratie heeft een duidelijke invloed op zowel signaalintensiteit als de ladingsverdeling. Een verhoging van het FA percentage in de mobiele fase resulteert in een verschuiving naar lagere m/z waarden. Al bij een FA percentage van 1%, treedt echter een sterke vermindering van signaalintensiteit op. De hoogste signaalintensiteit wordt bereikt met gecoate naalden die een uiteinde met een kleine interne diameter (ID) hebben.
De meeste traditionele chromatografische stationaire fasen voor de analyse van eiwitten, zijn gebaseerd op natuurlijke organische polymeren terwijl silica deeltjes voornamelijk voor LC-MS analyse van peptiden worden gebruikt. Hoe kleiner de silica deeltjes, hoe hoger de tegendruk. Hoe groter de deeltjes, hoe lager de scheidingsefficiency en de stroomweerstand. Bovendien hebben de meest poreuze deeltjes een hogere capaciteit. Aldus, zal de structuur van een stationaire fase in aanzienlijke mate de efficintie, snelheid en gevoeligheid van een scheiding benvloeden. Op silica gebaseerde monolithische fasen zijn een vrij recente innovatie op het gebied van chromatografische stationaire fasen, die tevens in dit proefschrift beschreven zijn voor wat betreft het gebruik voor scheiding en analyse van peptiden. Een overzicht van de synthese van op silica gebaseerde monolieten, hun karakterisering en toepassingen word gegeven in Hoofdstuk 3, terwijl in Hoofdstuk 4 de chromatografische prestaties van een nieuwe 50-μm-ID monolithische kolom worden gevalueerd en zijn toepassing in de peptidenanalyse wordt gedemonstreerd.
De bimodale poriestructuur van silica monolieten vertoont grote, verbonden throughpores' en kleinere mesopores binnen in een dun silica skelet, hetgeen resulteert in een hoge poreuziteit en slechts kleine afstanden waarover analieten zich middels diffusie moeten verplaatsen. Bij de productie van monolieten worden twee belangrijke synthesebenaderingen gebruikt die resulteren in verschillende poriestructuren. Enerzijds worden monolieten geproduceerd met grote throughpores', die een zeer lage stroomweerstand hebben ten koste van de scheidingsefficintie. An-

derzijds zijn er monolieten met kleine throughpores' en een relatief dik skelet, wat zeer efficinte scheidingen mogelijk maakt, waarvoor echter een hogere druk vereist is. De door ons gekarakteriseerde monoliet kenmerkt zich door throughpores' van 2-3 μm, een skelet van 1.0-1.5 μm en mesopores' van 18 nm, hetgeen een compromis tussen de twee eerdergenoemde synthesebenaderingen inhoudt. Een hoge efficintie en lage stroomweerstand maakt de scheiding van zeer complexe mengsels mogelijk in een veel kortere tijd dan wat gewoonlijk met gepakte kolommen wordt bereikt. De piekbreedte op halve hoogte is in de orde van 10 s en de scheidingen zijn zeer reproduceerbaar. Een grote verscheidenheid van stroomsnelheden (tot $\approx$ 20 keer de stroomsnelheid die met gepakte kolommen wordt gebruikt) en gradinthellingen (tot 9% ACN/min) kunnen worden gebruikt, afhankelijk van de complexiteit van de scheiding. Bovendien maakt de specifieke oppervlakte het opbrengen van grote monstervolumes mogelijk, hetgeen resulteert in een goede detectie van analieten met een lage concentratie.

In Hoofdstuk 5, wordt een nieuwe opstelling beschreven die de on-line koppeling van albumine depletie en monsterfractionering met nanoLC-MS mogelijk maakt. Door het verhogen van de efficintie, selectiviteit en het ladingscapaciteit van een analytisch systeem, met een multidimensionale benadering wordt het aantal peptiden dat kan worden geanalyseerd in complexe monsters vergroot.

Een aantal zeer overvloedige aanwezige eiwitten (b.v. albumine) maskeren vaak eiwitten en peptiden die in lagere hoeveelheid aanwezig zijn en verhinderen hun detectie en identificatie. Daarom moeten de monsters effectief van deze overvloedige protenen worden gezuiverd alvorens de monsters te analyseren. Daartoe, worden drie kolommen on-line gekoppeld in een nieuwe, eenvoudige en robuuste opstelling voor multidimensionele nanoLC-MS. Deze opstelling vereist geen extra schakelkraan of pomp om de drie verschillende kolommen aan elkaar te koppelen. Een cartridge gepakt met 'restricted access' materiaal (RAM) werd hierbij gekoppeld aan nanoLC-MS voor de depletie van runder serum albumine (BSA) uit een monster dat een neuropeptide bevat. Na optimalisering, was het mogelijk het monster van vrijwel alle BSA te ontdoen. De scheidingen waren zeer efficint, met piekbreedten op halve hoogte van 10s. De totale cyclustijd, inclusief albuminedepletie, scheiding van analieten, wassen en herequilibreren van het systeem, is ongeveer 40 min.

In Hoofdstuk 6, wordt een studie van de herhaalbaarheidkwesties in LC-MS gepresenteerd. De slechte reproduceerbaarheid van piekoppervlaktes is een probleem dat vaak voorkomt in peptideanalyse met nanoLC-MS. Dientengevolge, is de kwantitatieve analyse moeilijk, tenzij voor de signaalvariatie kan worden gecorrigeerd. Labelingstechnieken of de toevoeging van een interne standaard kunnen

daarbij worden toegepast. Deze procedures zijn echter vaak gecompliceerd, arbeidsintensief en verbeteren de reproduceerbaarheid niet altijd.
Er werd aangetoond dat de adsorptie van proteolytische peptides aan de oppervlakte van monsterbuisjes, de oorzaak was van de reproduceerbaarheidsproblemen in de kwantitatieve analyse van peptiden met nanoLC-MS. Het verbeteren van de peptidenopbrengst en een hogere signaalreproduceerbaarheid werden bereikt door de oplosbaarheid van de peptiden te verbeteren, door direct het adsorptie-evenwicht van peptiden tussen het oplossingmiddel en het oppervlak van het monsterbuisje te benvloeden. De toevoeging van verschillende hoeveelheden DMSO aan het monsterbuisje vermindert peptidenadsorptie tot, in sommige gevallen, meer dan 90%, hetgeen leidt tot een hogere reproduceerbaarheid en lagere detectielimieten.
Concluderend, wordt een oplossing geboden voor verscheidene beperkingen van nanoLC-MS die het bereiken van de noodzakelijk zeer hoge throughput en gebruiksgemak in routinematige vergelijkende proteomicsstudies verhinderden, zoals lage signaalreproduceerbaarheid, lange analysetijden en de slechte systeemrobuustheid. Hoewel er over het algemeen veel vooruitgang op het gebied is geboekt, is nanoLC-MS nog geen gebruiksvriendelijke techniek en is veel ervaring vereist. Niettemin, zijn de technologische ontwikkelingen genitieerd die het gebruik van nanoLC-MS voor onervaren onderzoekers zullen vereenvoudigen.

Acknowledgments

Though I mostly worked alone for the last years, I would not have been able to complete this work without receiving help from and collaborating with a certain number of people.
First of all, I would like to thank my promotors, Prof. Dr Rainer Bischoff and Prof. Dr Sabeth Verpoorte. Their knowledge of analytical systems in general and of protein analysis and miniaturised systems in particular was of great help.
Thanks to my copromotor, Harm Niederländer, who made the completion of this work possible due to his presence and daily supervision.
Thanks to the reading committee, Prof. Dr Ben Westerink, Prof. Dr Erik Frijlink and Prof. Dr Thomas Hankemeier, for accepting to spend time reading my thesis.
Thanks to Prof. Dr Ben Westerink, Dr Thomas Cremers and Marieke van der Hart for collaborating on the project aiming at the analysis of Substance P in microdialysates.
Thanks to Merck KGaA and Dr Dieter Lubda for providing me with silica-based monolithic columns.
Thanks to the Pharmaceutical Analysis and Analytical Biochemistry groups.
Thanks to all my friends in Groningen and abroad.
Merci à ma famille et à mes parents en particulier. A mes grand-parents, vous êtes mes modèles et ma fierté ainsi qu'une source d'inspiration et de motivation. Sans vous tous, je ne serai pas celui que je suis maintenant.

Mylène, grâce à toi, j'ai gagné des batailles que je croyais perdues, ravivé des feux que je croyais éteints et traversé des océans que je croyais sans fin. Tu m'as montré la voie, la nôtre, je l'espère la plus longue possible. Je t'aime.

Publications

Silica Monolithic columns : Synthesis, characterisation and application to the analysis of biological molecules, Rieux L., Niederländer H.A.G., Verpoorte E., Bischoff R.P.H., Journal of Separation Sciences, **2005**, *28*, 1628-1641

Chemically modified, immobilized trypsin reactor with improved digestion efficiency, Freije J.R., Mulder P.P.M.F.A., Werkman W., Rieux L., Niederländer H.A.G., Verpoorte E., Bischoff R.P.H., Journal of Proteome Research, **2005**, *4*, 1805-1813

Fast, high-efficiency peptide separations on a 50-μm reversed-phase silica monolith in a nanoLC-MS set-up, Rieux L., Lubda D., Niederländer H.A.G., Verpoorte E., Bischoff R.P.H., Journal of Chromatography A, **2006**, *1120*, 165-172

Improvement of repeatability and reproducibility in peptide analysis, van Midwoud P., Rieux L., Bischoff R.P.H., Verpoorte E., Niederländer H.A.G., (Submitted)

RAM-based albumin depletion coupled on-line to nanoLC-MS for the analysis of complex proteomics samples, Rieux L., Bischoff R.P.H., Verpoorte E., Niederländer H.A.G., (Submitted)